UNIVERSITÀ DEGLI STUDI DI MILANO

PhD Course in Molecular and Cellular Biology

XXXI Cycle

eIF6 phosphorylation on Ser235 is required for mammalian development and for T-cell lymphomagenesis, establishing a functional network between translation and senescence.

Alessandra Scagliola

PhD Thesis

Scientific tutor: Prof. Stefano Biffo

Supervisor: Dr. Annarita Miluzio

Academic year:

2017-2018

SSD: BIO/11

Thesis performed at Molecular Histology and Cell Growth Unit, INGM, Istituto di Genetica Molecolare and at the Department of Bioscience, University of Milan.

Contents

Abstract

Deregulated translation control is a hallmark of human cancers and is critical for tumorigenesis downstream of multiple oncogenic signaling pathways. eIF6 is an oncogenic translation factor, which regulates the initiation phase of translation controlling active 80S complex formation. eIF6 depletion and dephosphorylation slow cell growth and cell transformation *in vitro* and protect from tumor development in mice. eIF6 activation is mTORC1-independent and driven by PKCβ mediated phosphorylation on Ser235. Intriguingly, both eIF6 overexpression and PKC hyperactivation are found in T-cell lymphomas, such as in Anaplastic Large Cell Lymphoma (ALCL). We hypothesized that eIF6 phosphorylation drives T cell lymphomagenesis and mammalian development. We used a conditional eIF6^{SA} KI mouse model in which Ser235 is replaced by an Ala. We discovered that homozygous point mutation (eIF6$^{SA/SA}$) is lethal after gastrulation. Heterozygous mice (eIF6$^{SA/+}$) are viable but resistant to NPM-ALK induced lymphomagenesis. The survival of eIF6$^{SA/SA}$ NPM-ALK mice is significantly increased and the appearance of lymphoma is delayed up to 6 months. Surprisingly, *ex vivo* eIF6$^{SA/SA}$ NPM-ALK primary thymocytes have a striking senescence-like phenotype. Similarly, in vitro generated eIF6$^{SA/SA}$ MEFs show a markedly reduced proliferation and increased senescence. This phenotype is completely rescued by transducing eIF6^{wt}, but not by eIF6^{SA}. In eIF6$^{SA/SA}$ MEFs, the direct interaction between mutant eIF6^{SA} protein with the 60S ribosomal subunit surface is extremely increased, suggesting that 60S viability, required for active translation, could be compromised.

In conclusion, our work demonstrates for the first time that eIF6 phosphorylation on Ser235 is essential for mammalian development, cell homeostasis and is rate-limiting for T-cell lymphomagenesis *in vivo*. Finally, we suggest that the translational control driven by eIF6 activity induces cellular premature senescence, resulting in a protective mechanism against tumor progression.

eIF6 è un fattore di inizio della traduzione che regola la disponibilità della subunità maggiore del ribosoma 60S nel citoplasma, controllando la formazione del complesso attivo 80S. I livelli di eIF6 sono limitanti per la trasformazione cellulare e la progressione tumorale *in vivo*. L'attivazione di eIF6 è determinata dalla sua fosforilazione sulla Ser235, mediata dall'asse RACK1/PKCβ. eIF6 è overespresso e iperfosforilato in diverse linee cellulari tumorali e alti livelli proteici di eIF6 e PKC sono presenti in linfomi a cellule T. Il nostro studio ha l'obiettivo di definire il ruolo della fosforilazione di eIF6 in condizioni fisiologiche e nei linfomi a cellule T. Abbiamo dunque generato un modello murino condizionale $eIF6^{SA}$ KI che è stato incrociato con topi CMV-Cre e con topi transgenici NPM-ALK, i quali sviluppano spontaneamente linfomi a cellule T e la cui resistenza alla terapia farmacologica è determinata dall'attivazione della chinasi PKC. I nostri risultati indicano che l'espressione in omozigosi della mutazione puntiforme di eIF6 in tutti i tessuti è letale a livello embrionale, dopo lo stadio di gastrulazione. Topi eterozigoti per la mutazione ($eIF6^{SA/+}$) sono invece vitali ma resistenti allo sviluppo di linfomi indotto dall'oncogene NPM-ALK. Per determinare gli effetti anti-tumorali della mutazione di eIF6 a livello cellulare, abbiamo generato topi $eIF6^{SA/SA}$ CD4Cre NPM-ALK: lo sviluppo tumorale in questo modello murino è notevolmente rallentato. Analisi istologiche condotte sui tumori $eIF6^{SA/SA}$ hanno evidenziato un accumulo di cellule senescenti, le quali rappresentano una barriera per la progressione tumorale. Nei fibroblasti murini senescenti omozigoti ($eIF6^{SA/SA}$) l'interazione tra la proteina mutata $eIF6^{SA}$ con la subunità 60S è aumentata, suggerendo che la disponibilità della 60S, necessaria per un'attiva sintesi proteica, potrebbe essere compromessa. Il nostro studio dimostra per la prima volta che la fosforilazione di eIF6 sulla Ser235 è essenziale per lo sviluppo embrionale, l'omeostasi cellulare e per lo sviluppo di linfomi a cellule T. La nostra ipotesi è che il controllo traduzionale svolto da eIF6 induca prematura senescenza cellulare, proteggendo dalla progressione del tumore.

1. Introduction

1.1 Translation

Translation is the process by which mRNAs are translated into proteins. It is the most energy-consuming process in the cell and this consumption is tightly coupled to the cellular energy status (Buttgereit and Brand 1995, Warner 1999). The translation of mRNAs into proteins serves as a critical regulatory event in gene expression (Pradet-Balade, Boulmé et al. 2001).
Translation requires the orchestrated interaction of tRNA, ribosomes, auxiliary factors and mRNA (Bhat, Robichaud et al. 2015).
The established phases of translation are initiation, elongation, termination and ribosomal recycling. Initiation consists of the formation of a translational competent ribosome 80S at the mRNA start codon; elongation is the process by which active 80S decodes the mRNA into proteins; termination is the release of mRNA, protein and dissociation of the 80S in the individual ribosomes at the stop codon; next, ribosomes recycle to the 5' of the mRNA. These processes are assisted by the coordinated activity of initiation factors, elongation factors and termination factors. Most regulation of the process of translation is exerted at the first stage, considered the rate-limiting event of translation (Sonenberg and Hinnebusch 2009).

1.1.1 Cap-dependent translation

The majority of eukaryotic mRNAs initiate translation through a canonical cap-dependent mechanism. Briefly, this mechanism consists of the events that led up to the positioning of an elongation-competent 80S ribosome at the start codon of the mRNA.
This process can be divided into four steps:

1. formation of the 43S pre-initiation complex (PIC), formed by the 40S small ribosomal subunit, the ternary complex (eIF2-GTP and the initiating methionyl tRNA) and by a group of eukaryotic initiation factors (eIF3, eIF1, eIF1A, eIF5);

2. recruitment of the 43S complex to the 5' end of the mRNA, marked by an inverted m^7GpppN cap. Association of the 43S ribosome complex with the cap is mediated by the eIF4F complex-composed of cap-binding protein eIF4E, eIF4G, and RNA helicase eIF4A and by poly(A)-binding protein (PABP);

3. scanning of the 5' untranslated region (UTR) towards its 3’ end for an AUG nucleotide triplet start codon; this process requires the activity of the PIC that scans in an open conformation. Once the start codon is recognized, a conformational change from open to closed occurs and the iMet-tRNA adapts (Hinnebusch 2017).

4. when the anticodon of Met-tRNAi base-pairs with the start codon, hydrolysis of the GTP bound to eIF2 produce a stable 48S PIC. The release of eIF2-GDP is followed by joining of the large (60S) ribosome subunit, catalyzed by eIF5B, producing an 80S elongation-competent ribosome.

Eukaryotes ribosomes, which are evolutionarily conserved and constituted by ribosomal proteins and rRNA (Ben-Shem, Garreau de Loubresse et al. 2011), are represented by the small subunit (40S) and by the large subunit (60S). They are assembled in the nucleolus, exported to the cytoplasm and recruited for translation.
Ribosomes can associate in the absence of mRNA and form inactive 80S ribosomes. Thus, the 80S can exist in two forms: active and inactive. As physiological conditions favor the association of the 40S and 60S ribosomal subunits, it is fundamental that post-termination ribosomes dissociate.
As reported in Figure 1, the binding of the preinitiation complex to the mRNA involves the cooperative activities of eIF4F, eIF3, eIF4B and PABP. PABP was identified as a protein that associated with polyA tail at the 3’UTR of the mRNA. The PABP-eIF4G interaction is thought to promote a circularization of the mRNA molecule forming a closed loop. This circularization provides a possible framework by which 3’UTR-binding proteins can regulate translation initiation (Gebauer and Hentze 2004).

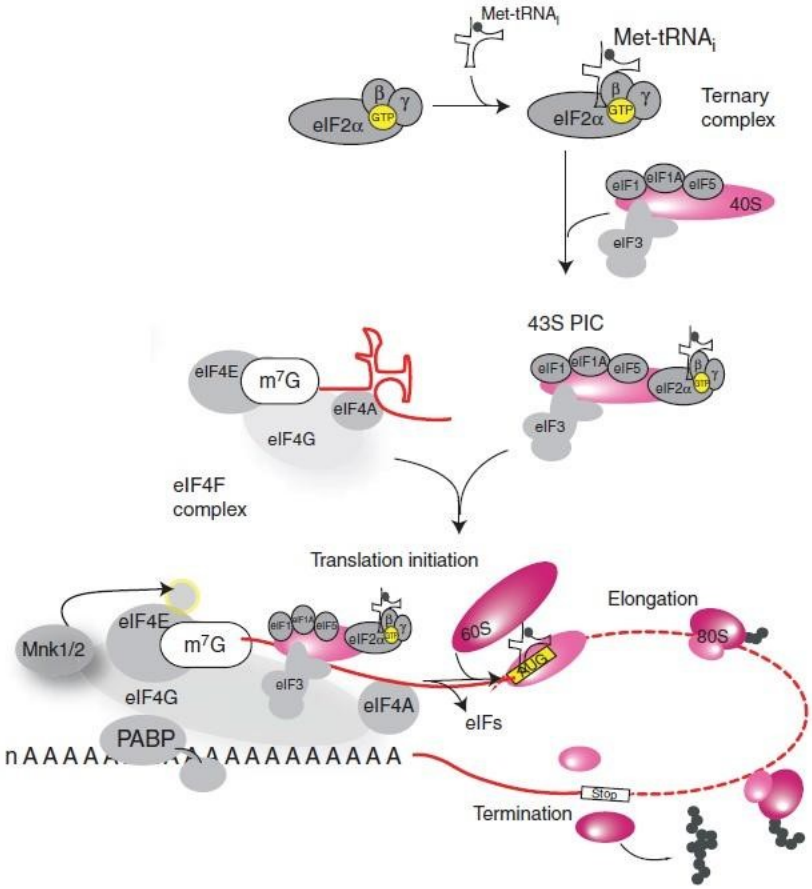

Figure 1. Cap-mediated translation initiation. Overview of translation initiation. (Bottom) Initiation proceeds via a scanning mechanism, whereby the 40S ribosomal subunit is recruited to the 5' extremity of the messenger RNA (mRNA) and scans the 5' untranslated region (UTR) of the mRNA toward its 3' end. When the anticodon of the initiator methionyl-transfer RNA (tRNA) (Met-tRNAi) base-pairs with the start codon, the 60S subunit is recruited and elongation begins with the sequential addition of amino acids until a stop codon is reached and termination occurs. (Top) Formation of the ternary complex (TC): eukaryotic initiation factor (eIF)2—composed of α, β, and γ subunits—GTP and Met-tRNAi. TCs associate with the 40S ribosome and other initiation factors, forming the preinitiation complex (PIC). (Middle) The eIF4F complex consists of the cap-binding protein eIF4E, the scaffolding protein eIF4G, and the eIF4A helicase. Figure adapted by (Robichaud, Sonenberg et al. 2018).

1.1.2 Translation Elongation, Termination and ribosome recycling

Following translation initiation, an 80S ribosome is poised on a messenger RNA (mRNA) with the anticodon of Met-tRNA$_i$ in the P site base-paired with the start codon. The second codon of the open reading frame (ORF) is present in the A (acceptor) site of the ribosome awaiting binding of the corresponding aminoacyl-tRNA. The eukaryotic elongation factor

eEF1A binds aminoacyl-tRNA in a GTP-dependent manner and then directs the tRNA to the A site of the ribosome. Following accommodation of the aminoacyl-tRNA into the A site, peptide bond formation with the P-site peptidyl-tRNA occurs rapidly.

eEF2 promotes tRNA translocation within the ribosome sites and allows mRNA to move by one codon. Termination is triggered when a stop codon (UAA, UGA, UAG) enters the A site of the ribosome. Post-termination ribosomes dissociate through release factors eRF1 and eRF3, which form a ternary eRF1/eRF3–guanosine triphosphate (GTP) complex. The post-termination complex is then disassembled, enabling its constituents to participate in further rounds of translation (Hellen 2018). Ribosome recycling involves splitting of the 80S ribosome by the ATP-binding cassette protein ABCE1 to release the 60S subunit (Pisarev, Skabkin et al. 2010). *In vitro*, eIF6 is necessary to clamp free ribosomal subunits (Jackson, Hellen et al. 2010).

1.1.3 The translational regulation

Translational control refers to the multiple mechanisms that drive the complexity of translation. Translational control exerts a major role in shaping gene expression that responds to endogenous or exogenous signals and it is crucial for determining cell homeostasis and cell function during nutrient deprivation and stress, development and differentiation, aging and disease (Hershey, Sonenberg et al. 2012). Regulation of protein synthesis may occur at different steps of the pathway, with the initiation phase being the most common target. Translational control can be divided into the global regulation of translation and mRNA-specific regulation (Gebauer and Hentze 2004). Global regulation affects the translation efficiency of most mRNAs through a general tuning of protein synthesis. Global regulation of translation is largely achieved via modulation of the activity of translation initiation factors, such as eIF4E and eIF2 factors (Sonenberg and Hinnebusch 2009, Hershey, Sonenberg et al. 2018). mRNA-specific regulation only affects the translation of selected mRNAs. mRNA-specific translational regulation happens mostly via trans-acting factors that bind cis-regulatory elements on the mRNA, but also through the action of microRNA and a variety of untranslated regions (UTRs), aside to the coding open reading frame (ORF), that mRNAs have evolved. These sequences account as powerful regulators of translation efficiency. Sequences on the mRNA regulate their sensitivity to eIF availability, which in turn is controlled by signaling pathways. The interplay among eIFs, mRNA sequences and signaling

pathways generate the specificity of translational control. Finally, also the ribosome itself can be targeted to exert translational regulation. Several of its protein constituents can stand post-translational modifications (Lackner and Bahler 2008) and heterogeneity in the composition of the ribosome may account for functional roles in controlling gene expression (Genuth and Barna 2018).

1.1.3.1 Regulation of ternary complex formation

One of the best-studied examples of global translational regulation occurs with the control of the active ternary complex formation. Exposure of cells to stress conditions results often in a global downregulation of translation (Holcik and Sonenberg 2005). Formation of active ternary complexes is strongly reduced, and consequently translation is downregulated globally, in the presence of four activated eIF2α kinases that are sensing of either amino acid deprivation (GCN2), or unfolded proteins (PERK) or double-stranded RNA in virus infection (PKR) or heme deficiency (HRI) (Figure 2). These different eIF2α kinases phosphorylate the same residue in eIF2α and, hence, elicit the same "integrated stress response". Phosphorylation of the α-subunit of eIF2 reduces the dissociation of eIF2 from eIF2B. As a result, less eIF2α is available and the global translation is inhibited (Holcik and Sonenberg 2005). Induction of phospho-eIF2α serves as an important regulator, under which general protein synthesis and cell proliferation are blocked, thus allowing cells to recuperate from stress or be eliminated if the damage is beyond repair (Koromilas 2015, Pavitt 2018).

Whereas translation of most mRNAs is downregulated by eIF2α phosphorylation, translation of several specific mRNAs can be upregulated in response to the reduced availability of ternary complex. This upregulation is achieved by regulatory upstream open reading frames (uORFs). For instance, the mammalian transcription factor ATF4 is regulated by uORFs in response to ER stress or amino acid starvation (Holcik and Sonenberg 2005, Holcik and Pestova 2007, Oyadomari, Harding et al. 2008).

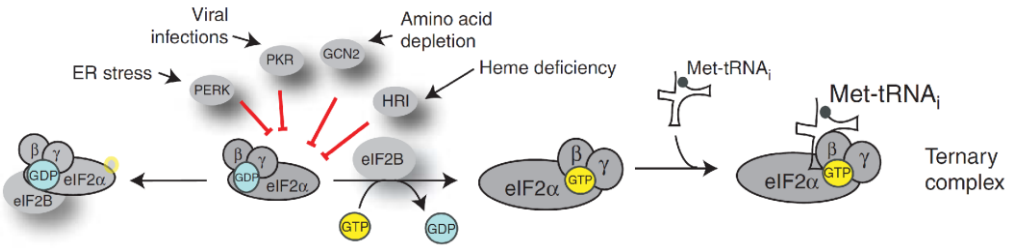

Figure 2. Integration of stress responses by the phosphorylation of eIF2α. eIF2α can be phosphorylated by PKR, PERK, GCN2, or HRI, responding to different stresses such as double-stranded RNA, misfolded proteins, amino acid deficiency, and heme deficiency, respectively. Phosphorylation of eIF2α leads to stabilization of the GDP-loaded complex with the guanine nucleotide exchange factor eIF2B and reduced cycling to the active, GTP-bound TC. Figure adapted by (Robichaud, Sonenberg et al. 2018).

1.1.3.2 Regulation of cap-dependent translation by signaling pathways

Cap-dependent translation is regulated by the pathway of the mammalian Target of Rapamycin (mTOR). mTOR is a downstream Ser/Thr kinase in the PI3K/Akt signaling pathway, which regulates proliferation and growth in response to extracellular stimuli, amino acid availability, oxygen and energy status of the cells (Zoncu, Efeyan et al. 2011, Roux and Topisirovic 2018).

mTOR exists in two functionally and structurally distinct protein complexes: mTOR complex 1 and 2 (mTORC1 and mTORC2). These two complexes regulate disparate cellular functions by phosphorylating distinct sets of substrates. mTORC1 signaling to the translational apparatus is regulated by a multitude of cellular pathways including phosphoinositide 3-kinase (PI3K), Ras/MAPK, Rag GTPase and AMP (Hay and Sonenberg 2004, Laplante and Sabatini 2012). Several substrates of mTORC1 have been identified, including the eIF4E-binding proteins (4E-BPs), S6 kinases 1 and 2 (S6Ks), PRAS40, the transcription factor TFEB, Ser/Thr kinase Ulk1 (also known as hATG1), and growth factor receptor-bound protein 10 (Grb10) (Caron, Ghosh et al. 2010, Peña-Llopis, Vega-Rubin-de-Celis et al. 2011). On activation, mTORC1 phosphorylates residues corresponding to Thr37 and Thr46 on human 4E-BP1, which act as priming sites for the phosphorylation of Ser65 and Thr70. Phosphorylation of 4E-BPs on these four residues leads to their dissociation from eIF4E, allowing the assembly of the eIF4F complex (Preiss and Hentze 1999). eIF4F assembles in conditions of mTORC1 activation, binds mRNAs, brings them to the small ribosomal subunit

and unwinds complex hairpin structures that prevent the scanning of the 40S ribosome to the start codon. Conversely, under conditions in which energy production, oxygen supply and nutrients are inadequate, mTORC1 signaling is down-regulated, resulting in inhibition of translation, reduction in cellular growth proliferation, and induction of autophagy. In addition to 4E-BPs, mTORC1 regulates translation by activating the S6Ks (Ma and Blenis 2009). Mammals express two variants of S6K: S6K1 and S6K2. Several S6Ks substrates have been implicated in the regulation of translation including ribosomal protein S6 (rpS6), eukaryotic initiation factor 4B (eIF4B) and programmed cell death protein 4 (PDCD4) (Roux and Topisirovic 2012). S6K1 regulates translation initiation through the phosphorylation of the cap-binding complex component eIF4B at Ser422 (Raught, Peiretti et al. 2004). S6K2 appears to be the predominant kinase that phosphorylates rpS6 on its five phosphorylation sites. The study of rpS6P$^{-/-}$knock-in mice (in which alanine residues replaced the rpS6 phosphorylation sites) established that rpS6 phosphorylation is crucial for cell size and proliferation since cells isolated from rpS6P$^{-/-}$ displayed defective cell growth (Montagne, Stewart et al. 1999, Ruvinsky, Sharon et al. 2005). Expression of the non phosphorylatable rpS6 mutant, however, moderately upregulates overall protein synthesis, whereas loss of S6Ks has only a marginal effect on global translation (Pende, Um et al. 2004, Ruvinsky, Sharon et al. 2005). In addition, the S6K/rpS6 axis has been implicated in ribosome biogenesis (Chauvin, Koka et al. 2014).

PDCD4 is a pro-apoptotic factor that binds to eIF4A and competes with eIF4G for eIF4A binding, leading to a consequent repression of cap-dependent translation (Yang, Jansen et al. 2003). S6Ks phosphorylates PDCD4 leading to its degradation. Additionally, mTORC1 directly phosphorylates eIF4G at multiple residues (Raught, Gingras et al. 2000), but the functional consequences remain unknown.

Rapamycin is a naturally occurring allosteric inhibitor of mTORC1 (Guertin and Sabatini 2007). mTOR inactivation, by treatment with rapamycin, mimics deprivation of nutrients, both in mammals and in yeasts.

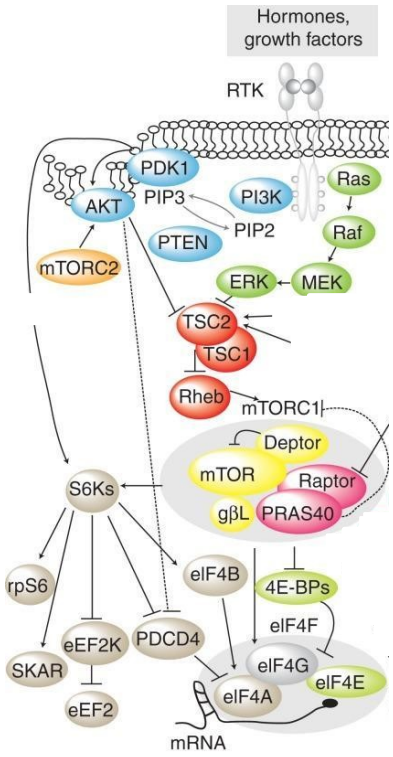

Figure 3. mTORC1 signaling to the translational machinery. Growth factors and hormones stimulate mTORC1 by acting receptor tyrosine kinase (RTK) signaling via PI3K/AKT (light blue) and Ras/ERL (green) pathways. TSC1/2 (red) suppresses mTORC1 signaling by inhibiting GTPase activity of Rheb (red). mTORC1 modulates translation via the phosphorylation of downstream targets including 4E-BPs, S6Ks and their downstream effectors. Image adapted from (Roux and Topisirovic 2012).

The mitogen-activated protein kinases (MAPKs) are Ser/Thr kinases that, by phosphorylating specific serines and threonines of target protein substrates, regulate many essential processes, including gene expression, mitosis, metabolism, motility, survival, apoptosis, and differentiation (Cargnello and Roux 2011).MAPKs consist of growth factor-regulated extracellular signal-related kinases (ERKs), and the stress-activated MAPKs, c-jun N-terminal kinases (JNKs) and p38 MAPKs (Roux and Topisirovic 2012). In the MAP kinase signaling pathway a MAP kinase is activated by a MAP kinase kinase (MKK or MAP2K), which is in turn activated by a MAP kinase/ERK kinase (MEK) kinase or MAP kinase kinase kinase (MEKK or MAP3K). The MAPK-activated protein kinases (MAPKAPKs) are a family of Ser/Thr kinases which includes the p90 ribosomal S6 kinases (RSKs) and the MAPK interacting kinases (MNKs). The RSKs and MNKs have been directly implicated in the regulation of mRNA translation (Nandagopal and Roux 2015). The activity of eIF4E is regulated by MNK1 and MNK2. MNKs are recruited to eIF4E through association with

eIF4G. Despite variable effects on global translation, phosphorylation of eIF4E specifically affects translation of a subset of mRNAs, involved in inflammation and tumor progression (Wendel, Silva et al. 2007).

The RSK family comprises four highly similar members (RSK1, RSK2, RSK3, and RSK4) that are activated by Ras/MAPK signaling. S6K1 and S6K2 are the predominant rpS6 kinases in somatic cells. Other studies using cells null for SK1 and SK2 showed rpS6 phosphorylation mediated by RSK. Both RSK1 and RSK2 were found to specifically phosphorylate rpS6 on Ser235 and Ser236 (Carriere, Ray et al. 2008). RSK provides a mTOR/S6K-independent input linking MAPK signaling to the potential regulation of mRNA translation (Roux and Topisirovic 2012).

1.1.3.3 Regulation of cap-independent translation

Studies of viral gene expression in the late 1980s led to the discovery of a cap-independent mode of translation initiation that bypasses the requirement for cap-dependent scanning and allows the 40S ribosome to be directly recruited to the vicinity of the initiation codon (Jackson, Hellen et al. 2010). The mRNA regions required for this direct recruitment of the 40S ribosomal subunit were termed Internal Ribosome Entry Sites (IRESs). IRES are long, highly structured sequence elements. It is well known that viral mRNAs can bypass the requirement for Initiation Factors by IRES. Viruses evolved IRES to efficiently hijack the host translational machinery overcoming the cellular block of cap-dependent translation initiation upon viral infection. Hepatitis C virus (HCV) contains one of the first discovered and characterized IRESs. The IRES of HCV regulates viral protein expression by directly recruiting the ribosome to the start site of translation (Pestova, Kolupaeva et al. 2001).

Also, some cellular IRES-containing mRNAs bypass the conventional scanning mechanism by directly recruit ribosomes (Johannes and Sarnow 1998, Hellen and Sarnow 2001, Hellen 2018). These mRNAs can be efficiently translated following environmental changes that reduce the cap-dependent translation, such as stress, mitosis and apoptosis (Holcik and Sonenberg 2005, Komar and Hatzoglou 2011). For example, hypoxia has been shown to induce a switch from cap-dependent to IRES-dependent translation (Braunstein, Karpisheva et al. 2007). The potential diversity of cellular functions regulated by IRES-dependent translation may reflect a role for distinct structural features of the IRES as well as associated IRES *trans*-acting factors (ITAFs) in directing the expression of specific mRNA classes (Truitt and Ruggero 2016).

Another recent mechanism of cap-independent translation is based on the multi-subunit initiation factor eIF3, which appears to repress or activate a specific subset of mRNAs by directly binding to stem-loop structures in their 5'UTRs (Leppek, Das et al. 2018). Also, RNA modifications employ the eIF3 complex for cap-independent ribosome recruitment, such as the N^6-methyladenosine (m^6A) modification (Meyer, Patil et al. 2015). Stress conditions, such as heat shock, selectively increase m^6A modifications in 5'UTR (Zhou, Wan et al. 2015).

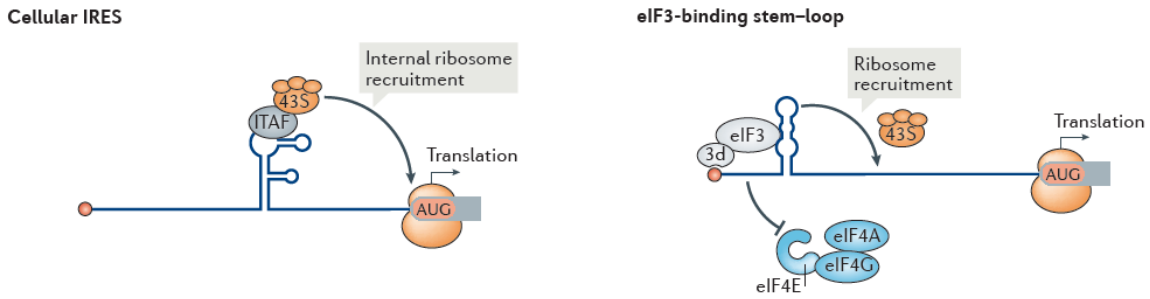

Figure 4. Cap-independent translation: cellular IRES and eIF3-binding stem loop. LEFT: Transcripts containing a structural element called internal ribosome entry site (IRES), can be selectively translated in a cap-independent manner by directly recruiting the ribosome to the 5´UTR, frequently with the aid of IRES *trans*-acting factors (ITAFs). RIGHT:structural elements in the 5´UTR have even been shown to interact with eIF3, which can internally assemble the translation machinery onto the mRNA. Figure adapted from (Leppek, Das et al. 2018).

1.1.3.4 mRNA specific translational regulation

Specific regulation of mRNA occurs through different mechanisms. Sequence and structural motifs present in mRNAs determinate their translational efficiency and translational regulation.

Of great importance in the translational control are some regulatory sequences in 5'-untranslated regions of eukaryotic mRNAs. The scanning process proceeds in 5' to 3' direction and the initiation codon is frequently the AUG triplet closet to the 5' end. The first AUG can be skipped when it is flanked by an unfavorable sequence. This process is termed "leaky scanning". When an upstream AUG (uAUG) is in frame with a downstream AUG without a stop codon, leaky scanning may occur to allow production of two protein isomers different only in the N-terminus. If the uAUG is followed by a stop codon in the same open reading frame (ORF), the translation of the upstream ORF (uORF) will interfere with the translation of the downstream ORF, because reinitiation is generally inefficient or because ribosomes stall during elongation or termination (Hinnebusch, Ivanov et al. 2016). uORFs interpose a barrier to prevent ribosomal access to initiation codon, preventing the translation of the downstream ORF and affecting gene expression and mRNA stability. Leaky scanning of an inhibitory uORF is increased under conditions of reduced translation, typically driven by impaired eIF2-GTP-Met-tRNA ternary complex formation during specific cellular stress, as amino acid deprivation and unfolded protein response (UPR) (Baird and Wek 2012). For instance, when misfolded proteins accumulate in Endoplasmic Reticulum (ER), eIF2α may be phosphorylated by PERK causing a reduction in global translation while inducing translation of uORF-containing mRNAs, including the transcription factor ATF4 (Hinnebusch 2014).

Some mRNAs contain special features that influence their lifespan or translation efficiency. These additional features are mostly found in the 5′untranslated region (5′UTR), less commonly in 3′untranslated region (3′UTR) or in main ORF (mORF). For example, hairpin secondary structures in 5'UTR are found to be a barrier in the scanning process and can be surpassed by additional helicases. Certain mRNAs that harbor long 5'UTR and high GC content require a tight control of their expression and they are particularly sensitive to eIF4A RNA helicase activity. Cap-proximal structures can also impede eIF4F binding to the cap (Hinnebusch, Ivanov et al. 2016). Another mechanism of mRNA specific translational control involves the translation initiator of short 5'UTR (TISU) element. This element allows cap-dependent but scanning-independent initiation on mRNAs with very short 5'UTR. TISU

elements appear to function in the absence of a number of the canonical initiation factors (Shirokikh and Spirin 2008) and are enriched in mRNA encoding mitochondrial proteins (Sinvani, Haimov et al. 2015).

Specific regulation of mRNA occurs also through the action of microRNA. In a conventional mode, miRNAs act through seed elements in the 3' of mRNA. miRNAs generally stimulate the degradation of mRNAs. A single microRNA may affect a number of different mRNAs (Braun, Huntzinger et al. 2012).

1.1.4 Translational control in cancer

Dysregulation of translation is associated with various diseases, including cancer (Calkhoven, Müller et al. 2002, Ruggero and Pandolfi 2003). Alterations in ribosome synthesis and activity are a defining feature of cancer cells (Silvera, Formenti et al. 2010, Loreni, Mancino et al. 2014) and most cancers are caused by dysregulation of signaling pathways that feed into the translation machinery (Ganapathi and Shimamura 2008).

Often tumors show an enlargement of the nucleolus and increased ribosomal proteins (Montanaro, Treré et al. 2008). For a long time, ribosomal amplification was considered a by-stander effect of increased growth and proliferation. It is now evident that ribosome biogenesis and activity are highly regulated. Depletion of RPs reduces tumor growth, as in the case of rpL24 deficiency in mice, which limits Myc-induced lymphomagenesis (Barna, Pusic et al. 2008), while their overexpression has been implicated in cancer progression (Shuda, Kondoh et al. 2000, Kondoh, Shuda et al. 2001, Shi, Zhai et al. 2004, Yang, Cui et al. 2016). Also, the occurrence of ribosomal protein gene mutations plays important roles in cancer development (Goudarzi and Lindström 2016). A class of inherited syndromes collectively referred to as ribosomopathies harbor mutations in distinct ribosome components and is characterized by increased cancer susceptibility (Ganapathi and Shimamura 2008).

Although global translation rates are increased in cancer cells, oncogenic signaling induces transcript-specific changes in translation. Cyclins, antiapoptotic factors, proangiogenic factors, regulators of metabolism and prometastatic factors are specifically translationally regulated in cancer (Robichaud, Sonenberg et al. 2018). Cancer cells are characterized by increased activity of signaling pathways, that regulates the expression or availability of certain translation initiation factors and, consequently, the selective translation of poorly translated mRNA (Ruggero and Pandolfi 2003, Silvera, Formenti et al. 2010, Bhat, Robichaud et al. 2015, Truitt, Conn et al. 2015, Truitt and Ruggero 2016). For example,

formation and activity of the eIF4F complex are tightly regulated by signaling pathways, as mTOR. Activation of the mTOR pathway by the PI3K-AKT signaling is consistently observed in cancer.

Many commonly mutated genes encoding key proteins that regulate signaling pathways are deregulated in human cancers, including PTEN, WNT-β-catenin, MYC, RAS-MAPK, KRAS, and others (Truitt and Ruggero 2016).

Oncogenic signaling pathways regulate activity and expression of translation initiation factors and many of them are frequently amplified or dysregulated in tumors (Table 1).

Factor	Dysregulation	Clinical correlates in cancers
eIF4E	Overexpression	• Decreased survival in breast, head and neck, liver, prostate, bladder and stomach cancers • Correlates with disease progression and aggressive subtypes in many cancers, and with resistance to chemotherapy
eIF4E	Phosphorylation	• Elevated in early stages of development of breast, colon, gastric and lung cancers • Increased in prostate cancer and correlates with androgen independence • Poor-prognosis marker in non-small-cell lung cancer
4E-BP1	Overexpression	• Inversely correlates with tumour grade • Correlates with better survival in lung and prostate cancers • Correlates with absence of lymph node and distant metastases in gastric cancer
4E-BP1	Loss	Possibly responsible for loss of translational control in 50% of pancreatic tumours
4E-BP1	Phosphorylation	Correlates with tumour grade and poor prognosis in breast, lung, ovarian and prostate cancers
eIF4G	Increased expression	• Amplification correlates with aggressive stages in lung cancer • Overexpressed in inflammatory breast cancer and cervical cancer • Correlates with poor prognosis in nasopharyngeal carcinoma
eIF4A	Increased expression	Overexpressed in lung and cervical cancer; lowered expression after radiation predicts better survival in cervical cancer
PDCD4	Decreased expression	• Associated with poor prognosis in breast, lung, colon and ovarian cancers and gliomas • Inversely correlated with advanced tumour stage in renal cell carcinoma
eIF2α	Increased expression	Correlates with aggressive lymphoma subtypes
eIF5A	Increased expression and hypusination	Correlates with poor prognosis in early-onset colorectal cancer. Overexpression of eIF5A2 correlates with local invasion in non-small-cell lung cancer and hepatocellular carcinoma
eIF6	Altered expression and function	• Regulates ribosome biogenesis and 40S–60S joining. Promotes transformation and lymphomagenesis • Elevated in colorectal cancer, head and neck carcinomas and ovarian serous carcinoma; low expression correlates with reduced disease-free survival in ovarian serous carcinoma; mediates lymphomagenesis in Shwachman–Diamond syndrome
eIF3a	Increased expression	Associated with breast, cervical, oesophagal, lung and stomach cancers
eIF3b	Increased expression	Associated with bladder, breast and prostate cancers
eIF3c	Increased expression	Associated with meningioma and testicular seminoma
eIF3h	Increased expression	Associated with breast, colon, liver and prostate cancers
eIF3i	Increased expression	Associated with breast, head and neck, and liver cancers, as well as melanoma and neuroblastoma
eIF3m	Increased expression	Associated with colon cancer
eIF3e	Decreased expression	Associated with breast, lung and prostate cancers
eIF3f	Decreased expression	Associated with breast, colon, small intestine, ovarian, pancreatic and vulval cancers and melanoma

Table 1. Dysregulation of translation initiation factors and regulators in human cancers. 4E-BP, 4E-binding protein; eIF, eukaryotic translation initiation factor; PDCD4, programmed cell death 4. (Bhat, Robichaud et al. 2015).

The eIF4F cap-binding initiation complex is the best-characterized translation complex in cancer development. eIF4F, as described before, is composed by the cap-binding protein eIF4E, the ATP-dependent RNA helicase eIF4A and the large scaffolding protein eIF4G. All three eIF4F subunits are amplified in human tumors (Silvera, Formenti et al. 2010, Ruggero 2013). Increased eIF4E levels were documented in human cancers, due to gene amplification and transcriptional upregulation (Raught and Gingras 1999, Haydon, Googe et al. 2000). eIF4E and eIF4G overexpression is sufficient to drive transformation in cell lines and spontaneous tumorigenesis in mice (Fukuchi-Shimogori, Ishii et al. 1997, Furic, Rong et al. 2010). Moreover, eIF4E-haploinsufficient mice are physiologically normal but resistant to tumor formation. eIF4E is also essential for the translation of specific mRNAs regulating reactive oxygen species that are essential for transformation and cancer cell survival *in vivo* (Truitt, Conn et al. 2015). Translational initiation of cancer cells can also be regulated by phosphorylation of eIF4 components: eIF4E phosphorylation promotes tumor development and it is elevated in several human cancers (Furic, Rong et al. 2010). The MAPK-interacting kinases (MNK1 and MNK2) phosphorylates eIF4E on a single serine residue, Ser209 in mammals (Fukunaga and Hunter 1997). Loss of eIF4F phosphorylation attenuates its oncogenic potential *in vitro* and in *vivo*. Mice expressing a nonphosphorylatable eIF4E mutant allele show delayed development of prostate and breast tumor (Furic, Rong et al. 2010).

4E-BP controls the assembly of the eIF4F complex, controlling the availability and, therefore, the activity of eIF4E. Hyperphosphorylation of 4E-BPs by mTOR inactivates them. In most tumors, the function of 4E-BP1 is compromised by reduction of its expression or phosphorylation mediated by oncogenic signaling pathways (Martineau, Azar et al. 2014) and high levels of phospho-4EBP1 were found in advanced prostate cancers (D'Abronzo and Ghosh 2018).

Oncogenic mRNAs generally have long and stable 5'UTR and are particularly sensitive to the formation of eIF4F. They are defined "eIF4E-sensitive mRNAs" (Kozak 1987). These mRNAs include cMYC, cyclin and cyclin-dependent kinases, VEGFA and FGF2. eIF4E overexpression increases also the selective recruitment to polyribosomes of various mRNA encoding cancer-promoting genes (Larsson, Li et al. 2007).

eIF3 is a multisubunit complex that binds directly to eIF4G, bringing it to the PIC. Many eIF3 subunits are overexpressed in several human cancers. However expression of eIF3f and eIF3e are downregulated during cancer development and several evidence indicate that they may

function as translational tumor suppressors (Silvera, Formenti et al. 2010). Furthermore, recently it has been demonstrated that eIF3 binds mRNA structures in the 5'UTR of mRNA relevant in oncogenic processes such as c-Jun and Btg1 (Lee, Kranzusch et al. 2015).

Sequence and structural motifs present in mRNAs determinate their translational efficiency and translational regulation. Importantly, these sequences are over-represented in oncogenic mRNAs. Sequence and structural motivs are often present in 5'UTR and they recruit RNA-binding proteins. Genes encoding cellular oncogenes and growth factors are enriched in uORFs and alternative initiation codons. uORFs can act as functional barriers (Johnstone, Bazzini et al. 2016) which interfere with the correct scanning of the downstream ORFs. Such inhibitory effects can be lost under specific stress conditions which trigger eIF2α phosphorylationand consequent inhibition of ternary complex formation, thus eliciting a global drop in translation but a specific increase in the translation of uORF-containing mRNAs (Jackson, Hellen et al. 2010). In cancer cells, the translation of uORF-containing stress-response mRNAs, such as ATF4, is promoted (Wek 2018). In fact, cancer cells must modulate their growth in a variety of many stresses, including hypoxia, metabolic and proteotoxic stress and nutrients deprivation. These stresses inhibit cap-dependent translation, due to the inhibition of eIF4E and eIF2α phosphorylation, but simultaneously increase the ability of cancer cells to respond to a stress condition. Even if there is a strong evidence for the deregulation of eIF2α phosphorylation in cancer development, its contribution to oncogenic processes is still controversial. Increased expression of aIF2α kinases are associated with increased tumor cell differentiation and in some studies, tumorigenesis in mice was promoted by inhibiting eIF2α phosphorylation (Silvera, Formenti et al. 2010). By contrast, in other cases, eIF2α phosphorylation was associated with cancer development and progression (Tejada, Lobo et al. 2009).

In addition, in the condition of cap-dependent translation inhibition, IRESs, mRNA methylation and others non-canonical mechanism of translation initiation maintain protein synthesis and enables selective translation of mRNA involves in stress response. For example, IRES-mediated translation of select transcripts as HIF1a, VEGFA and BCL-2 has been shown to support tumor growth and survival under hypoxia (Braunstein, Karpisheva et al. 2007). Also increased Myc expression can be acquired by IRES-dependent mechanisms (Jopling and Willis 2001).

Motivs or sequences in 5'UTRs that mediate the recruitment of RNA-binding proteins, alternative translation start site and sequences recognized by miRNA are particularly present in oncogenic mRNAs and drive translational control of specific mRNAs in cancer.

In summary, the understanding of the interaction among translation factors in cancer, the signaling cascades that converge on them and the resulting specialized mRNA translation could have a fundamental therapeutic value.

1.2 Eukaryotic Initiation Factor 6 (eIF6)

Eukaryotic Initiation Factor 6 (eIF6), also known as integrin β4 binding protein or p27BBP, is a protein of 245 amino acid long and it is 77% identical between humans and yeast (Biffo, Sanvito et al. 1997). eIF6 primary sequence is evolutionarily unique, with no homologs or conserved motifs. No evidence for gene duplication exists, suggesting a strong evolutionary pressure for control of the protein concentration. Human eIF6 is constitutively expressed *in vitro*, but highly modulated *in vivo*: levels of eIF6 vary among different organs. Studies on many metazoan tissues demonstrated that the protein is highly expressed in brain but has low levels in muscles. Furthermore, eIF6 shows high levels in stem or cycling cells but is almost undetectable in several post-mitotic cells (Donadini, Giodini et al. 2001).

The structure of eIF6 was resolved by X-ray crystallography: eIF6 is a highly rigid protein, organized with a cyclic fold known as pentein or star-like structure formed by five stretches of α/β subdomains arrayed about a five-fold axis of pseudosymmetry (Groft, Beckmann et al. 2000). The structure encloses a cavity that contains sixteen well-ordered water molecules, with a limited degree of motility (Figure 5). The eIF6 C-terminal sequence was not resolved in the crystal structure.

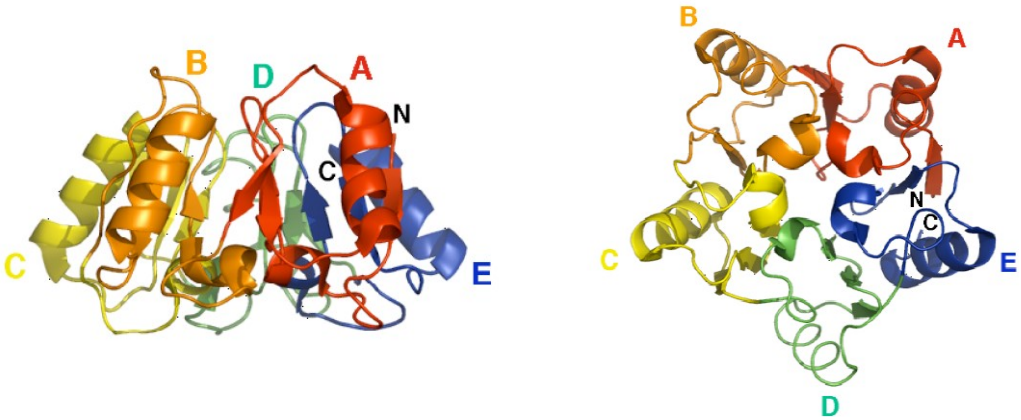

Figure 5. Unique structure of eIF6 protein. The eIF6 protein has a unique star-like structure known as pentein, which is formed by five identical subdomains (A–E) (Groft, Beckmann et al. 2000).

eIF6 has a dual function: it is necessary for the biogenesis and the maturation of 60S ribosomal subunit in the nucleus and it possesses an anti-association activity necessary for the protein synthesis in the cytoplasm (Miluzio, Beugnet et al. 2009).
Ribosome biogenesis occurs in the nucleolus and leads to the production of large and small mature ribosomal subunits and to their export to the cytoplasm. The presence of eIF6 in the nucleolus supports a role in ribosome biogenesis, both in yeast and in mammalian cells (Sanvito, Vivoli et al. 2000). Genetic evidence has shown that Tif6, the yeast homolog of eIF6, is necessary for the production of 60S subunits. Accordingly, Tif6 deletion is lethal. Human eIF6 can complement the lethal effect of Tif6 mutation (Sanvito, Piatti et al. 1999, Si and Maitra 1999, Brina, Grosso et al. 2011). rRNA pulse-chain has shown that yeast cells depleted of eIF6 have defective pre-RNA processing (Basu, Si et al. 2001, Woolford and Baserga 2013). However, the eIF6 mechanistic function in the biogenesis of the 60S subunit is still not clear.
eIF6/Tif6 shuttling from the nucleus to the cytoplasm is regulated by its phosphorylation. Two conserved amino acids in the C-terminus of eIF6 seems to have a function in the export of eIF6 from the nucleus in the cytoplasm: mutation of both Ser-174 and Ser-175 to alanine abolishes phosphorylation of Tif6 and causes a loss of viability. Furthermore, the double Tif6 mutant Ser174Ala/Ser175Ala is a constitutive nuclear protein (Basu, Si et al. 2003).

eIF6 was first identified for its anti-association activity in calf liver (Valenzuela, Chaudhuri et al. 1982) and wheat germ (Russell and Spremulli 1979). eIF6 has a relevant biochemical activity *in vitro*, preventing binding of 40S and 60S in the absence of mRNA and thus avoiding an accumulation of inactive 80S subunit. In this way eIF6 is able to keep the small and large subunit available for initiation of translation (Ceci, Gaviraghi et al. 2003). eIF6 cannot dissociate preformed 80S complexes. Structural data have identified that eIF6 binds to intersubunit space of the large subunit of the ribosome, the 60S (Klinge, Voigts-Hoffmann et al. 2011), close to sarcin-ricin loop (SRL) and ribosomal protein rpL23 and rpL24. Due to its position in the intersubunit space, that causes a steric hindrance, the binding of eIF6 to the 60S prevents its joining with the small ribosomal subunit, the 40S. The phosphorylation sites Ser174 and Ser175 are located to the accessible surface of eIF6, not involved with the interaction with the 60S subunit. Also the more flexible C-terminal sequence, that contains the Ser235 phosphorylation site, is located at the outer surface of eIF6 (Gartmann, Blau et al.

2010) (Figure 6). Anti-association activity of eIF6, as observed *in vitro*, could be relevant for translational control *in vivo.*

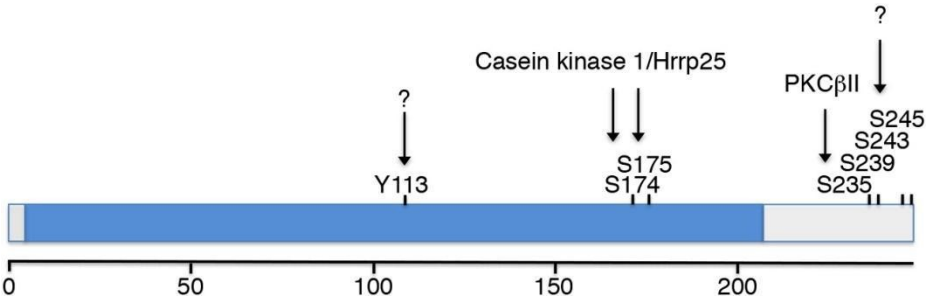

Figure 6. Phosphorylation sites identified by mass spectrometry in the eIF6 sequence. Casein Kinase 1 (tha mammalian homolog of the yeast Hrr25p) is responsible for the phosphorylation of Ser174/Ser175 in the nucleus. The C-terminal sequence of eIF6 presents multiple phosphorylation sites. PKCβII phosphorylates eIF6 on Ser235 (Brina, Miluzio et al. 2015).

1.2.1 eIF6 and translation

Mammalian and yeast eIF6 have common properties, such as the mainly cytoplasmic localization, which correlates with a role of eIF6 in the control of translation. Ceci et al showed that eIF6 is able to repress translation after binding to 60S ribosomal subunit (Ceci, Gaviraghi et al. 2003). Since the binding of eIF6 to the large ribosomal subunit is mutually exclusive to the binding of 40S subunit, in order to start translation eIF6 needs to be released from the 60S. For this event, two models have been proposed (Figure 7):

1) After the translocation of the eIF6-60S complex from the nucleus to the cytoplasm, the interaction between the Shwachman-Bodian-Diamond Syndrome protein (SBDS) and the GTPase Efl1p leads to an allosteric change of the 60S itself and causes the displacement of eIF6 protein (Wong, Traynor et al. 2011). This mechanism is relevant for the maturation of the 60S (Bussiere, Hashem et al. 2012), but it is still unclear if it is also involved in the translational control. Point mutation of eIF6 can rescue the loss of function phenotype of SBDS (Menne, Goyenechea et al. 2007).

2) The release of eIF6 is mediated by RACK/PKC complex. RACK1 is localized on the head region of the 40S subunit, in the immediate vicinity of the mRNA exit channel (Nilsson, Sengupta et al. 2004). RACK1 acts as a scaffold receptor protein for active PKC and binds to the small ribosomal subunit (Ceci, Gaviraghi et al. 2003, Volta, Beugnet et al. 2013). Activated PKC translocates from endomembrane to the small subunit, comes in close vicinity with eIF6 bound to the 60S subunit and catalyzes the phosphorylation of eIF6 on Ser235 and its subsequent release (Brina, Grosso et al. 2011).

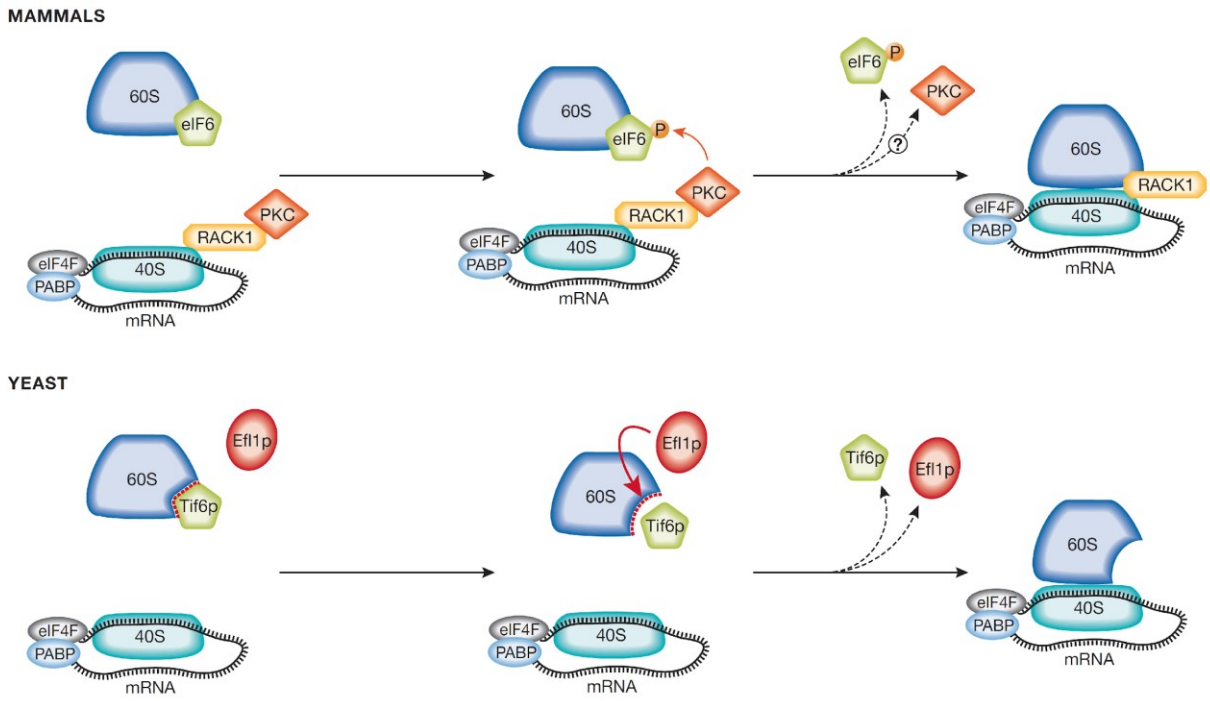

Figure 7. The two models of eIF6 release that regulate the interaction of the two ribosomal subunits, the 60S and the 40S . Two models for eIF6 release have been described for mammals and yeast. In mammalian cells, this event is modulated by the RACK1–PKC complex. PKC is recruited to the 40S subunit by RACK1 and phosphorylates eIF6 on Ser 235, leading to its release from 60S. In yeast, a structural rearrangement of the large subunit is mediated by the Efl1 protein, which facilitates the release of Tif6 from 60S and its subsequent recycling to the nucleolus. (Miluzio, Beugnet et al. 2009).

A mouse model of eIF6 haploinsufficiency shows that eIF6 is critical for translation initiation (Gandin, Miluzio et al. 2008). eIF6-null mice are embryonic lethal in mammals at the stage of pre-implantation, while heterozygous mice are viable. The 50% reduction of the eIF6 protein affects its cytoplasmic pool, and not the nuclear levels, and, accordingly, biogenesis of the 60S ribosomal subunit remains normal. In contrast, translation is impaired. The effects of eIF6 depletion are tissue specific: eIF6 heterozygous mice have smaller livers than wild-type ones and reduced white fat mass. Hepatocytes, mouse Embryonic Fibroblasts (MEFs) and adipocytes from heterozygous eIF6 mice show a delayed G1/S phase progression but are normal in size, apoptotic rate and senescence (Gandin, Miluzio et al. 2008).

The analysis of polysomal profiles of eIF6 heterozygous livers shows an increase in the 80S peak and a decrease in polysomes, confirming the role of eIF6 in the initiation of translation. eIF6 heterozygous hepatocytes and MEFs have a normal level of translation but they are not

able to regulate their response to insulin (Gandin, Miluzio et al. 2008). In conclusion, full levels of eIF6 are necessary to perform the translation program induced by insulin, *in vivo*.

1.2.2 eIF6 and metabolism

Reduction of insulin-regulated translation in eIF6 heterozygous mice results in a reduction in blood cholesterol and triglycerides levels, and in a reduction of ATP production, triglycerides and non-essential fatty acids levels in liver (Brina, Miluzio et al. 2015).

Interestingly, haploinsufficiency of eIF6 causes a decrease in translation of transcription factors that contain uORFs in their 5′-UTRs and which positively regulate lipogenesis, like ATF4 (Wang, Huang et al. 2010), C/EBPδ and C/EPBβ (Payne, Au et al. 2009).

The reduction in the translational efficiency of transcription factors involved in lipid synthesis upon eIF6 depletion causes a change in steady-state mRNA levels of enzymes involved in fatty acid synthesis and glycolysis and also their relative protein levels are reduced. eIF6 high levels correlate with insulin resistance and obesity in humans, thus its involvement in the metabolic syndrome has been partially investigated. Interestingly, eIF6 heterozygous mice have a reduced weight gain upon a high-fat diet (HFD) regimen, showing increased insulin sensitivity, reduced hepatic steatosis and circulating lipids (Brina, Miluzio et al. 2015). eIF6 heterozygosity protects from HFD-induced Non-alcoholic fatty liver disease (NAFLD).

The capability of eIF6 to regulate metabolism has been also confirmed in skeletal muscle. eIF6 haploinsufficiency leads to a reduced translation of a subset of mRNAs involved in oxidative phosphorylation, acetyl-coenzyme A (CoA) metabolism, TCA cycle, glycolysis, fatty acid metabolism and pyruvate metabolism. In particular Clarke et al. observed that depletion of eIF6 impacts functions of mitochondria, triggering ROS production and impairing mitochondrial respiration efficiency (Clarke, Ricciardi et al. 2017).

In addition, eIF6 is able to drive metabolic fluxes also in human lymphocytes. eIF6 expression is induced in activated $CD4^+$-T cells and eIF6 depletion determines a reduction in lactate secretion and ATP levels in human $CD4^+$ T-cells. In the same work it has been demonstrated that eIF6 is also essential for *in vitro* human $CD4^+$ T-cell acquisition of effector functions, such as inflammatory cytokine secretion (Manfrini, Ricciardi et al. 2017).

One important translational target of eIF6 is uORF-containing ATF4 (Brina, Miluzio et al. 2015). Interestingly, Myc-dependent activation of the PERK/eIF2α/ATF4 axis results in cellular transformation, establishing a link between ATF4 activity and tumorigenesis(Hart, Cunningham et al. 2012).

Finally, eIF6 drives the switch to glycolysis and fatty acid synthesis. One downstream target of eIF6 is Fatty acid synthase (Fasn), a critical regulator of lipid synthesis.The Warburg effect is a metabolic switch observed in cancer cells, where increased aerobic glycolysis is preferentially used as a source of energy over oxidative phosphorylation. Concordly, eIF6 depletion leads to a reduction in glycolytic flux, impairing lactate and ATP production in Malignant Pleural Mesothelioma (MPM) cells, leading to a reduction of tumoral cell growth (Miluzio, Oliveto et al. 2015).

1.2.3 eIF6 and cancer

eIF6 is overexpressed in several human tumors, such as head and neck cancer (Rosso, Cortesina et al. 2004), lung metastasis (Martin, Sanz et al. 2008), acute promyelocytic leukemia (Harris, Ozpolat et al. 2004). eIF6 is overexpressed in subsets of luminal breast cancer due to gene amplification (Gatza, Silva et al. 2014) and in some patients of colorectal cancer due to increased transcription (Sanvito, Vivoli et al. 2000). Copy gains of eIF6 are observed in many cancer patients. eIF6 is both overexpressed and hyperphosphorylated in Malignant Pleural Mesothelioma (Miluzio, Oliveto et al. 2015). eIF6 availability limits oncogene-induced transformation: eIF6 heterozygous mouse embryonic fibroblasts transduced with dominant negative p53 tumor suppressor plus H-ras^{V12} or with Myc plus H-ras^{V12} displayed a strong reduction in the formation of transformed colonies compared to the wild-type counterparts and impairment in G1/S cell cycle progression (Gandin, Miluzio et al. 2008). *In vivo*, haploinsufficiency of eIF6 levels is sufficient to increase the survival of a mouse model of Eμ-Myc driven B-cell lymphomagenesis from 4 to 9 months, in the absence of negative side effects (Miluzio, Beugnet et al. 2011).

1.2.4 Ser235 phosphorylation site in eIF6 activity

In the mammalian model of eIF6 release, the PKCβII kinase phosphorylates eIF6 on its unique consensus site Ser235, leading to its release from the 60S.

Corroborating this model, PMA-stimulated translation is associated to the phosphorylation of eIF6 at Serine 235 and a Ser235Ala mutant of eIF6 is unable to be released by 60S *in vitro* (Ceci, Gaviraghi et al. 2003), impeding growth factor-stimulated translation. eIF6 heterozygous MEFs reconstituted with wt eIF6 show increased translation in response to

insulin, but not if they are reconstituted with a Ser235Ala mutant of eIF6 (Gandin, Miluzio et al. 2008).

Ser235 is important also in the capability of eIF6 to regulate cellular metabolism: as described before, eIF6 regulates the Fasn mRNA levels. In Ear mesenchymal stem cells (EMSC) differentiated to adipocytes overexpression of eIF6 wt stimulates the expression of Fasn, in contrast, Fasn levels are not increased by Ser235Ala mutant (Brina, Miluzio et al. 2015).

eIF6 plays a critical role in cancer. As shown in web-based databases, Ser235 and the eIF6 C-terminus are phosphorylated in various cancer cells. In Myc-driven B-cell lymphoma samples, eIF6 is phosphorylated by PKCβII, but not by mTORC1 (Miluzio, Beugnet et al. 2011).

eIF6 heterozygous transformed fibroblasts with DNp53 plus H-rasV12 overexpressing a Ser235Ala mutant of eIF6 are resistant to oncogenic transformation *in vitro* and have an impaired growth *in vivo* as xenografts (Miluzio, Beugnet et al. 2011).

Recent studies have shown that eIF6 is overexpressed and hyperphosphorylated in human Malignant Pleural Mesothelioma (MPM). eIF6 hyperphosphorylation correlates with lower MPM patients survival. Concordly, eIF6 is overexpressed and hyperphosphorylated in MPM cell lines and the partial depletion of eIF6 or inhibition of PKCβII activity, using the PKCβ inhibitor Enzastaurin, restrict the growth of MPM cancer cells, *in vitro* as *in vivo* as xenografts (Miluzio, Oliveto et al. 2015).

Altogether, these evidence suggest a critical role for Ser235 residue in eIF6 functional activity and in its pro-tumorigenic activity.

1.3 Anaplastic Large Cell Lymphoma

Lymphomas are typically solid tumors, usually developing within lymph nodes but they can occur in any tissue (Shankland, Armitage et al. 2012). The classification of lymphoma comprises a vast range of subtypes belonging to either the Hodgkin (HL) or the Non-Hodgkin (NHL) category, identified by their morphological and cellular appearances. Lymphomas are further classified into T, B, null or even natural killer cell types. The majority of NHL is B-cell-derived accounting for 85-90 % of cases, the remaining, for the most part, is of a T-cell origin (Shankland, Armitage et al. 2012). Peripheral lymphoma (PTCL) is defined as a group of aggressive lymphomas. It is classified as a subtype of NHL, specifically affects T-cells, and results when T-cells develop and grow abnormally. The peripheral T cell lymphomas are considered to origin in the lymphoid tissues outside of the bone marrow. PTLC have a poor prognosis with a 5-year overall survival of 15-30% (Foss, Zinzani et al. 2011).

Anaplastic Large Cell Lymphoma (ALCL) is a rare peripheral T-cell lymphoma belongs to the Non-Hodgkin subtype. ALCL comprises approximately 3% of all adult NHLs and 10% to 20% of childhood lymphomas (Mora, Filippa et al. 2003). ALCLs have an unusual immunophenotype: tumor cells typically express CD30 indicating an activated T cell phenotype, but they rarely express a T cell receptor (TCR), they are often positive for CD4 but in the absence of CD8. In many cases, tumor cells do not express T-cell-associated antigens and hence are defined as "null-cells" (Krenacs, Wellmann et al. 1997, Medeiros and Elenitoba-Johnson 2007).ALCLs comprises 3 entities: Anaplastic Lymphoma kinase (ALK)-positive ALCL, ALK-negative ALCL and primary cutaneous ALCL (pcALCL) (Salaverria, Beà et al. 2008). The first two are systemic diseases, whereas the last presents in the skin.

ALK- and pcALCL diseases occur mainly in adults whereas ALK+ ALCL presents mainly in children and young adults and represents approximately 20% of childhood lymphomas. ALK+ ALCL occurs more frequently in males (Ferreri, Govi et al. 2013).

1.3.1 ALK+ Anaplastic Large Cell Lymphoma

ALK-positive ALCL is characterized by aberrant expression of anaplastic lymphoma kinase (ALK) due to rearrangements of the ALK gene which produces ALK fusion proteins.

ALK-positive ALCLs are characterized by generally large cells with a horseshoe-shaped nucleus that surrounds a prominent central Golgi zone and abundant cytoplasm. The tumor cells express an ALK fusion protein and also express CD30 (Xing and Feldman 2015).

The ALK protein, also known as CD246, belongs to a sub-family of the insulin receptor superfamily of tyrosine kinases. ALK gene encodes for a 177 kDa protein that undergoes N-linked glycosylation, resulting in the 220 kDa mature protein that is expressed on the cell surface and capable of being tyrosine phosphorylated (Chiarle, Voena et al. 2008). Structurally, ALK comprises of an extracellular domain, a transmembrane domain, and an intracellular domain that includes the tyrosine kinase region (Hallberg and Palmer 2013). Normal lymphocytes lack expression of ALK. Physiological ALK expression is restricted to the central and peripheral nervous system and it is associated with the development of the nervous system and its diminishes in all tissues after birth (Iwahara, Fujimoto et al. 1997, Hallberg and Palmer 2013).

The ALK locus has recently been identified as a hotspot for activating translocation events in many types of cancer, with over 22 different translocation partners identified (Hallberg and Palmer 2013).

Among these, the most predominant is the Nucleophosmin 1 (NPM1), which with ALK produces the fusion proteins NPM-ALK, expressed as a consequence of the t(2;5)(p23;q35) translocation (Morris, Kirstein et al. 1994) (Figure 8). NPM1, a nucleolar phosphoprotein, shuttles between the nucleus and cytoplasm. Due to oligomerization motif in NPM protein, NPM-ALK fusion protein is capable of forming homodimers, which can auto-phosphorylate and form a signal transduction complex activating multiple signaling pathways (Palmer, Vernersson et al. 2009).

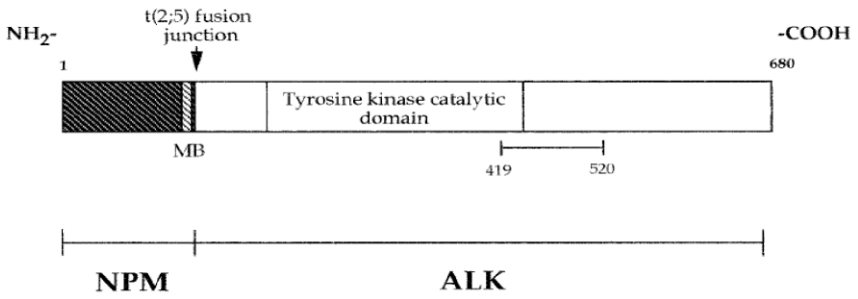

Figure 8. Schematic diagram of the NPM-ALK fusion protein. As a result of the 2:5 translocation, the amino-terminal portion of NPM is fused to the intracellular region of ALK (Pulford, Lamant et al. 1997).

A direct role for NPM-ALK in cellular transformation has been demonstrated *in vitro* with immortalized MEFs and *in vivo* (Bai, Dieter et al. 1998, Chiarle, Gong et al. 2003, Chiarle, Simmons et al. 2005, Zhang, Wei et al. 2013).

In the last years, the generation of mouse models of ALK+ tumors has provided a setting in which to examine the oncogenic events that promote tumor development and the signaling pathways involved in tumor progression.

Transgenic mouse models were generated using different lineage-restricted promoters. In particular, using CD4-restricted promoters, transgenic mice have been established in which NPM–ALK expression leads to T-cell transformation (Turner, Tooze et al. 2003, Chiarle, Simmons et al. 2005). The CD4 transgene cassette allows the expression of the target protein in all T-cells, including early progenitor thymocytes (CD4+/CD8+) and single positive T-cells (CD4+/CD8- and CD4-/CD8+). Expression of NPM-ALK in mice from the T-cell specific CD4 promoter gives rise to thymic lymphomas after a short period of latency. In NPM-ALK transgenic mice, fusion protein is detected in the cytoplasm and nucleus, a pattern similar to that observed in human NPM-ALK+ cells and histological analysis show that the transgenic NPM-ALK protein is localized in cortical and medullary thymocytes, in lymphocytes within the interfollicular areas of lymph nodes, and in the T-cell areas of the splenic white pulp (Chiarle, Gong et al. 2003).

In these mice, NPM–ALK engages a series of adaptor molecules in both premalignant and transformed mouse T-cells, and activates multiple pathways that are similar to human ALCL (Chiarle, Gong et al. 2003), including signal transducer and activator of transcription 3 (STAT3), which is required for the maintenance of the neoplastic phenotype (Chiarle, Simmons et al. 2005).

Signalling pathways activated through NPM-ALK, such as phospholipase Cγ (PLCγ), Janus kinase (JAK)-STAT, PI3K-AKT, mTOR, Wnt, sonic hedgehog (SHH), interleukins (ILs), JUNB, Myc, CRKL-C3G (also known as RAPGEF1)-RAP1 GTPase and MAPK signaling cascades and finally GRB/SHC/IRS1-VAV1-CDC42 pathway (Palmer, Vernersson et al. 2009, Choudhari, Minero et al. 2016) affect cell growth, transformation and antiapoptotic signaling. Recent studies have demonstrated that also the AP-1 members, JUN and JUNB,

control lymphoma development and tumor dissemination through transcriptional regulation of platelet-derived growth factor receptor-β (PDGFRB) (Laimer, Dolznig et al. 2012).

Aberrant expression of anaplastic lymphoma kinase (ALK) due to rearrangement of the ALK gene is also present in a subgroup of non–small cell lung cancers. It causes a specific type of adenocarcinoma of the lung, namely ALK-positive lung cancer (Soda, Choi et al. 2007, Koivunen, Mermel et al. 2008).

In the past years, several ALK inhibitors have been developed: in 2011 Crizotinib was identified as a potent ALK inhibitor and approved for the treatment of advanced non-small cell lung cancer (NSCLC) harboring ALK rearrangements. However, disease relapses in the majority of crizotinib-treated patients within one year, under various mechanisms including ALK fusion gene amplification, secondary ALK kinase domain mutations, activation of bypass signaling pathways and others (Isozaki, Takigawa et al. 2015). Second generation (ceritinib, alectinib, PF-06463922, X-396, AP26113 and TSR-011) and third generation (Lorlatinib) ALK inhibitors were developed (Wu, Savooji et al. 2016).

The determination of the molecular mechanisms that occur in NPM-ALK mediated tumorigenesis is fundamental to the determination of new possible pharmacological targets. The simultaneously blocking of ALK and these downstream targets could increase the efficacy of ALK inhibitors. In this context, a recent work has shown that the combined ALK/mTOR inhibition (obtained using crizotinib, alectinib and lorlatinib as ALK inhibitors and temsirolimus as mTOR inhibitor) leads to a specific synergistic effect, impairing the proliferation of ALK+ cells and their capability to form colonies *in vitro*, as their growth *in vivo* as xenografts (Redaelli, Ceccon et al. 2016). This work underlines the active role played by translation in ALK+ cells and the therapeutic value of inhibition of the translation machinery.

A large-scale functional genetic study, aimed to characterize mechanisms of resistance to ALK inhibition in ALK-dependent lung cancer cells, showed that PKC activation alone is sufficient to confer resistance to ALK inhibitors, whereas combined ALK and PKC inhibition restored sensitivity in ALK+ cancer cells (Wilson, Johannessen et al. 2015). The fact that PKC drives resistance to ALK inhibitors raises the question of the meaning of eIF6 phosphorylation in ALK-driven T cell lymphomas.

2. Aim

eIF6 (eukaryotic Initiation Factor 6) is a mTORC1-independent oncogenic translation factor, which is required for regulation of translation in the cytosol, working as an anti-association factor: it binds 60S subunit averting its premature joining with 40S in absence of mRNA. To allow ribosomal joining and thus translation, eIF6 needs to be released from 60S subunit. eIF6 anti-association activity is modulated by phosphorylation: PKCβII kinase phosphorylates eIF6 on its unique consensus site Ser235, leading to eIF6 release from the 60S and to the consequent formation of translationally active 80S complexes. Corroborating this model, a Ser235Ala mutant of eIF6 is unable to be released by 60S *in vitro*, impeding growth factors stimulated translation. These data suggest a critical role for this residue in eIF6 functional activity. eIF6 is overexpressed and hyperphosphorylated in several cancer cell lines and human tumors. eIF6 dephosphorylation slows cancer cell growth and overexpression of mutant $eIF6^{SA}$ in murine fibroblasts causes oncogenic resistance *in vitro* and impaired growth *in vivo* as xenografts. All these evidence suggest a fundamental role for Ser235 phosphorylation in the pro-tumorigenic activity of eIF6. eIF6 is hyperphosphorylated in lymphomas and in cells with NPM-ALK translocation. In addition, recent works have demonstrated that resistance to ALK inhibition is driven by PKC activation.

We hypothesize that the phosphorylation of Ser235 is fundamental for eIF6 activity, both in physiological and pathological contexts, particularly in ALK mediated T-cell lymphomagenesis. To provide genetic evidence for the relevance of eIF6 phosphorylation on Ser235, we developed a conditional $eIF6^{SA}$ Knock-In mouse model, in which Ser235 is replaced by an Ala. This mouse model was first crossed to CMV-Cre mice, to investigate the role of eIF6 phosphorylation in mammalian development, and then to the NPM-ALK transgenic mouse model. In short, we have developed an array of models and experiments that unequivocally demonstrate for the first time that eIF6 phosphorylation plays an essential role in mammalian development, cell homeostasis and is rate-limiting for T-cell lymphomagenesis *in vivo*.

3. Results

3.1 eIF6 phosphorylation on Ser235 is essential for mammalian development

In order to genetically address the *in vivo* relevance of eIF6 phosphorylation on Ser235, we generated a conditional eIF6^{SA} Knock-In mouse model, taking advantage of gene targeting strategy (Figure 9A). A targeted mutational approach, based onCre-lox recombinase technology, was used: after Cre recombinase-mediated excision of floxed sequence, a mutant form of eIF6 in which Ser235 is replaced by an Ala is expressed.

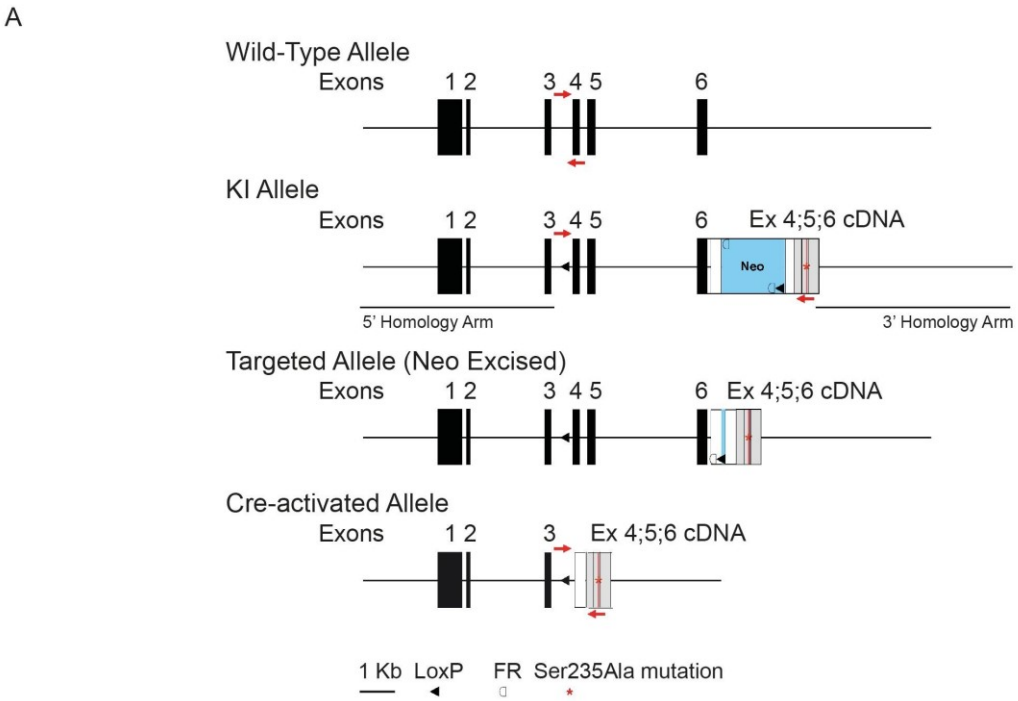

Figure 9. Generation of conditionally activatable knock-in allele. A) From top to bottom: genomic locus encoding eIF6 protein; KI targeting construct; targeted locus in the embryonic stem cells (ES) after removal of the neomycin cassette; eIF6^{SA} allele following Cre recombinase-mediated activation. Positions of genotyping primers are indicated by arrows.

We crossed KI mice with ubiquitous CMV-Cre mice to obtain the constitutive expression of the mutant form of eIF6. Cre-driven excision of floxed sequence was confirmed by PCR genotyping (Figure 10A). eIF6$^{SA/+}$ embryos revealed no significant changes in embryonic development and eIF6$^{SA/+}$ mice were born at normal Mendelian ratios (Figure 10C, D). Intercrossing of eIF6$^{SA/+}$ mice failed to produce eIF6$^{SA/SA}$ live offspring and eIF6$^{SA/SA}$ aborts were found from embryonic day E10.5 to E13.5 (Figure 10B, C, D), indicating that eIF6^{SA}homozygosity causes embryonic lethality after gastrulation. To examine the effect of

the eIF6 mutation on early embryogenesis, we isolated blastocysts at 3.5 days post coitum (dpc). eIF6$^{SA/SA}$ blastocysts were recovered (Figure 10B, C). However, when cultured *in vitro* for five days on gelatin-coated plates, they failed to hatch and enlarge the inner cell mass, indicating a defect in *in vitro* development (Figure 10E).

The embryonic lethality caused by eIF6^{SA} homozygosity is consistent with a fundamental role for eIF6 phosphorylation in mammalian development.

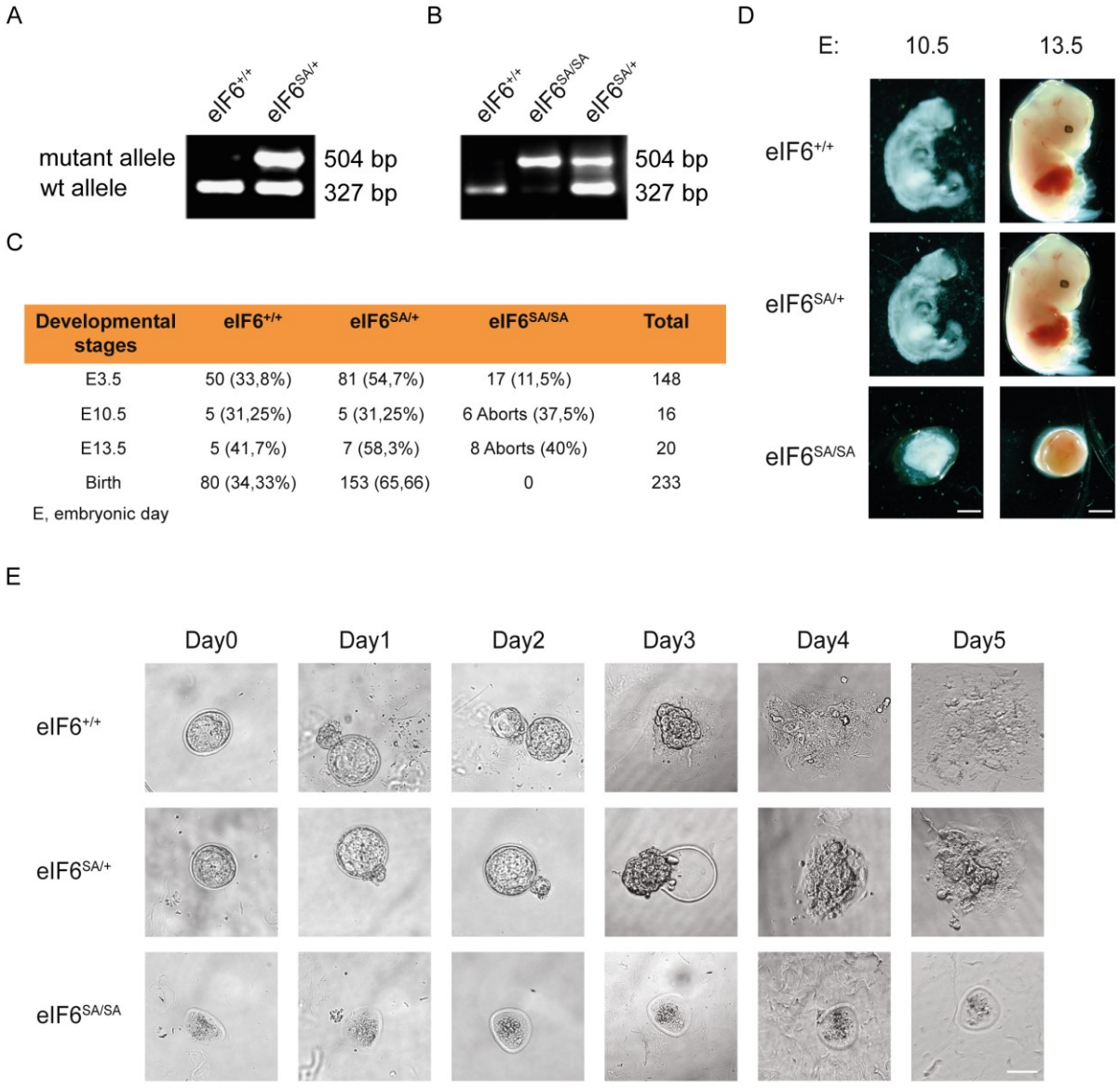

Developmental stages	eIF6$^{+/+}$	eIF6$^{SA/+}$	eIF6$^{SA/SA}$	Total
E3.5	50 (33,8%)	81 (54,7%)	17 (11,5%)	148
E10.5	5 (31,25%)	5 (31,25%)	6 Aborts (37,5%)	16
E13.5	5 (41,7%)	7 (58,3%)	8 Aborts (40%)	20
Birth	80 (34,33%)	153 (65,66)	0	233

E, embryonic day

Figure 10. eIF6 phosphorylation on Ser235 is essential for mammalian embryonic development. A) PCR-based genotyping (at weaning) of wild-type and heterozygous mice produced by intercrossing eIF6$^{SA/+}$. Wild-type and mutant alleles generate PCR products of 327 bp and 504 bp, respectively. B) PCR-based genotyping (at E13.5) of eIF6$^{+/+}$, eIF6$^{SA/+}$ embryos and eIF6$^{SA/SA}$aborts. C) Genotypes of offspring and embryos (E) at 3.5, 10.5 and at 13.5 dpc from eIF6$^{SA/+}$ intercross:no viable eIF6$^{SA/SA}$ embryos after implantation and no eIF6$^{SA/SA}$ offsprings were found. D) Gross morphology of eIF6$^{+/+}$, eIF6$^{SA/+}$ and eIF6$^{SA/SA}$ E10.5 and E13.5 embryos. Scale bar=2 mm for E10.5; scale bar=15 mm for E13.5. E).

Blastocysts from eIF6$^{SA/+}$ intercrosses were cultured *in vitro* and observed by phase-contrast microscopy on five consecutive days. Representative images of eIF6$^{+/+,}$ eIF6$^{SA/+}$ and eIF6$^{SA/SA}$ genotypes are shown. Scale bar=20 μm.

We decided to investigate whether heterozygous expression of eIF6^{SA} mutant could affect mouse growth after birth. At three months of age, heterozygous mice for the mutation of eIF6 were viable and indistinguishable from age-matched wt littermates. Measures of organs weights at autopsy revealed no differences between eIF6$^{SA/+}$ and eIF6$^{+/+}$ mice (Figure 11A). Qualitative Western Blot analysis of eIF6 levels showed that the Ser235Ala mutation did not affect eIF6 protein levels, in all analyzed tissues (Figure 11B).

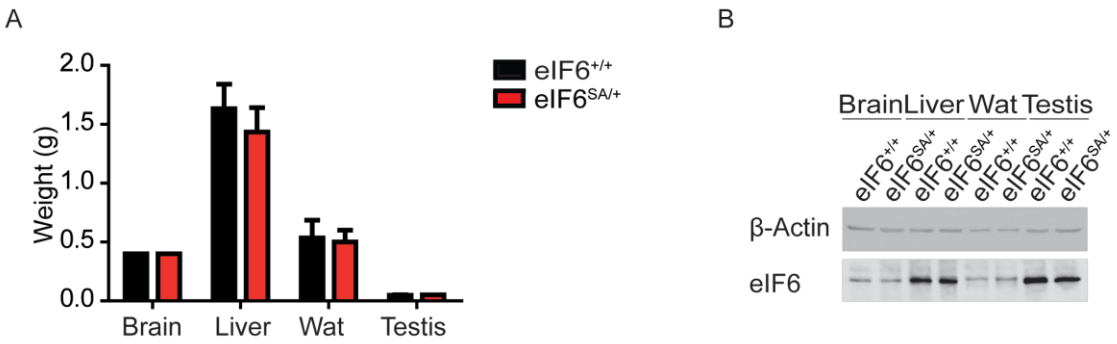

Figure 11. eIF6^{SA} heterozygosity does not impair mice growth. A) No differences in weight of indicated organs are observed in eIF6$^{+/+}$ and eIF6$^{SA/+}$ mice. Values represent mean ± SD (n=6 for genotype). B) Representative Western Blot analysis of eIF6 protein expression in all indicated organs. Data are normalized with β-Actin. eIF6 protein level is equal between eIF6$^{+/+}$ and eIF6$^{SA/+}$ mice.

We explored further primary MEFs from eIF6$^{SA/+}$ mice. eIF6$^{+/+}$ and eIF6$^{SA/+}$ MEFs were similar in cell size and in eIF6 protein levels (Figure 12A, B). We analyzed the effects of eIF6 mutation on cell cycle progression in highly proliferative cells, after synchronization by serum starvation and stimulation by serum refeeding. Data obtained by 5-Bromodeoxyuridine (BrdU) pulse labeling showed no differences in eIF6$^{SA/+}$ MEFs compared to wt ones (Fig. 12C). Since it has been demonstrated that the partial loss of eIF6 reduces insulin-stimulated translation (Gandin, Miluzio et al. 2008, Brina, Miluzio et al. 2015), we checked whether eIF6 mutant could affect the global translational rate too. We found no evidence for globally altered polysome profiles in eIF6$^{SA/+}$ cells under insulin stimulation, as shown by a representative experiment in Figure 12D.

Taken together, these findings demonstrate that the heterozygous expression of the Ser235Ala mutant is fully compatible with normal organismal development and physiology *in vivo*, as well as for cell cycle progression and normal translation *in vitro*.

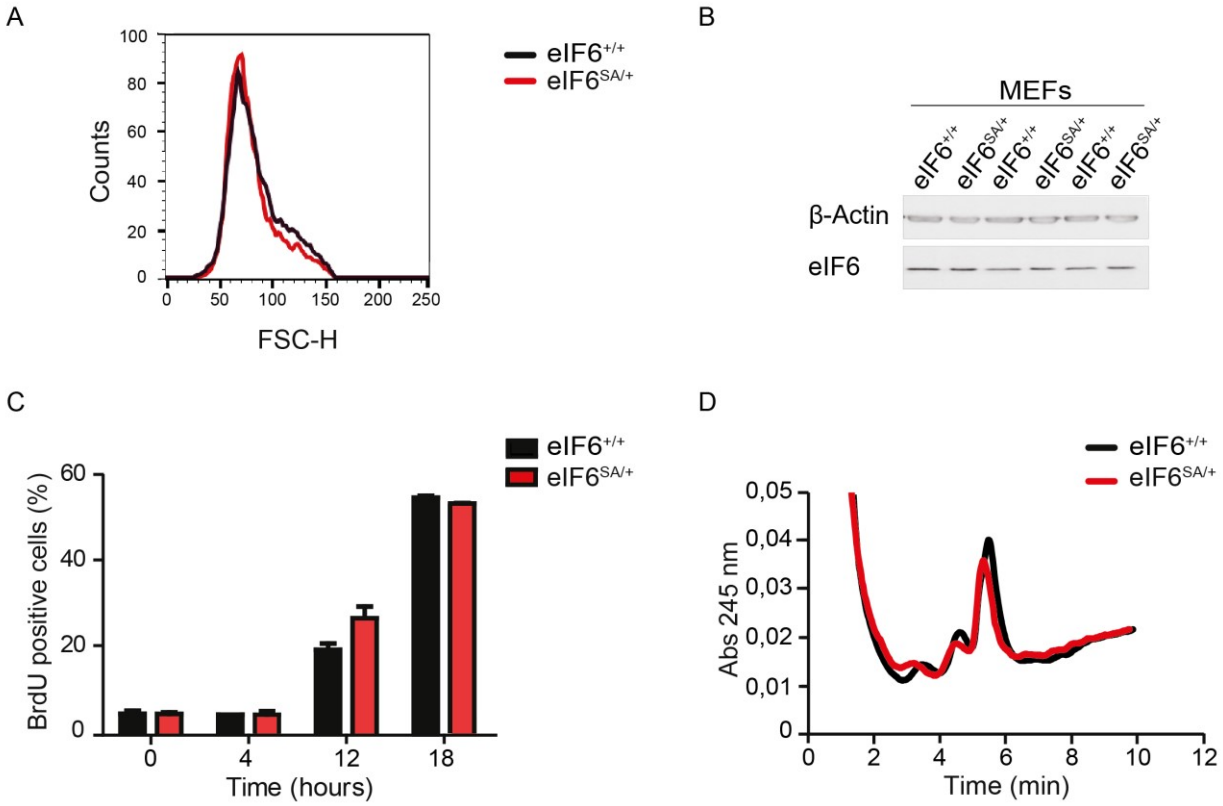

Figure 12. Characterization of eIF6$^{SA/+}$ MEFs reveals normal cell cycle progression and protein synthesis. A) Representative FACS analysis of eIF6$^{+/+}$ and eIF6$^{SA/+}$ MEFs. No differences in cell size were found. B) Representative Western Blot analysis of eIF6 expression in eIF6$^{+/+}$ and eIF6$^{SA/+}$ MEFs, normalized with β-Actin. eIF6 protein level is equal between eIF6$^{+/+}$ and eIF6$^{SA/+}$ MEFs. C) BrdU labeling of synchronized cells at the indicated time point after serum stimulation. No significant differences in S-phase entry distribution are observed between eIF6$^{+/+}$ and eIF6$^{SA/+}$ MEFs. D) Representative polysome profile of eIF6$^{+/+}$ and eIF6$^{SA/+}$ MEFs.

3.2 eIF6^{SA} mutation affects eIF6 phosphorylation

Given the detrimental effects of the homozygous eIF6 mutation in mammalian development, we decided to address the role of eIF6^{SA} mutation at the cellular level, without the bias of the partial expression of eIF6 wt protein. Thus, we generated a conditional system of eIF6^{SA} homozygosity in MEFs: KI homozygous MEFs were immortalized and transduced with a retrovirus expressing an inducible Cre-ER^{T2} recombinase. Treatment with 4-hydroxytamoxifen (4-OHT) allowed the activation of the Cre recombinase, generating eIF6$^{SA/SA}$ MEFs (Figure 13A,B).

This cellular model allowed us to analyze the phosphorylation pattern of eIF6 in condition of Ser235Ala mutation. 2-D electrophoresis on wt MEFs displayed several focused spots compatible with eIF6 phosphorylation sites. eIF6$^{SA/SA}$ MEFs showed a single focused spot, indicating that eIF6 phosphorylation is strongly reduced in eIF6$^{SA/SA}$ MEFs (Figure 13C).

In the mammalian model of eIF6 anti-association activity, the PKCβII kinase phosphorylates eIF6 on its unique consensus site Ser235, leading to its release from the 60S (Miluzio, Beugnet et al. 2009).

Measurement of eIF6 binding sites by Ribosomes Interaction Assay (iRIA) showed that eIF6$^{SA/SA}$ MEFs have less binding sites for exogenous biotinylated eIF6, suggesting a stronger interaction between mutant eIF6^{SA} protein with the 60S ribosomal subunit (Figure 13D). This result corroborates the fundamental role of Ser235 phosphorylation in eIF6 release from the 60S.

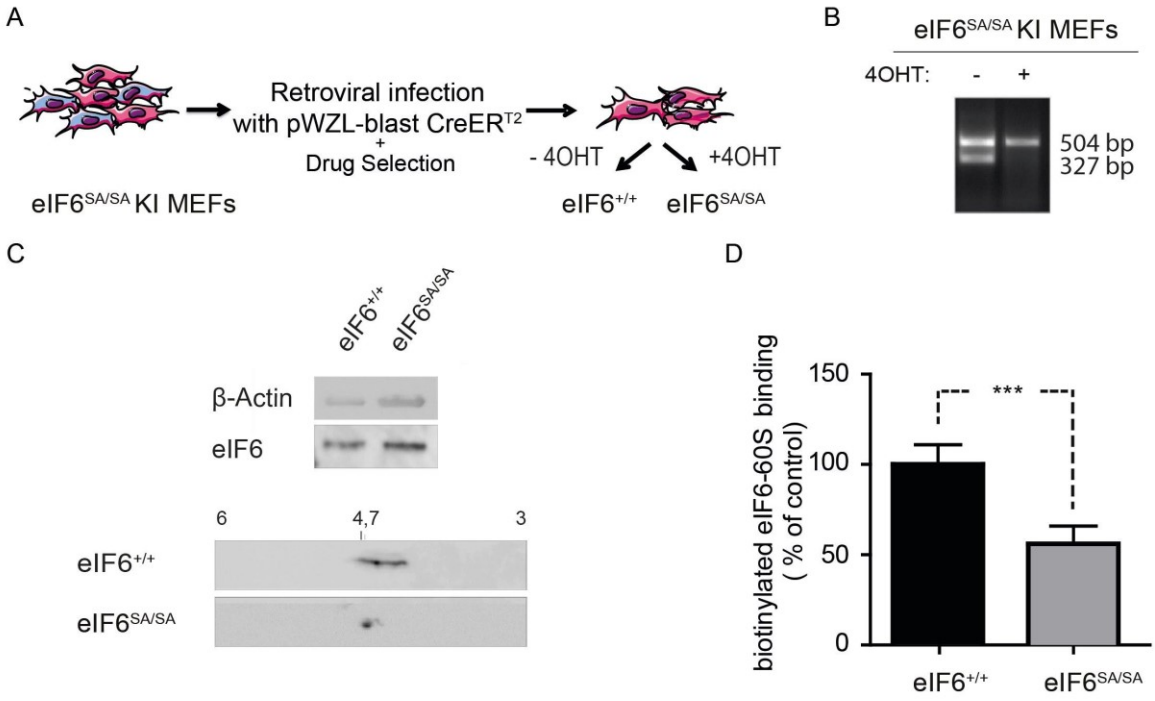

Figure 13. eIF6^{SA} homozygosity causes loss of eIF6 phosphorylation and impairs 60S availability. A) Scheme of *in vitro* eIF6$^{SA/SA}$ MEFs generation: eIF6^{SA} KI homozygous MEFs were transduced with a 4OHT-inducible CreER^{T2} recombinase. After 4-OHT treatment, eIF6$^{SA/SA}$ MEFs were generated. B) PCR-based genotyping of eIF6$^{+/+}$ and eIF6$^{SA/SA}$ MEFs. C) Up: representative Western Blot analysis of eIF6 expression in eIF6$^{+/+}$ and eIF6$^{SA/SA}$ MEFs, normalized with β-Actin. eIF6 protein level is equal between eIF6$^{+/+}$ and eIF6$^{SA/SA}$ MEFs. Bottom: representative 2D-Gel electrophoresis of eIF6 protein from eIF6$^{+/+}$ and eIF6$^{SA/SA}$ MEFs: S235A mutation causes loss of eIF6 phosphorylation. D) Measurement of eIF6 binding sites by iRIA technique shows that eIF6$^{SA/SA}$ MEFs have less binding sites for exogenous biotinylated eIF6. Representative technical triplicate experiment of n=3 biological replicates are presented in a graph as mean ± SD. ***P<0.001.

3.3 eIF6 phosphorylation modulates cell proliferation and premature cellular senescence

eIF6$^{SA/SA}$ MEFs showed markedly reduced proliferation, compared to wt ones, suggesting that eIF6 phosphorylation on Ser235 is essential for cell proliferation *in vitro* (Figure 14A).

To determine whether eIF6^{SA} protein has any effects on the cell cycle, we examined the cell cycle profile of MEFs by flow cytometry after BrdU pulse-labeling. eIF6$^{SA/SA}$ MEFs showed impaired G1/S progression, as shown in Figure 14B.

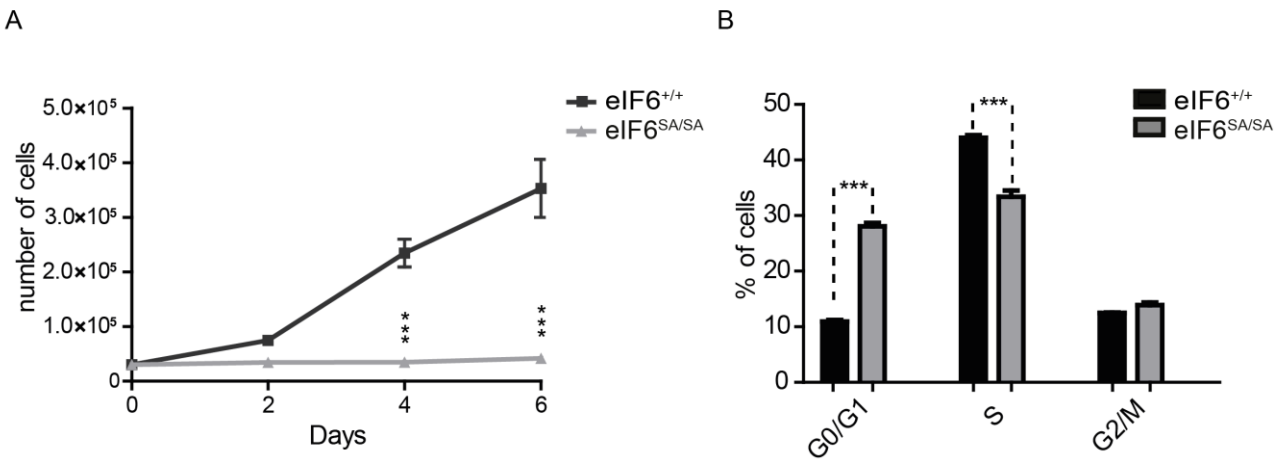

Figure 14. eIF6^{SA} causes impaired cell proliferation and G1/S progression. A) eIF6$^{SA/SA}$ MEFs show a markedly reduced proliferation. eIF6$^{+/+}$ and eIF6$^{SA/SA}$ MEFs were seeded and cell numbers were counted at the indicated time points. Values are mean ± SD of three independent experiments. ***P<0.001. B) FACS analysis of eIF6$^{+/+}$ and eIF6$^{SA/SA}$ MEFs. eIF6 mutation impairs G1/S progression. Data are presented in a graph as mean ± SD (n=3 independent experiments). ***P<0.001.

Reduced growth of eIF6$^{SA/SA}$ MEFs could be caused by increased cell death or senescence. Increased apoptosis was not observed (data not shown). However, eIF6$^{SA/SA}$ MEFs exhibited full-blown characteristics of cellular senescence, such as flattened large shape and positive senescence-associated β-galactosidase (SA β-gal) staining, compared with wt MEFs (Figure 15A,B).

The induced senescence observed in eIF6$^{SA/SA}$ MEFs was associated with a robust induction of the cyclin-dependent kinase inhibitor p21CIP1/WAF1 (thereafter referred to as p21). Commonly, cellular senescence requires the function of multiple tumor suppressors including p53 and p16^{INK4A} (thereafter referred to as p16) (Serrano, Lin et al. 1997, Schmitt, Fridman et al. 2002). We examined the expression of these additional senescence-molecular markers in eIF6$^{SA/SA}$ MEFs. Notably, we found that p16 and p53 protein levels in eIF6$^{SA/SA}$ MEFs were comparable to levels in wild-type, suggesting that in our model p21 can induce senescence independently from p53 and p16 activation (Figure 15C).

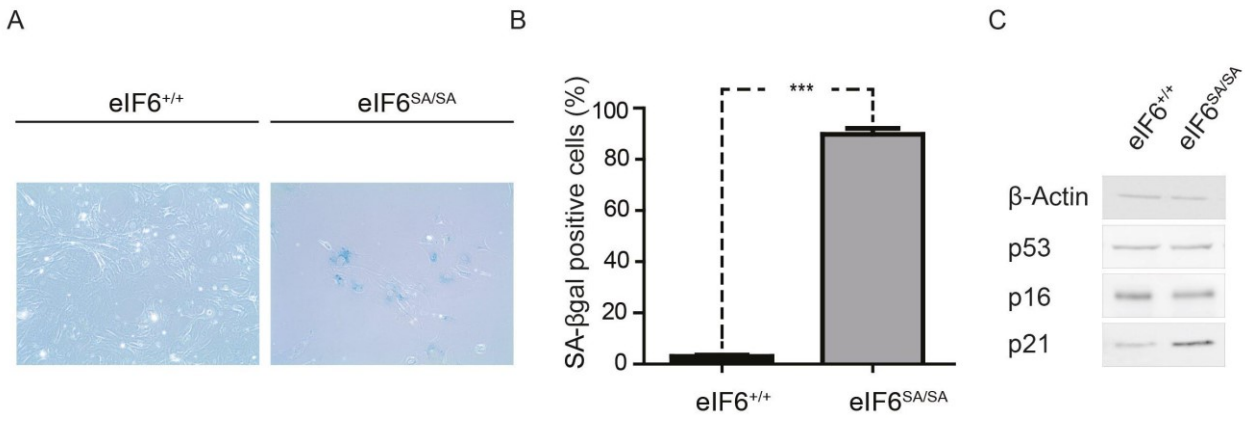

Figure 15. *In vitro* generated eIF6$^{SA/SA}$ MEFs have a senescence-like phenotype. A) Representative bright-field images of SA-β galactosidase staining performed on eIF6$^{+/+}$ and eIF6$^{SA/SA}$ MEFs. Scale bar=20 μm. B) Data are presented in a graph as mean ± SD of at least three independent experiments. ***P<0.001. C) Western blot analysis for p53, p21 and p16 in eIF6$^{+/+}$ and eIF6$^{SA/SA}$ MEFs. P21 expression is higher in eIF6$^{SA/SA}$ MEFs compared to wt ones. Data are normalized with antibody anti β-Actin.

We performed a rescue experiment in which KI homozygous MEFs, expressing the inducible Cre-ER^{T2} recombinase, were re-supplemented with control GFP, or WT and Ser235Ala eIF6 proteins. Analysis of eIF6 protein levels indicated that both eIF6 forms were overexpressed at similar levels (Figure 16A). Of note, after 4-OHT treatment, we observed that high levels of the mutant form of eIF6 did not rescue cell proliferation (data not shown) nor the increased SA-βgal positivity, as for GFP control. On the contrary, high levels of the eIF6 wild-type form did (Figure 16B,C). These results indicate that the senescence phenotype observed in eIF6$^{SA/SA}$ MEFs can be ascribed specifically to eIF6 Ser235Ala mutation. Taken together, these data suggest that eIF6 phosphorylation on Ser235 is essential for cell growth and proliferation and that its inhibition modulates premature cellular senescence *in vitro*.

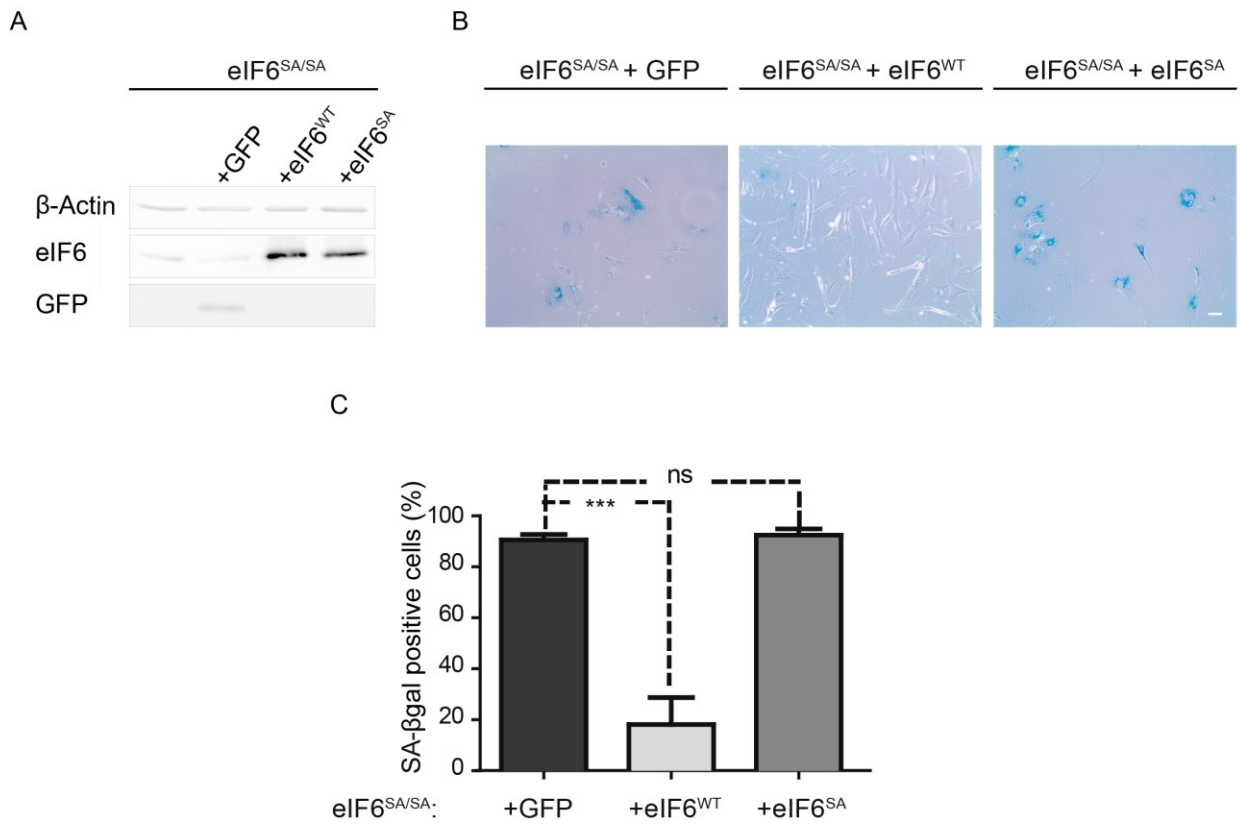

Figure 16. Reconstitution of eIF6 wt, but not of eIF6^{SA} mutant, rescues premature cellular senescence. A) Representative Western Blot analysis of eIF6 levels in eIF6 WT and SA transduced MEFs, normalized with β-Actin. GFP transduced MEFs were used as control. B) The viability of eIF6$^{SA/SA}$ MEFs is rescued by transducing wild-type but not SA protein. Representative bright-field images of SA-β gal staining are reported. Scale bar=20 μm. C) Quantification of SA-β gal positive MEFs. Results are presented as mean ± SD from a representative experiment performed in triplicate. ***<P 0.001.

3.4 eIF6 is overexpressed and hyperactivated in ALK+ T-cell lymphomas

Next, we asked whether eIF6 phosphorylation on Ser235 is critical during oncogenic events. Considering the relevance of PKCBII kinase on eIF6 activation, first we data-mined eIF6 and PKCβ (PRKCB) mRNA levels from Rna-Seq studies, conducted on several types of human tumors. Data showed that T-cell lymphoma patients express higher levels of both eIF6 and PRKCB mRNA in tumor samples when compared to normal tissues, indicating a possible role for eIF6 phosphorylation in T-cell lymphomagenesis (Figure 17A).

Particularly, we decided to focus on Anaplastic Large Cell Lymphoma (ALCL), a subset of T-cell non Hodgkin Lymphoma, which frequently carries a chromosomal translocation resulting in the expression of the oncogenic NPM-ALK fusion protein (Pulford, Lamant et al. 1997).

Our data-mining studies showed that higher levels of eIF6 protein emerged in human ALK-positive ALCL cell lines compared to ALK-negative ALCL and normal cell lines (Figure 17B). Moreover, Western Blotting analysis showed that eIF6 and PKCβII are overexpressed in ALK-driven lymphomas (Figure 17C). To evaluate eIF6 phosphorylation, we performed a 2D gel electrophoresis on a pool of three ALK-positive tumor samples. Tumors derived from NPM-ALK mice showed focused spots compatible with eIF6 phosphorylation state, indicating that eIF6 is phosphorylated in ALK-tumors (Figure 17D). Our results establish that eIF6 is hyperexpressed and phosphorylated in NPM-ALK driven lymphomas, confirming that upregulation of eIF6 activity is part of the oncogenic process driven by NPM-ALK.

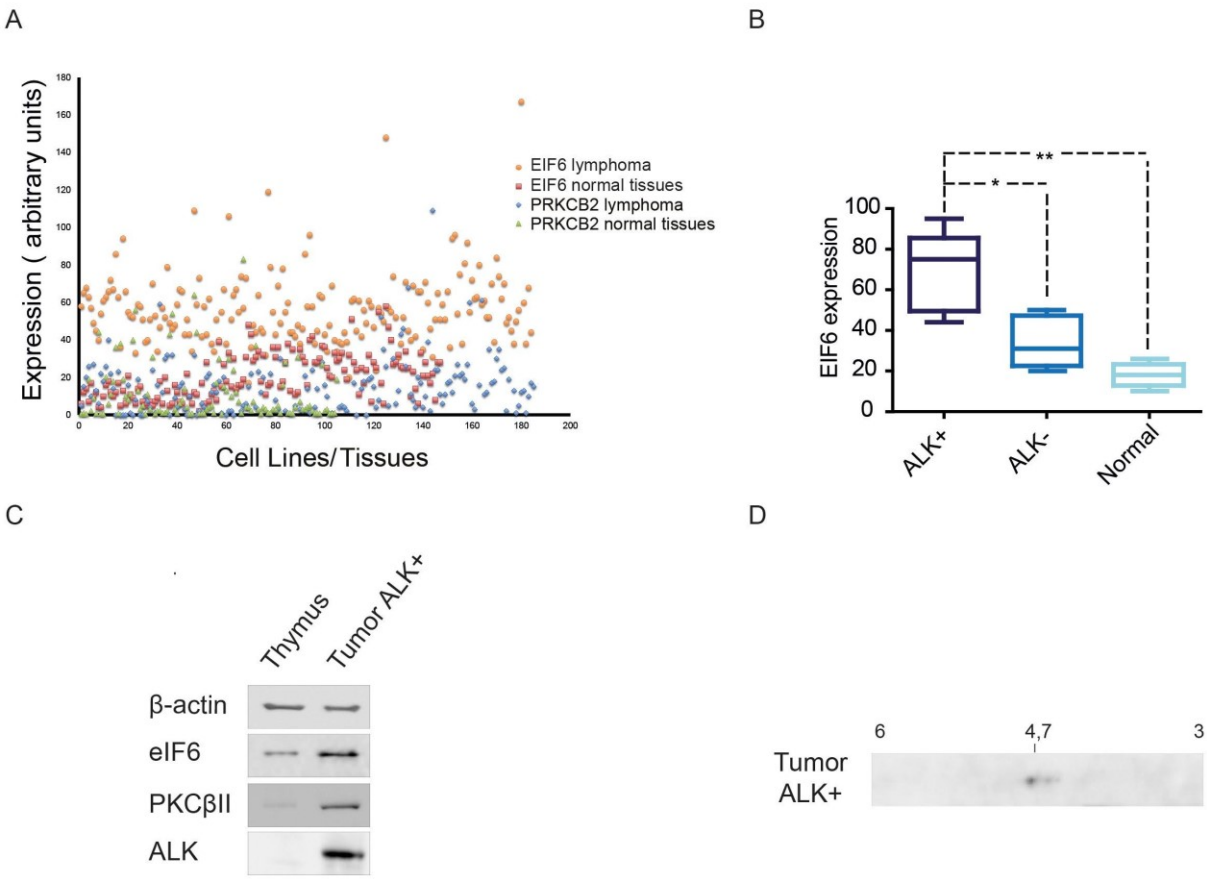

Figure 17. eIF6 is overexpressed and hyperactivated in ALK+ T-cell lymphomas. A) Meta-analysis shows that both EIF6 and PRKCB2 are overexpressed in T-cell lymphomas compared to normal tissues. B) Computational analysis of EIF6 expression level in normal, ALK-positive and ALK-negative human cell lines. C) Representative Western Blot analysis of eIF6, PKCβII and ALK levels in normal thymus and ALK-positive tumor, normalized with β-Actin. D) Representative bidimensional electrophoresis performed on a pool of three tumoral extracts. Focused spots indicate that eIF6 is hyperphosphorylated in ALK-positive lymphomas.

3.5 Constitutive expression of eIF6^{SA} delays NPM-ALK-induced lymphomagenesis

Established that eIF6 is overexpressed and hyperphosphorylate in NPM-ALK induced lymphomagenesis, we asked whether Ser235 phosphorylation is required for ALK-mediated transformation.

First, we used immortalized MEFs derived from eIF6$^{+/+}$ and eIF6$^{SA/+}$ mice. We compared transformation of eIF6$^{+/+}$ and eIF6$^{SA/+}$ MEFs after infection with a retrovirus expressing the NPM-ALK transgene and the reporter gene GFP. eIF6$^{+/+}$ and eIF6$^{SA/+}$ MEFs were infected also with a MOCK, as control. Western Blot analysis of GFP protein showed that the rate of infection was similar between wt and mutant MEFs (Figure 18A).

eIF6$^{+/+}$ nor eIF6$^{SA/+}$ cells infected with the MOCK did not establish colonies. In contrast, after infection with NPM-ALK virus, eIF6$^{+/+}$ MEFs formed colonies. eIF6$^{SA/+}$ cells were resistant to transformation, forming fewer colonies, compared to eIF6$^{+/+}$ MEFs (Figure 18B). Notably, larger foci were obtained from eIF6$^{+/+}$ MEFs expressing NPM-ALK transgene compared to eIF6$^{SA/+}$ ones (Figure 18C).

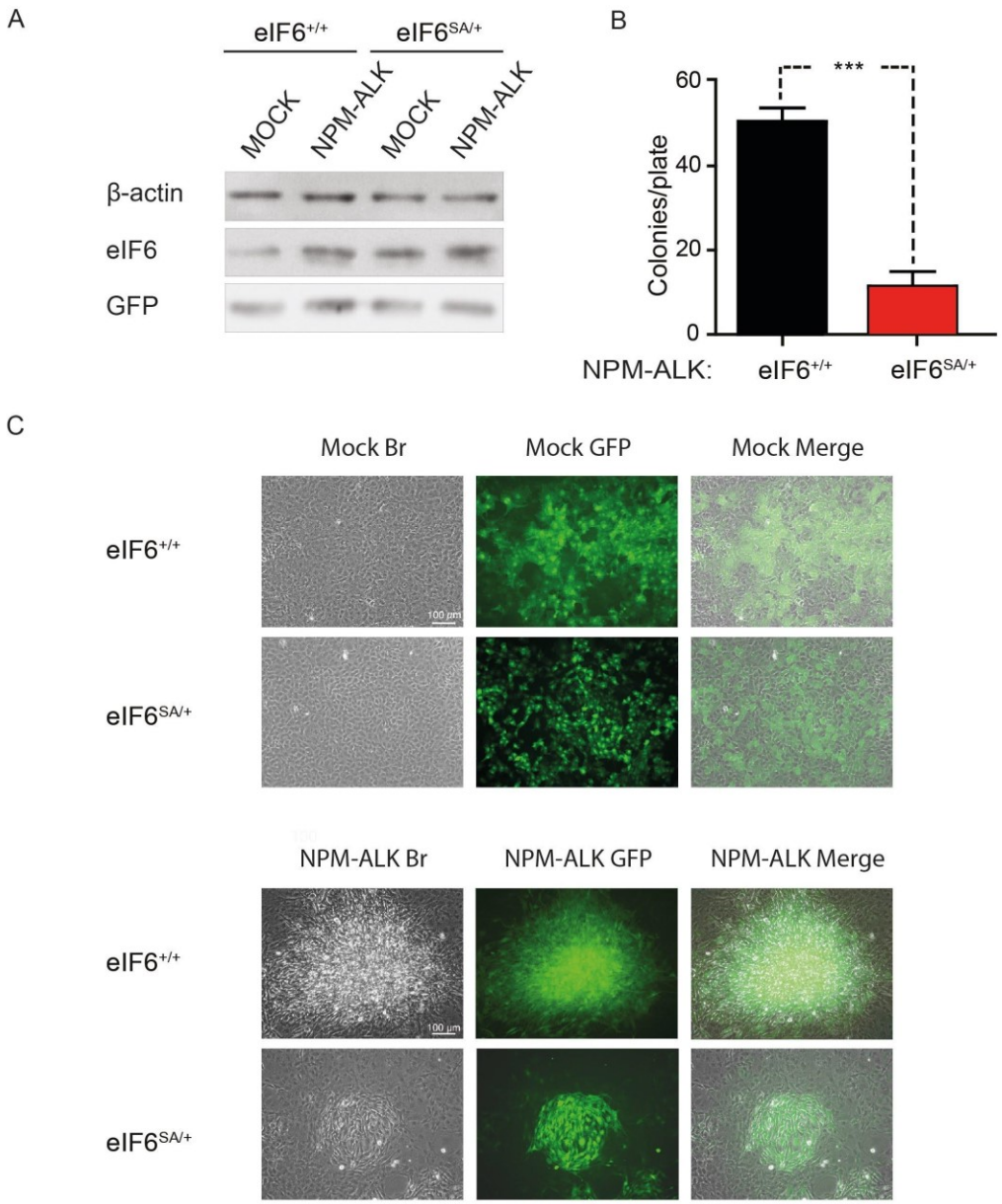

Figure 18. eIF6$^{SA/+}$ mutation impairs ALK-induced transformation of MEFs. A) eIF6$^{+/+}$ and eIF6$^{SA/+}$ MEFs were transduced with MOCK and NPM-ALK retrovirus. Western Blot analysis for GFP and eIF6 in eIF6$^{+/+}$ and eIF6$^{SA/+}$ MEFs. Data are normalized on β-Actin levels. Anti-GFP antibody was used as a control of retroviral infection. B) Number of transformed colonies derived from three independent experiments, represented as mean ± SD. Data show that transformation is dramatically impaired in eIF6$^{SA/+}$ MEFs, ***P<0.001. C) eIF6$^{+/+}$ and eIF6$^{SA/+}$ MEFs were imaged for green fluorescence during transformation. Images were merged with brightfield images. Scale bar=100µm. eIF6$^{SA/+}$ MEFs form smaller colonies compared to eIF6$^{+/+}$ ones.

Then, we addressed eIF6 phosphorylation requirement for NPM-ALK-induced lymphomagenesis *in vivo*. We crossed eIF6$^{SA/+}$ mice with NPM-ALK mice to generate eIF6$^{+/+}$

NPM-ALK and eIF6$^{SA/+}$ NPM-ALK mice. The expression of ALK oncogene was comparable between eIF6$^{SA/+}$ NPM-ALK mice and wt counterparts (Figure 19A). Expression of NPM-ALK acts as a strong driver oncogene, as all mice develop lymphoma. However, as shown in Figure 19B, the constitutive expression of the mutant form of eIF6 slightly increased the overall survival of NPM-ALK mice.

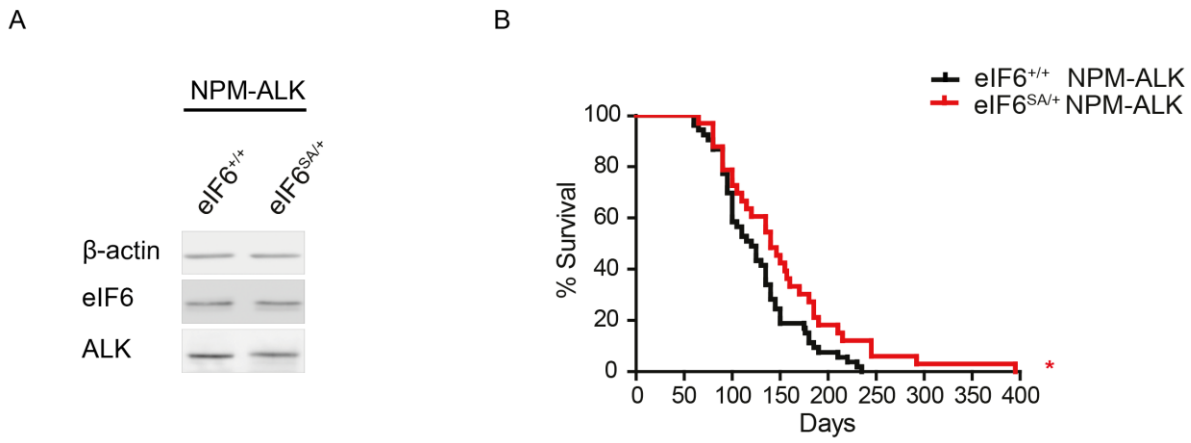

Figure 19. eIF6$^{SA/+}$ mutation slightly affects NPM-ALK induced lymphomagenesis *in vivo*. A) Representative Western Blot analysis of eIF6 and ALK expression on tumors derived from control and eIF6$^{SA/+}$ NPM-ALK mice. B) Kaplan-Meier curves depicting overall survival of eIF6$^{+/+}$ NPM-ALK+ mice (n=53) compared to eIF6$^{SA/+}$ NPM-ALK+ mice (n=32). Constitutive eIF6 partial mutation increases the survival of NPM-ALK mice. *P< 0.05.

3.6 eIF6 inactivation in T-cells protects from NPM-ALK-induced lymphomagenesis

Next, we asked whether the homozygous expression of the mutant form of eIF6 could prevent the onset of T-cell lymphomas induced by NPM-ALK.

First, we addressed the role of eIF6 activity in ALK induced oncogenic transformation *in vitro*.We observed that eIF6$^{SA/SA}$ MEFs transformed at lower efficiency than do wt cells (Figure 20A). We then proceeded to conduct a reconstitution experiment. MEFs were reconstituted with eIF6 wt, eIF6^{SA} or control GFP. Analysis of the levels of eIF6 in each population indicated that each construct was overexpressed (data not shown). Reconstitution of eIF6$^{SA/SA}$ MEFs with wt eIF6, but not with eIF6^{SA}, increased their capability to form transformed colonies (Figure 20B).

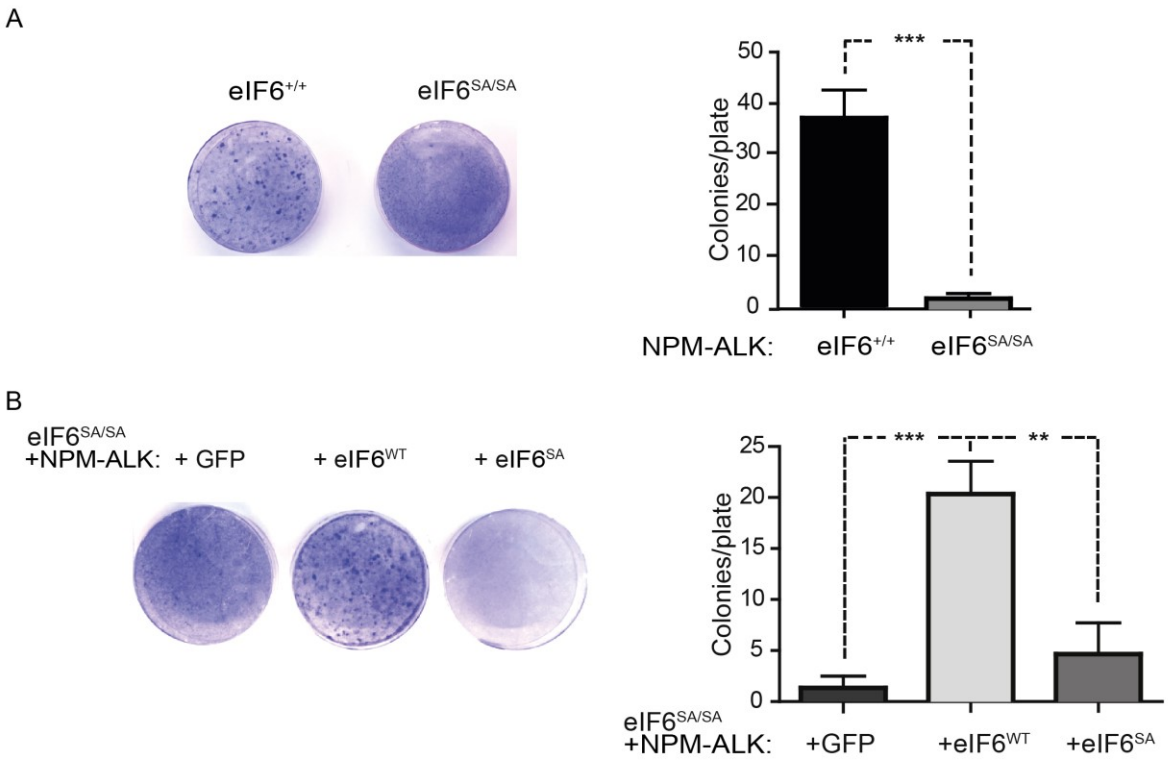

Figure 20. Effect of eIF6 mutation on transformation of immortalized MEFs. A) After 3 weeks from ALK-infection, colonies were stained with crystal violet and enumerated. Mean colony number per plate ± SD for each genotype is represented graphically (n=3 independent experiments performed in triplicates). ***P<0.001. B) Transduction of eIF6$^{SA/SA}$ MEFs with eIF6^{WT} rescued the transformation capability of eIF6$^{SA/SA}$ MEFs. GFP transduced MEFs were used as control. Mean colony number per plate ± SD for each genotype is represented graphically (n=3 independent experiments performed in triplicates). **P<0.01 and ***P <0.001.

To study the effects of homozygous eIF6^{SA} in NPM-ALK–mediated lymphomagenesis, we developed a murine mouse model of inducible expression of the eIF6 mutant form simultaneously with the NPM-ALK oncogene. First, to achieve a T-cell–restricted expression of eIF6 SA mutant, we crossed KI homozygous mice with CD4Cre mice.

Gene recombination in eIF6$^{SA/SA}$ CD4Cre mice was confirmed by DNA genotyping (data not shown) and normal T-cell development and functions were observed in these mice (data not show). Then, we crossed eIF6$^{SA/SA}$ CD4Cre mice with NPM-ALK mice (Figure 21A).

A

Figure 21. Generation of NPM-ALK mouse strain with T-cell-specific expression of homozygous eIF6^{SA} protein. Scheme of the strategy used to generate eIF6$^{SA/SA}$ CD4Cre NPM-ALK mice. CD4 enh./prom., CD4 enhancer and promoter.

Control mice (eIF6$^{SA/SA}$ NPM-ALK mice) developed T-cell lymphomas around 8 weeks after birth, in contrast, eIF6$^{SA/SA}$ CD4Cre NPM-ALK mice showed a delay in lymphoma appearance up to 6 months and significantly extended survival (Figure 22A). Mice were sacrificed at different time-points of lymphoma development. By autopsy, we measured the weight of tumor mass: eIF6$^{SA/SA}$ CD4Cre NPM-ALK lymphoma showed reduced tumor mass weight at all time points analyzed, indicating that Ser235Ala mutation provided a protective effect against tumor growth (Figure 22B). Histological analysis performed on thymi and lymph nodes showed that of eIF6$^{SA/SA}$ ALK-positive lymphoma cells have a markedly reduced proliferation when compared to eIF6$^{+/+}$ cells. Interestingly, in terms of morphology, eIF6$^{SA/SA}$ ALK lymphoma cells showed smaller size and rounder morphology (Figure 22C).

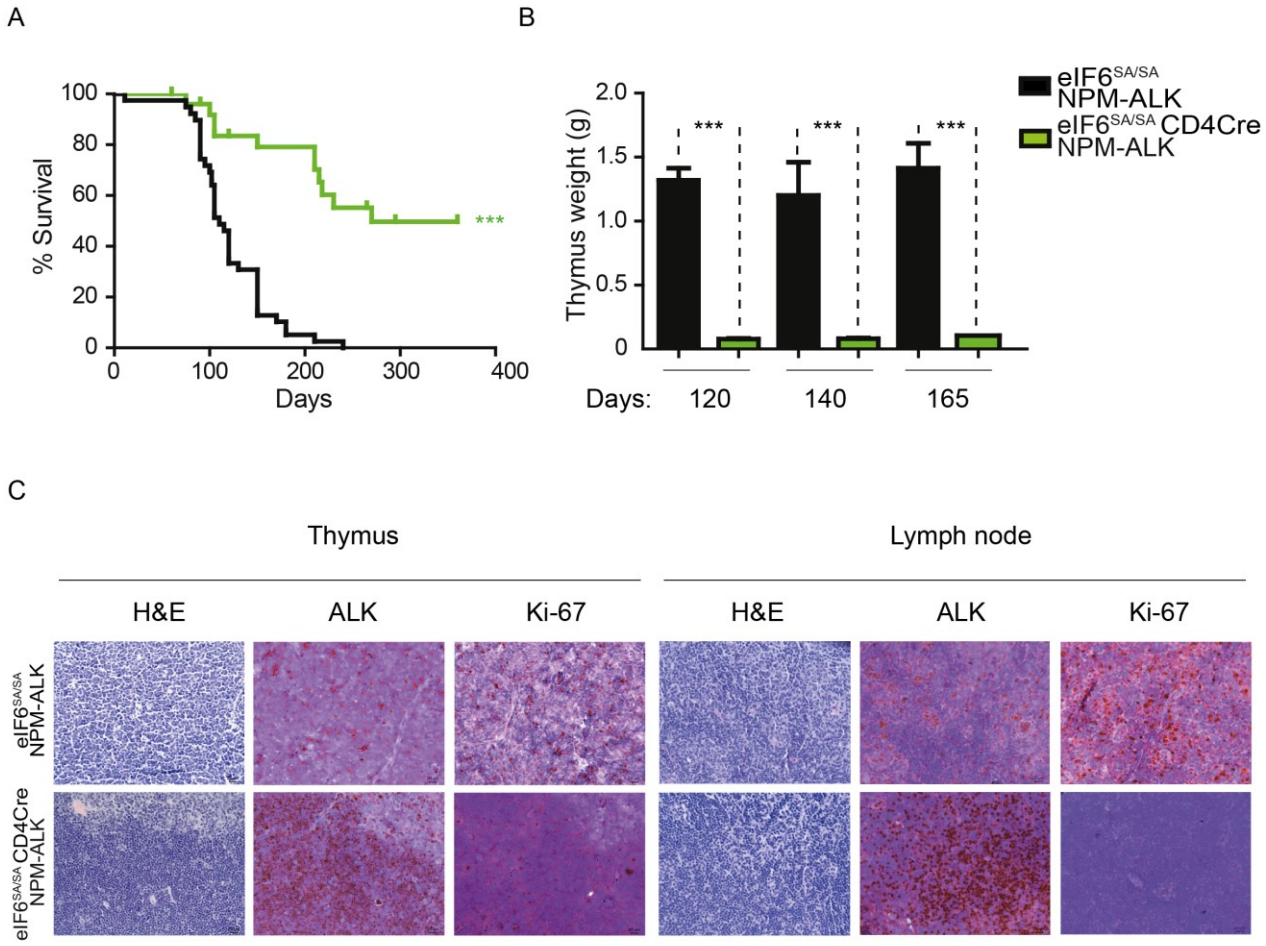

Figure 22. eIF6 inactivation in T-cells protects from NPM-ALK induced lymphomagenesis. A) Kaplan-Meier curves depicting overall survival of eIF6$^{SA/SA}$ NPM-ALK+ mice (n=34) compared to eIF6$^{SA/SA}$ CD4Cre NPM-ALK+ mice (n=26). The overall survival of homozygous eIF6$^{SA/SA}$ mice is significantly increased. ***P<0.001. B) Weight of tumors of NPM-ALK mice (n=6 for genotype). Values represent mean ± SD ***P<0.001. C) H&E, IHC stainings for ALK and Ki-67 of thymi and lymph nodes of eIF6$^{SA/SA}$ NPM-ALK and eIF6$^{SA/SA}$ CD4Cre NPM-ALK mice demonstrate a delay in T-cell lymphomagenesis in eIF6$^{SA/SA}$ CD4Cre NPM-ALK mice. Scale bar=20µm.

To address the effects of eIF6 mutation at the cellular level, we cultured *in vitro* freshly isolated lymphoma cells obtained from eIF6$^{SA/SA}$ CD4Cre NPM-ALK and age-matched wt littermates. We analyzed cells growth at 24, 48 and 72 hours after plating. Cell-Titer Assay revealed that the proliferation rate of eIF6 mutant cells was reduced compared to control cells, *in vitro* (Figure 23A). NPM-ALK oncogene deeply changes CD4+ T lymphocytes morphology, increasing their size and inducing a polarized shape (Choudhari, Minero et al.

2016). FACS analysis of cell size revealed that cells expressing the mutant form of eIF6 have a smaller size compared to wt counterparts, resulting more similar to normal thymocytes rather than transformed lymphoma cells (Figure 23B). Taken together, these results confirmed that eIF6 Ser235Ala mutation decreases the viability and the cell size of NPM-ALK lymphoma cells.

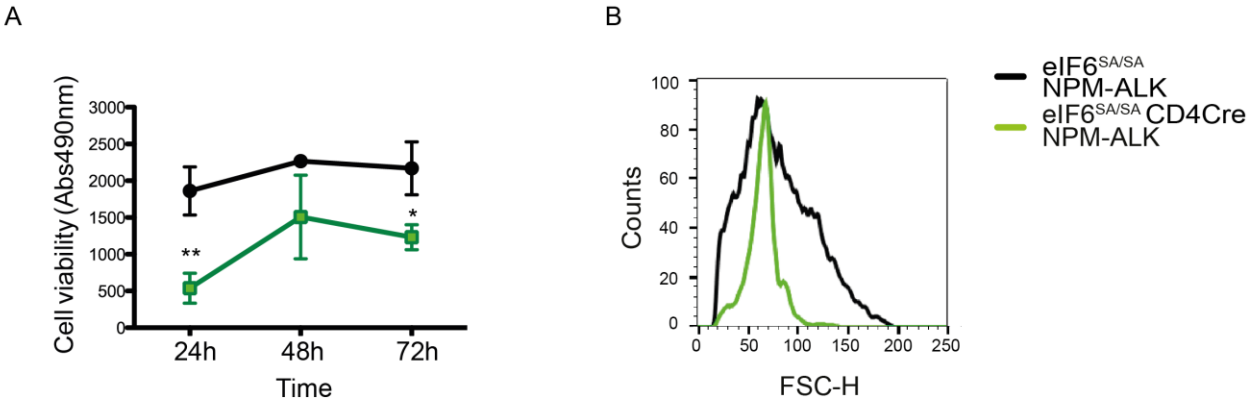

Figure 23. eIF6^{SA} affects the proliferation and the cell size of NPM-ALK thymocytes. A) eIF6$^{SA/SA}$ CD4Cre NPM-ALK primary thymocytes have reduced viability compared to eIF6$^{SA/SA}$ ones. Cell viability was analyzed at the indicated time points from plating. Data are presented as mean ± SD (n=3 independent experiments). *P<0.05 and **P<0.01. B) Representative FACS analysis show that eIF6$^{SA/SA}$ CD4Cre NPM-ALK thymocytes are smaller compared to wt ones (n=3 independent experiments).

3.7 eIF6^{SA} induces cellular senescence, *in vivo*

Cellular senescence can act as an important tumor-suppressive mechanism to restrict tumor development *in vivo* (Campisi 2001). Given the premature senescence induced by eIF6^{SA} mutation in MEFs, we questioned whether the delay of lymphoma onset observed in eIF6$^{SA/SA}$ CD4Cre NPM-ALK could be caused by cellular senescence.

To identify senescent cells in situ, we stained lymphoma sections from eIF6$^{SA/SA}$ CD4Cre NPM-ALK and eIF6$^{SA/SA}$ NPM-ALK mice for β-galactosidase activity and p21 protein. As shown in Figure 24A, Ser235Ala mutant expression significantly increased the SA-βgal-positive cell population and p21 expression in tumor tissues already after 30 days after birth. Moreover, when the disease became full-blown in adult mice, these senescence markers were

even more expressed. We further confirmed these results on freshly isolated lymphoma cells cultured *in vitro* (Figure 24B, C). Our results suggest that the Ser235Ala mutation elicits cellular premature senescence, resulting in a protective mechanism against tumor progression, *in vivo*.

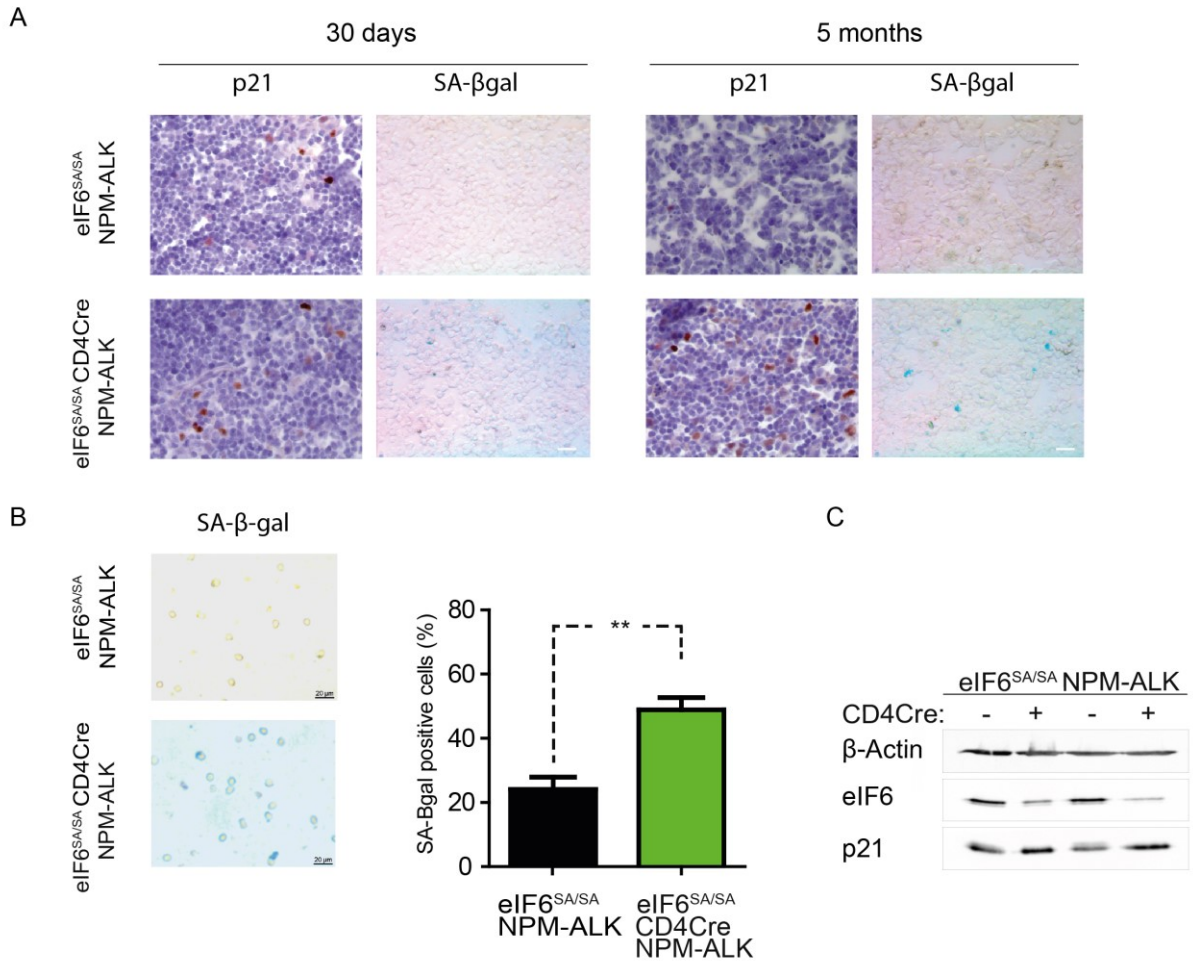

Figure 24. eIF6^{SA} induces senescence in NPM-ALK lymphomas. A) Representative histology of lymphoma arising in eIF6$^{SA/SA}$ NPM-ALK and eIF6$^{SA/SA}$ CD4Cre NPM-ALK mice. Immunostainings for p21 and β-gal activity in tumors of the indicated genotype are shown, at 30 days (left) and 5 months (right) after birth. Scale bar=20 μm. B) Left: representative bright-field images of SA-βgal staining performed on eIF6$^{SA/SA}$ NPM-ALK and eIF6$^{SA/SA}$ CD4Cre NPM-ALK primary thymocytes cultured *in vitro*. Right: quantification of SA β-gal positive thymocytes. Results are presented as mean ± SD from a representative experiment performed in triplicate. **<P 0.01. C) Western Blot analysis of eIF6 and p21 expression in eIF6$^{SA/SA}$ CD4Cre NPM-ALK and control primary thymocytes. P21 expression is increased in eIF6$^{SA/SA}$ CD4Cre NPM-ALK thymocytes compared to wt ones.

4. Discussion and Conclusions

Eukaryotic Initiation Factor 6 (eIF6) controls the initiation phase of translation by regulating the availability of free 60S ribosomes and consequently the active 80S complexes assembly (Ceci, Gaviraghi et al. 2003, Gandin, Miluzio et al. 2008).eIF6 activation is mTORC1-independent but rather it is driven by PKCβ kinase, which mediates eIF6 phosphorylation on the Ser235, its unique consensus site (Miluzio, Beugnet et al. 2009, Miluzio, Beugnet et al. 2011).

eIF6 is overexpressed in several types of human cancers and eIF6 protein levels are limiting in cellular transformation *in vitro* and in cancer progression *in vivo* (Sanvito, Vivoli et al. 2000, Gandin, Miluzio et al. 2008, Miluzio, Beugnet et al. 2011, Gatza, Silva et al. 2014). In this context, the relevance of eIF6 activation *in vivo* is less well known. To investigate the role of eIF6 phosphorylation in mammalian development and in cancer, we have genetically designed and generated an eIF6 Ser235Ala KI mouse model. We showed that complete inactivation of eIF6 ($eIF6^{SA/SA}$) causes embryonic lethality after gastrulation. Moreover, homozygous $eIF6^{SA/SA}$ mutation induces cell cycle arrest, and drives premature cellular senescence, *in vitro* and *in vivo*, resulting in a protective mechanism against cellular transformation and tumor growth. Overall, we demonstrated for the first time that eIF6 phosphorylation on Ser235 is a rate-limiting event necessary for normal mammalian development and for tumorigenesis, and we provided evidence for a new connection between translational control driven by eIF6 activity, cellular premature senescence and cancer.

Our data showed that complete inactivation of eIF6 ($eIF6^{SA/SA}$) causes loss of eIF6 phosphorylation using 2D gel electrophoresis. We are currently trying to produce a phospho-eIF6 antibody to confirm this result. Measurement of eIF6 binding sites by iRIA showed that the direct interaction between mutant $eIF6^{SA}$ protein with the 60S ribosomal subunit surface is extremely increased, suggesting that 60S viability, required for active translation, could be compromised. We will further investigate this possibility performing polysome profiles on $eIF6^{SA/SA}$ MEFs.

In the past, in our lab it has been shown that eIF6 null embryos died prior to the implantation stage (Gandin, Miluzio et al. 2008). This was explained by the fact that total protein depletion caused severe defects in ribosome biogenesis, a process essential to sustain the earliest stages

of mammalian development. Instead, eIF6 mutation induced embryonic lethality later, precisely after gastrulation. Our data from mutant eIF6$^{SA/SA}$ cells do not reveal diminished eIF6 protein levels in the nucleolar compartment (data not shown), suggesting that ribosomal biogenesis could not be impaired. Moreover, even thought eIF6 activation is mTOR-independent, both eIF6 inactivation and mTOR kinase inhibition have highly similar embryonic lethal phenotypes. In both cases, mammalian embryonic lethality occurred after gastrulation and the development of blastocysts is arrested *in vitro* (Gangloff, Mueller et al. 2004, Murakami, Ichisaka et al. 2004, Shor, Cavender et al. 2009). In addition, treatment with the mTOR inhibitor rapamycin impaired the proliferation of the ICM cells of murine blastocysts (Murakami, Ichisaka et al. 2004). mTORC1 and eIF6 are considered central regulators of translation initiation: we can suggest that the activity of both eIF6 and mTORC1 on the control of downstream mRNAs translation represents a rate-limiting mechanism essential for mammalian development and survival.

Consistent with the effects on early embryogenesis, eIF6 mutation has a significant impact on cell proliferation and cell-cycle progression. eIF6$^{SA/SA}$ cells showed a delay in G1/S cell cycle progression and a senescence-like phenotype. We found that eIF6^{SA}-induced cellular senescence is associated with p21, but not p53, upregulation: p21 binds and inhibits cyclin E/CDK2 complexes, leading to G1/S cell cycle arrest (Adams, Sellers et al. 1996, Poon, Jiang et al. 1996, Brugarolas, Moberg et al. 1999). Performing polysome profiles on eIF6$^{SA/SA}$ MEFs, we will investigate whether the mutation of eIF6 is critical in regulating the translation of cellular senescence-specific genes, such as p21.

Programmed cellular senescence during mammalian development has been well proven to be p21-dependent, but p53- and p16-independent (Muñoz-Espín, Cañamero et al. 2013, Storer, Mas et al. 2013). On the basis of this evidence, we can speculate that lethality of eIF6$^{SA/SA}$ embryos may be mediated by an eIF6-induced ectopic activation of p21-dependent senescence. This is still unclear, and it will be further addressed.

The observation that mutant eIF6^{SA} drives premature cellular senescence was unexpected. The role of the translational apparatus during senescence is controversial. For instance, it has been shown that the inhibition of the TOR pathway by rapamycin treatment significantly extends life-spans in yeast, nematodes, fruit flies and mice (Kaeberlein, Powers et al. 2005, Powers, Kaeberlein et al. 2006, Harrison, Strong et al. 2009, Bjedov, Toivonen et al. 2010). Conversely, loss-of-function mutations in TSC1/TSC2, that lead to unrestrained mTOR activity, induces premature senescence (Powers, Kaeberlein et al. 2006). The mTOR substrates 4EBP1 and 4EBP2 have been previously shown to be involved in senescence,

downstream of mTORC1and 4EBP1/4EBP2-deficient cells undergo faster replicative senescence as compared to wild-type control (Powers, Kaeberlein et al. 2006). Another well-known mTORC1 downstream target is S6K: it has been demonstrated that S6K is also involved in cell cycle arrest and senescence response (Nicke, Bastien et al. 2005, Leontieva, Demidenko et al. 2013). So far, no evidence for a role of eIF6 in premature senescence was found.

Senescence is a form of cell-cycle arrest linked to aging (Baker, Perez-Terzic et al. 2008, Baker, Wijshake et al. 2011, McHugh and Gil 2018). The lethal phenotype of constitutive $eIF6^{SA/SA}$ mice does not permit us to investigate whether $eIF6^{SA}$ induces organ premature senescence and aging. It will be interesting to define if the inducible expression of $eIF6^{SA}$ mutant, in adulthood, causes precocious aging phenotype.

Another critical role of cellular senescence is its action as a tumor suppressor mechanism. Cellular senescence is considered a powerful barrier to the clonal expansion of primary cells and a potent tumor-suppressor mechanism *in vivo* (Collado, Blasco et al. 2007). Here, we demonstrated that $eIF6^{SA}$-induced premature senescence results in a protective mechanism against NPM-ALK mediated lymphomagenesis. Our findings are consistent with a report demonstrating that suppression of cellular senescence increments NPM-ALK-induced cellular transformation *in vitro* and accelerates NPM-ALK mediated lymphomagenesis *in vivo* (Martinelli, Bonetti et al. 2011). Moreover, we observed p21, but not p53, induction in $eIF6^{SA/SA}$ ALK+ lymphomas: these data are consistent with recent findings proving p21-dependent cellular senescence as a mechanism to prevent tumor development *in vivo* (Lin, Chen et al. 2010). A possible relationship between the regulation of p21 protein expression and eIF6 activity is still unclear. Future studies are needed to investigate this mechanism. Finally, it has been established that HDAC inhibitors induce p21 without p53 involvement (Huang, Sowa et al. 2000). We previously demonstrated that eIF6 inhibition led to a gene expression signature overlapping with the treatment with HDAC inhibitors and that eIF6 inhibition is associated with increased histone acetylation (Brina, Miluzio et al. 2015, Clarke, Ricciardi et al. 2017). Recently it has been demonstrated that pharmacological inhibition of histone acetylation induces cellular senescence and arrest lymphoma growth *in vivo* (Baell, Leaver et al. 2018). Future studies will reveal whether eIF6 phosphorylation could modulate histone acetylation inducing a senescence-like state during cancer development.

Despite maintaining a non-dividing state, senescent cells display a high metabolic rate. Metabolic changes characteristic of replicative senescence include altered mitochondrial function, enhanced glycolysis, fatty acid catabolism and perturbations in growth signaling

pathways (Nacarelli and Sell 2017). Recent evidence has raised the possibility that these metabolic changes may be the drivers of the senescent induction (Favaro, Bensaad et al. 2012, Jiang, Du et al. 2013, Kaplon, Zheng et al. 2013, Zheng, Cardaci et al. 2015, Wiley, Velarde et al. 2016, Rizza, Cardaci et al. 2018). The translational activity of eIF6 is particularly relevant in the regulation of metabolism, both in physiological condition and in cancer cells (Brina, Miluzio et al. 2015, Miluzio, Oliveto et al. 2015).eIF6 acts as a master regulator of metabolism through specific translation of uORF-containing mRNAs encoding for lipogenic transcription factors, as ATF4 (Brina, Miluzio et al. 2015). Intriguingly, ATF4 is known to promote neoplastic transformation by suppressing the expression of cell senescence factors (Horiguchi, Koyanagi et al. 2012). Thus, we will define: a) the metabolic changes induced by S235A mutation and b) the effects of eIF6 phosphorylation on the crosstalk between senescence, metabolism and translation.

We preliminarily investigated the glycolytic rate and ATF4 expression in eIF6$^{SA/SA}$ cells: ATP accumulation and ATF4 reduction were found in eIF6$^{SA/SA}$ senescent cells (data not shown). Further metabolomic and translational analysis, as ribosome profiling, will be performed to define whether eIF6 phosphorylation control senescence through translation-driven metabolic changes. Our future aim will be the identification of potential oncometabolites that are crucial for cancer growth and that are directly susceptible to eIF6 phosphorylation during active translation.

In conclusion, these data prompt the translational control to a center stage in the crosstalk between senescence and tumor progression. Our study discloses for the first time a regulation of a senescence program dependent on eIF6 activity that slows tumor formation. This evidence suggests that eIF6 can be considered an anti-cancer molecular target. Besides this, the transgenic eIF6$^{SA/SA}$ mouse model may be used for predicting the effects of putative small molecules able to directly modulate eIF6 activation and their anti-tumoral value.

5. Materials and Methods

Generation of eIF6^{Ser235Ala} knock-In mice and *in vivo* experimental procedures

The conditional eIF6 point mutant allele and the eIF6^{SA} knock-In mouse model were designed and created in collaboration with the Ingenious Targeting Laboratory (Ronkonkoma, NY, USA). Briefly, murine eIF6 genomic locus was modified by recombineering to create the specific point mutation (AG-to-GC change) on exon 5 of eIF6 gene, leading to a Serine to Alanine amino acid changing. The conditional targeting vector was performed by the insertion of the SV40pA *frt*-Neo-*frt*-LoxP positive selection cassette downstream of exon 6, followed by a cDNA sequence that contains exons 4, 5 (with the point mutation on Ser235) and exon 6. *Frt* sites were inserted for later excision by *Flp* recombinase. An additional distal single LoxP site was inserted upstream of exon 4. The constructed targeting vector was introduced into the ES cells by electroporation and homologous recombinant ES cell clones were identified and microinjected into C57BL/6 blastocysts. Resulting chimeras were mated to C57BL/6 mice and heterozygous eIF6^{SA} Knock-In mice were intercrossed with CMV-Cre and CD4-Cre murine lines to generate mutant eIF6^{SA} allele. Mutant eIF6^{SA} transgenic mice, CMV-Cre, CD4-Cre (kindly provided by the laboratory of Prof. Paolo Dellabona, San Raffaele Hospital, Milan) and NPM-ALK transgenic mice (kindly provided by the laboratory of Prof. Roberto Chiarle, University of Turin) were intercrossed to obtain all the genotypic combinations, as described in the manuscript. Genotyping analysis was performed by PCR on tail genomic DNA. The detection of LoxP sites was performed using the following primers: FwLoxp1 5'-GTG GCA GCT TGG TCT GGA AGT TAC-3'; RwSDL2 5'-AAC CAC AAA TCT GCA CAT GGA AGC-3'. The identification of Cre-activated alleles was performed using the specific primers: 5'-FwSDL2 GCT TCC ATG TGC AGA TTT GTG GTT-3'; RwINT5 5'-GGT ACC TAG AAA CCC TGT CTC-3'; RwEx4-5 5'-CAC AGT GCC TGC CAC AAG-3'. CMV-Cre genotyping was performed using the specific primers: Rw: 5'-GTGGCAGATGGCGCCGGCAACACC-3'; Fw: 5'-GCCTGCATTACCGGTCGATGCAA-3'. CD4-Cre genotyping was performed using the specific primers: Fw: 5'-GCCTGCATTACCGGTCGATGCAAG-3'; Rw: 5'-GTGGCAGATGGCGCGGCA-3'. NPM-ALK genotyping was performed using the specific primers: Fw 5′-TCCCTTGGGGGCTTTGAAATA-3′, Rw 5′-CGAGGTGCGGAGCTTGCTCAG-3′. PCR products were resolved on 2% agarose gels. Mice were monitored daily for the tumor development until they died spontaneously or they were sacrificed if showing evident signs of

distress. Kaplan-Meier curve was used to examine the survival rate of all considered animals. Axillary lymph nodes, thymi and spleens of these mice were recovered, weighted, and used for further analysis. Mice were maintained under specific pathogen-free conditions and all experiments involving animals were performed in accordance with Ethical Committee of San Raffaele and covered by experimental protocols reviewed by the E.C. regulations, the Institutional Animal Care and Use Committees (IACUC n.688).

Cell lines

Primary Embryo Fibroblasts (MEFs) were isolated from 13.5 d.p.c. eIF6 $^{SA/+}$ and eIF6$^{SA/SA}$ KI embryos as previously described (Gandin, Miluzio et al. 2008). Primary MEFs were grown in DMEM (Lonza), supplemented with 10% Fetal Bovine Serum (FBS) and 1% penicillin, streptomycin, L-glutamine, and maintained at 37°C and 9% CO_2. Primary MEFs were infected at early passages with hTERT lentiviral vector. After immortalization, cells were maintained at 37°C and 5% CO_2. Primary thymocytes were isolated from tumors of 4-month-old NPM-ALK transgenic mice with mechanic disaggregation and isolated with a 40-µm nylon cell strainer. Cells were maintained in RPMI 1640 (Lonza) with 10% fetal bovine serum, 2% penicillin, streptomycin 5 mg/mL (Gibco), and 1% glutamine (Gibco). Cell lines were grown at 37°C and 5% CO_2. All the analyses were performed at least three times on different genetic backgrounds.

Retrovirus preparation and cell transduction

Retroviruses were generated by transient transfection of pWZLblast vector expressing CreER^{T2} in 293 Phoenix packaging cells. After 48 hours of incubation at 37°C, supernatants containing viral particles were collected and used for further transduction. For the retroviral transduction, 300 µL supernatant was used to infect eIF6$^{SA/SA}$ KI MEFs. CreER^{T2} transduced cells were selected using blasticidin (Calbiochem, San Diego, CA) at 2,5 µg/mL for 6 days. To induce recombination of the floxed alleles, cells were treated with 2 µM 4-OHT dissolved in EtOH for 2 days. For cell proliferation assays, 3 x 10^4 cells/mL were grown in 6-well plates and cell numbers were recorded every 24 h for 6 days.

Transformation assay and lentiviral vectors

Immortalized fibroblasts expressing the CreER^{T2} recombinase were infected with retrovirus carrying GFP together with NPM-ALK oncogene, as previously described (Chiarle, Simmons et al. 2005). As a control, an empty retroviral vector expressing GFP was used. After 5 days, these cells were also infected with lentiviral vectors.The lentiviral vectors used in this study express full-length wt eIF6, mutant eIF6^{SA}and GFP as internal control, as previously described (Gandin, Miluzio et al. 2008). For transformation analysis, cells were fixed and stained with Crystal violet; foci were counted 2-3 weeks after infections.

Antibodies and reagents

The following antibodies were used: rabbit polyclonal antibodies against eIF6 (Biffo, Sanvito et al. 1997), Ki-67 (Abcam); mouse monoclonal antibodies against BrdU (Sigma), p53 (Cell Signaling), ALK (Invitrogen), p21 and p16 (Santa Cruz Biotechnology), β-Actin (Sigma). 4-hydroxytamoxifen (OHT) and all powders and reagents were from Sigma.

Cell proliferation and cell cycle analysis

Proliferation rate of thymocytes was analyzed by Cell Titer-Blue assay (Promega). Briefly, different densities of cells were plated at 100 ml/well in a 96-well plate, and assayed after 24, 48 and 72 hours, as indicated in the manuscript. CTB was added and left on cells for 3 hours at 37° C and 5% CO2. The number of viable cells was measured by recording fluorescence at 560Ex/590Em nm in a Victor3 multilabel counter (PerkinElmer, Germany). Cell cycle analysis was performed on MEFs. Sub-confluent cells were cultured for 36 h in medium supplemented with 0.1% fetal bovine serum to arrest growth, and then switched to 10% fetal bovine serum. At 4, 8, 12 and 18 h after serum stimulation, 5-Bromo-2-deoxyuridine was added for 2 h to label cells undergoing DNA synthesis. Cells were then harvested by trypsinization and fixed in 70% ethanol at 4 °C for 24 h, then treated with RNase (1 mg/ml) for 30 min. Cells were stained with FITC-conjugated anti-5-Bromo-2-deoxyuridine for 1 h at

37 °C and with 7-Aminoactinomycin D (7-AAD) for 2 min at room temperature. Samples were acquired on a BD FACS CANTO II flow cytometer. Cell cycle analysis was performed using the FCS Express software (BD). Each experiment was done at least in triplicate.

Polysome profiles

eIF6$^{SA/+}$ and eIF6$^{SA/SA}$ MEFs were lysed in 50mM Tris HCl pH 7.8, 240mM KCl, 10mM $MgSO_4$, 5mM DTT, 250mM sucrose, 2% Triton X-100, 90 mg/ml Cicloheximide, 30 U/ml RNasin using a glass douncer. 10 OD of RNA was loaded on a 15-55% sucrose gradient dissolved in 25mM Tris HCl pH 7.4, 25mM NaCl, 5mM $MgCl_2$, 1mM DTT and run at 39,000 rpm for 3h30min with SW41Ti swing rotor (Beckman Coulter). Absorbance at 254 nm was recorded by BioLogic LP software (BioRad) and 40S, 60S, 80S peaks and polysomes were defined.

***In vitro* culture of murine blastocysts**

All blastocysts were isolated from synchronized and superovulated adult eIF6$^{SA/+}$ female, mated with 2-3 months old eIF6$^{SA/+}$ males. After vaginal plug detection, blastocyst were collected at 3.5 days post coitum (d.p.c.) by uterine flushing with M2 medium (Sigma) and cultured on gelatin-coated wells. Each blastocyst was daily photographed using a Zeiss Axio Observer Z1 system. Images were exported as jpeg files, subsequently cropped and adjusted for brightness and contrast. At the day 5, the blastocyst-outgrowing cells or the undeveloped blastocysts were collected and suspended in 50 µl lysis buffer (60mM Tris-HCl, ph 9.0, 15 mM$[NH_4]_2SO_4$, 2mM $MgCl_2$, 0.5% tween-20(v/v) and 250 mg/ml proteinase K) for PCR-based genotyping. Genotyping was successful for all the blastocysts collected.

Histological Staining and Immunohistochemistry

Immunohistochemical and histological analyses were performed on paraffin-embedded sections obtained from thymi, spleens and lymph nodes of eIF6$^{+/+}$ NPM-ALK and eIF6$^{SA/SA}$ CD4-Cre NPM-ALK mice. Immunohistochemistry for the considered targets was done using the Vectastain Elite ABC kit (Vector), according to the manufacturer's instructions. Some sections were counterstained with Hematoxylin-Eosin (H&E).

SA β-gal activity

SA β-gal staining of cultured cells was performed using the senescence β-Galactosidase Staining Kit (Cell Signaling). The percentage of cells stained for SA β-gal activity was determined using an inverted microscope (Olympus IX51), by counting cells in four random fields of view at a magnification of 10/20X. Images were taken with Canon 1100D digital camera. For SA-β-Gal activity on thymi, 5-µm frozen sections were fixed with 0.5% glutaraldehyde for 15 min, washed with PBS and incubated in SA-β-Gal staining solution: 1 mg of 5-bromo-4-chloro-3-indolyl P3-D-galactoside (X-Gal) per ml (stock=20 mg of dimethylformamide per ml)/40mM citric acid/sodium phosphate, pH 5.5/5mM potassium ferrocyanide/5mM potassium ferricyanide/150mM NaCl/2mM MgCl2) for 18 h at 37 °C. All sections were washed after incubation and counterstained with Haematoxylin. Sections were dehydrated and mounted and 10–15 random fields per section were imaged.

Two-dimensional (2D) gel electrophoresis

Total protein extracts from MEFs and tumor samples were examined in 2D gel electrophoresis. Samples were lysed in SDS-free RIPA buffer and proteins were precipitated with 10% TCA. Pellets were resuspended in 2-D buffer (7 M Urea, 2 M Thiourea, 50 mM DTT and 4% CHAPS) and 100 µg of proteins were isoelectrofocused. The first dimension was performed on Ready Strip IPG (pH 3.9–5.1; Biorad). For the reduction/alkylation step, the strips were incubated with re-equlibration buffer (50 mM Tris-HCl, pH 8.8, 6 M urea, 30% glycerol, 2% SDS, bromophenol blue) plus 10 mg/ml of DTT and re-equilibration buffer plus 45 mg/ml of iodoacetamide, respectively. Then, the strips were subjected to SDS/PAGE for the second dimension. Proteins were transferred on PVDF membrane and subsequently incubated with eIF6 monoclonal antibody. The signal was detected with an anti-mouse secondary antibody and ECL substrate kit (GE Healthcare). Each experimental sample was run at least twice, and at least three different biological replicates were analyzed.

***In vitro* Ribosome Interaction Assay (iRIA)**

iRIA assay was performed as described in (Pesce, Minici et al. 2015). Briefly, 96-well plates were coated with $eIF6^{+/+}$ and $eIF6^{SA/SA}$ cellular extracts diluited in 50 µL of PBS, 0.01% Tween-20 O/N at 4°C in humid chamber. Coating solution was removed and aspecific sites

were blocked with 10% BSA, dissolved in PBS, 0.01% Tween-20 for 30 minutes at 37 °C. Plates were washed with 100 µL/well with PBS-Tween. 0.5 µg of exogenous recombinant biotinylated eIF6 protein were resuspended into a reaction mix (2.5 mM MgCl2, 2% DMSO and PBS-0.01%Tween) to reach 50µL of final Volume/Well, added to the wells and incubated with coated ribosomes for 1 hour at room temperature. To remove unbound proteins, each well was washed 3 times with PBS, 0.01% Tween-20. Diluted HRP-conjugated streptavidin (1:7000 in PBS, 0.01% Tween-20) was added and incubated for 30 minutes at room temperature. Excess of streptavidin was removed through three washes with PBS-Tween. OPD (o-phenylenediamine dihydrochloride) was used according to the manufacturer's protocol (Sigma-Aldrich) as a soluble substrate for the detection of streptavidin peroxidase activity. The signal was detected after the incubation, plates were read at 450 nm on a multiwell plate reader (Microplate Bio-Rad model 680).

Statistical analysis

Each experiment was repeated at least three times, as biological replicates; means and standard deviations between different experiments were calculated. Statistical P-values obtained by Student *t*-test were indicated: three asterisks *** for P-values less than 0.001, two asterisks ** for P-values less than 0.01 and one asterisk * for P-values less than 0.05.

6. References

Adams, P. D., W. R. Sellers, S. K. Sharma, A. D. Wu, C. M. Nalin and W. G. Kaelin (1996). "Identification of a cyclin-cdk2 recognition motif present in substrates and p21-like cyclin-dependent kinase inhibitors." Mol Cell Biol**16**(12): 6623-6633.

Baell, J. B., D. J. Leaver, S. J. Hermans, G. L. Kelly, M. S. Brennan, N. L. Downer, N. Nguyen, J. Wichmann, H. M. McRae, Y. Yang, B. Cleary, H. R. Lagiakos, S. Mieruszynski, G. Pacini, H. K. Vanyai, M. I. Bergamasco, R. E. May, B. K. Davey, K. J. Morgan, A. J. Sealey, B. Wang, N. Zamudio, S. Wilcox, A. L. Garnham, B. N. Sheikh, B. J. Aubrey, K. Doggett, M. C. Chung, M. de Silva, J. Bentley, P. Pilling, M. Hattarki, O. Dolezal, M. L. Dennis, H. Falk, B. Ren, S. A. Charman, K. L. White, J. Rautela, A. Newbold, E. D. Hawkins, R. W. Johnstone, N. D. Huntington, T. S. Peat, J. K. Heath, A. Strasser, M. W. Parker, G. K. Smyth, I. P. Street, B. J. Monahan, A. K. Voss and T. Thomas (2018). "Inhibitors of histone acetyltransferases KAT6A/B induce senescence and arrest tumour growth." Nature**560**(7717): 253-257.

Bai, R. Y., P. Dieter, C. Peschel, S. W. Morris and J. Duyster (1998). "Nucleophosmin-anaplastic lymphoma kinase of large-cell anaplastic lymphoma is a constitutively active tyrosine kinase that utilizes phospholipase C-gamma to mediate its mitogenicity." Mol Cell Biol**18**(12): 6951-6961.

Baird, T. D. and R. C. Wek (2012). "Eukaryotic initiation factor 2 phosphorylation and translational control in metabolism." Advances in nutrition**3**(3): 307-321.

Baker, D. J., C. Perez-Terzic, F. Jin, K. S. Pitel, K. Pitel, N. J. Niederländer, K. Jeganathan, S. Yamada, S. Reyes, L. Rowe, H. J. Hiddinga, N. L. Eberhardt, A. Terzic and J. M. van Deursen (2008). "Opposing roles for p16Ink4a and p19Arf in senescence and ageing caused by BubR1 insufficiency." Nat Cell Biol**10**(7): 825-836.

Baker, D. J., T. Wijshake, T. Tchkonia, N. K. LeBrasseur, B. G. Childs, B. van de Sluis, J. L. Kirkland and J. M. van Deursen (2011). "Clearance of p16Ink4a-positive senescent cells delays ageing-associated disorders." Nature**479**(7372): 232-236.

Barna, M., A. Pusic, O. Zollo, M. Costa, N. Kondrashov, E. Rego, P. H. Rao and D. Ruggero (2008). "Suppression of Myc oncogenic activity by ribosomal protein haploinsufficiency." Nature**456**(7224): 971-975.

Basu, U., K. Si, H. Deng and U. Maitra (2003). "Phosphorylation of mammalian eukaryotic translation initiation factor 6 and its Saccharomyces cerevisiae homologue Tif6p: evidence that phosphorylation of Tif6p regulates its nucleocytoplasmic distribution and is required for yeast cell growth." Molecular and cellular biology**23**(17): 6187-6199.

Basu, U., K. Si, J. R. Warner and U. Maitra (2001). "The Saccharomyces cerevisiae TIF6 gene encoding translation initiation factor 6 is required for 60S ribosomal subunit biogenesis." Molecular and cellular biology**21**(5): 1453-1462.

Ben-Shem, A., N. Garreau de Loubresse, S. Melnikov, L. Jenner, G. Yusupova and M. Yusupov (2011). "The structure of the eukaryotic ribosome at 3.0 Å resolution." Science**334**(6062): 1524-1529.

Bhat, M., N. Robichaud, L. Hulea, N. Sonenberg, J. Pelletier and I. Topisirovic (2015). "Targeting the translation machinery in cancer." Nat Rev Drug Discov**14**(4): 261-278.

Biffo, S., F. Sanvito, S. Costa, L. Preve, R. Pignatelli, L. Spinardi and P. C. Marchisio (1997). "Isolation of a novel beta4 integrin-binding protein (p27(BBP)) highly expressed in epithelial cells." The Journal of biological chemistry**272**(48): 30314-30321.

Bjedov, I., J. M. Toivonen, F. Kerr, C. Slack, J. Jacobson, A. Foley and L. Partridge (2010). "Mechanisms of life span extension by rapamycin in the fruit fly Drosophila melanogaster." Cell Metab**11**(1): 35-46.

Braun, J. E., E. Huntzinger and E. Izaurralde (2012). "A molecular link between miRISCs and deadenylases provides new insight into the mechanism of gene silencing by microRNAs." Cold Spring Harb Perspect Biol**4**(12).

Braunstein, S., K. Karpisheva, C. Pola, J. Goldberg, T. Hochman, H. Yee, J. Cangiarella, R. Arju, S. C. Formenti and R. J. Schneider (2007). "A hypoxia-controlled cap-dependent to cap-independent translation switch in breast cancer." Mol Cell**28**(3): 501-512.

Brina, D., S. Grosso, A. Miluzio and S. Biffo (2011). "Translational control by 80S formation and 60S availability: the central role of eIF6, a rate limiting factor in cell cycle progression and tumorigenesis." Cell cycle**10**(20): 3441-3446.

Brina, D., A. Miluzio, S. Ricciardi and S. Biffo (2015). "eIF6 anti-association activity is required for ribosome biogenesis, translational control and tumor progression." Biochim Biophys Acta**1849**(7): 830-835.

Brina, D., A. Miluzio, S. Ricciardi, K. Clarke, P. K. Davidsen, G. Viero, T. Tebaldi, N. Offenhäuser, J. Rozman, B. Rathkolb, S. Neschen, M. Klingenspor, E. Wolf, V. Gailus-Durner, H. Fuchs, M. Hrabe de Angelis, A. Quattrone, F. Falciani and S. Biffo (2015). "eIF6 coordinates insulin sensitivity and lipid metabolism by coupling translation to transcription." Nat Commun**6**: 8261.

Brugarolas, J., K. Moberg, S. D. Boyd, Y. Taya, T. Jacks and J. A. Lees (1999). "Inhibition of cyclin-dependent kinase 2 by p21 is necessary for retinoblastoma protein-mediated G1 arrest after gamma-irradiation." Proc Natl Acad Sci U S A**96**(3): 1002-1007.

Bussiere, C., Y. Hashem, S. Arora, J. Frank and A. W. Johnson (2012). "Integrity of the P-site is probed during maturation of the 60S ribosomal subunit." The Journal of cell biology**197**(6): 747-759.

Buttgereit, F. and M. D. Brand (1995). "A hierarchy of ATP-consuming processes in mammalian cells." Biochem J**312 (Pt 1)**: 163-167.

Calkhoven, C. F., C. Müller and A. Leutz (2002). "Translational control of gene expression and disease." Trends Mol Med**8**(12): 577-583.

Campisi, J. (2001). "Cellular senescence as a tumor-suppressor mechanism." Trends Cell Biol**11**(11): S27-31.

Cargnello, M. and P. P. Roux (2011). "Activation and function of the MAPKs and their substrates, the MAPK-activated protein kinases." Microbiol Mol Biol Rev**75**(1): 50-83.

Caron, E., S. Ghosh, Y. Matsuoka, D. Ashton-Beaucage, M. Therrien, S. Lemieux, C. Perreault, P. P. Roux and H. Kitano (2010). "A comprehensive map of the mTOR signaling network." Molecular systems biology**6**: 453.

Carriere, A., H. Ray, J. Blenis and P. P. Roux (2008). "The RSK factors of activating the Ras/MAPK signaling cascade." Front Biosci**13**: 4258-4275.

Ceci, M., C. Gaviraghi, C. Gorrini, L. A. Sala, N. Offenhauser, P. C. Marchisio and S. Biffo (2003). "Release of eIF6 (p27BBP) from the 60S subunit allows 80S ribosome assembly." Nature**426**(6966): 579-584.

Chauvin, C., V. Koka, A. Nouschi, V. Mieulet, C. Hoareau-Aveilla, A. Dreazen, N. Cagnard, W. Carpentier, T. Kiss, O. Meyuhas and M. Pende (2014). "Ribosomal protein S6 kinase activity controls the ribosome biogenesis transcriptional program." Oncogene**33**(4): 474-483.

Chiarle, R., J. Z. Gong, I. Guasparri, A. Pesci, J. Cai, J. Liu, W. J. Simmons, G. Dhall, J. Howes, R. Piva and G. Inghirami (2003). "NPM-ALK transgenic mice spontaneously develop T-cell lymphomas and plasma cell tumors." Blood**101**(5): 1919-1927.

Chiarle, R., W. J. Simmons, H. Cai, G. Dhall, A. Zamo, R. Raz, J. G. Karras, D. E. Levy and G. Inghirami (2005). "Stat3 is required for ALK-mediated lymphomagenesis and provides a possible therapeutic target." Nat Med**11**(6): 623-629.

Chiarle, R., C. Voena, C. Ambrogio, R. Piva and G. Inghirami (2008). "The anaplastic lymphoma kinase in the pathogenesis of cancer." Nat Rev Cancer**8**(1): 11-23.

Choudhari, R., V. G. Minero, M. Menotti, R. Pulito, C. Brakebusch, M. Compagno, C. Voena, C. Ambrogio and R. Chiarle (2016). "Redundant and nonredundant roles for Cdc42 and Rac1 in lymphomas developed in NPM-ALK transgenic mice." Blood**127**(10): 1297-1306.

Clarke, K., S. Ricciardi, T. Pearson, I. Bharudin, P. K. Davidsen, M. Bonomo, D. Brina, A. Scagliola, D. M. Simpson, R. J. Beynon, F. Khanim, J. Ankers, M. A. Sarzynski, S. Ghosh, A. Pisconti, J. Rozman, M. Hrabe de Angelis, C. Bunce, C. Stewart, S. Egginton, M. Caddick, M. Jackson, C. Bouchard, S. Biffo and F. Falciani (2017). "The Role of Eif6 in Skeletal Muscle Homeostasis Revealed by Endurance Training Co-expression Networks." Cell Rep**21**(6): 1507-1520.

Collado, M., M. A. Blasco and M. Serrano (2007). "Cellular senescence in cancer and aging." Cell**130**(2): 223-233.

D'Abronzo, L. S. and P. M. Ghosh (2018). "eIF4E Phosphorylation in Prostate Cancer." Neoplasia**20**(6): 563-573.

Donadini, A., A. Giodini, F. Sanvito, P. C. Marchisio and S. Biffo (2001). "The human ITGB4BP gene is constitutively expressed in vitro, but highly modulated in vivo." Gene**266**(1-2): 35-43.

Favaro, E., K. Bensaad, M. G. Chong, D. A. Tennant, D. J. Ferguson, C. Snell, G. Steers, H. Turley, J. L. Li, U. L. Günther, F. M. Buffa, A. McIntyre and A. L. Harris (2012). "Glucose utilization via glycogen phosphorylase sustains proliferation and prevents premature senescence in cancer cells." Cell Metab**16**(6): 751-764.

Ferreri, A. J., S. Govi, S. A. Pileri and K. J. Savage (2013). "Anaplastic large cell lymphoma, ALK-negative." Crit Rev Oncol Hematol**85**(2): 206-215.

Foss, F. M., P. L. Zinzani, J. M. Vose, R. D. Gascoyne, S. T. Rosen and K. Tobinai (2011). "Peripheral T-cell lymphoma." Blood**117**(25): 6756-6767.

Fukuchi-Shimogori, T., I. Ishii, K. Kashiwagi, H. Mashiba, H. Ekimoto and K. Igarashi (1997). "Malignant transformation by overproduction of translation initiation factor eIF4G." Cancer Res**57**(22): 5041-5044.

Fukunaga, R. and T. Hunter (1997). "MNK1, a new MAP kinase-activated protein kinase, isolated by a novel expression screening method for identifying protein kinase substrates." EMBO J**16**(8): 1921-1933.

Furic, L., L. Rong, O. Larsson, I. H. Koumakpayi, K. Yoshida, A. Brueschke, E. Petroulakis, N. Robichaud, M. Pollak, L. A. Gaboury, P. P. Pandolfi, F. Saad and N. Sonenberg (2010). "eIF4E phosphorylation promotes tumorigenesis and is associated with prostate cancer progression." Proc Natl Acad Sci U S A**107**(32): 14134-14139.

Ganapathi, K. A. and A. Shimamura (2008). "Ribosomal dysfunction and inherited marrow failure." Br J Haematol**141**(3): 376-387.

Gandin, V., A. Miluzio, A. M. Barbieri, A. Beugnet, H. Kiyokawa, P. C. Marchisio and S. Biffo (2008). "Eukaryotic initiation factor 6 is rate-limiting in translation, growth and transformation." Nature**455**(7213): 684-688.

Gangloff, Y. G., M. Mueller, S. G. Dann, P. Svoboda, M. Sticker, J. F. Spetz, S. H. Um, E. J. Brown, S. Cereghini, G. Thomas and S. C. Kozma (2004). "Disruption of the mouse mTOR gene leads to early postimplantation lethality and prohibits embryonic stem cell development." Mol Cell Biol**24**(21): 9508-9516.

Gartmann, M., M. Blau, J. P. Armache, T. Mielke, M. Topf and R. Beckmann (2010). "Mechanism of eIF6-mediated inhibition of ribosomal subunit joining." The Journal of biological chemistry**285**(20): 14848-14851.

Gatza, M. L., G. O. Silva, J. S. Parker, C. Fan and C. M. Perou (2014). "An integrated genomics approach identifies drivers of proliferation in luminal-subtype human breast cancer." Nat Genet**46**(10): 1051-1059.

Gebauer, F. and M. W. Hentze (2004). "Molecular mechanisms of translational control." Nat Rev Mol Cell Biol**5**(10): 827-835.

Genuth, N. R. and M. Barna (2018). "Heterogeneity and specialized functions of translation machinery: from genes to organisms." Nat Rev Genet**19**(7): 431-452.

Goudarzi, K. M. and M. S. Lindström (2016). "Role of ribosomal protein mutations in tumor development (Review)." Int J Oncol**48**(4): 1313-1324.

Groft, C. M., R. Beckmann, A. Sali and S. K. Burley (2000). "Crystal structures of ribosome anti-association factor IF6." Nature structural biology**7**(12): 1156-1164.

Guertin, D. A. and D. M. Sabatini (2007). "Defining the role of mTOR in cancer." Cancer cell**12**(1): 9-22.

Hallberg, B. and R. H. Palmer (2013). "Mechanistic insight into ALK receptor tyrosine kinase in human cancer biology." Nat Rev Cancer**13**(10): 685-700.

Harris, M. N., B. Ozpolat, F. Abdi, S. Gu, A. Legler, K. G. Mawuenyega, M. Tirado-Gomez, G. Lopez-Berestein and X. Chen (2004). "Comparative proteomic analysis of all-trans-retinoic acid treatment reveals systematic posttranscriptional control mechanisms in acute promyelocytic leukemia." Blood**104**(5): 1314-1323.

Harrison, D. E., R. Strong, Z. D. Sharp, J. F. Nelson, C. M. Astle, K. Flurkey, N. L. Nadon, J. E. Wilkinson, K. Frenkel, C. S. Carter, M. Pahor, M. A. Javors, E. Fernandez and R. A. Miller (2009). "Rapamycin fed late in life extends lifespan in genetically heterogeneous mice." Nature**460**(7253): 392-395.

Hart, L. S., J. T. Cunningham, T. Datta, S. Dey, F. Tameire, S. L. Lehman, B. Qiu, H. Zhang, G. Cerniglia, M. Bi, Y. Li, Y. Gao, H. Liu, C. Li, A. Maity, A. Thomas-Tikhonenko, A. E. Perl, A. Koong, S. Y. Fuchs, J. A. Diehl, I. G. Mills, D. Ruggero and C. Koumenis (2012). "ER stress-mediated autophagy promotes Myc-dependent transformation and tumor growth." J Clin Invest**122**(12): 4621-4634.

Hay, N. and N. Sonenberg (2004). "Upstream and downstream of mTOR." Genes Dev**18**(16): 1926-1945.

Haydon, M. S., J. D. Googe, D. S. Sorrells, G. E. Ghali and B. D. Li (2000). "Progression of eIF4e gene amplification and overexpression in benign and malignant tumors of the head and neck." Cancer**88**(12): 2803-2810.

Hellen, C. U. and P. Sarnow (2001). "Internal ribosome entry sites in eukaryotic mRNA molecules." Genes & development**15**(13): 1593-1612.

Hellen, C. U. T. (2018). "Translation Termination and Ribosome Recycling in Eukaryotes." Cold Spring Harb Perspect Biol.

Hershey, J. W., N. Sonenberg and M. B. Mathews (2012). "Principles of translational control: an overview." Cold Spring Harb Perspect Biol**4**(12).

Hershey, J. W. B., N. Sonenberg and M. B. Mathews (2018). "Principles of Translational Control." Cold Spring Harb Perspect Biol.

Hinnebusch, A. G. (2014). "The scanning mechanism of eukaryotic translation initiation." Annu Rev Biochem**83**: 779-812.

Hinnebusch, A. G. (2017). "Structural Insights into the Mechanism of Scanning and Start Codon Recognition in Eukaryotic Translation Initiation." Trends Biochem Sci**42**(8): 589-611.

Hinnebusch, A. G., I. P. Ivanov and N. Sonenberg (2016). "Translational control by 5'-untranslated regions of eukaryotic mRNAs." Science**352**(6292): 1413-1416.

Holcik, M. and T. V. Pestova (2007). "Translation mechanism and regulation: old players, new concepts. Meeting on translational control and non-coding RNA." EMBO reports**8**(7): 639-643.

Holcik, M. and N. Sonenberg (2005). "Translational control in stress and apoptosis." Nature reviews. Molecular cell biology**6**(4): 318-327.

Horiguchi, M., S. Koyanagi, A. Okamoto, S. O. Suzuki, N. Matsunaga and S. Ohdo (2012). "Stress-regulated transcription factor ATF4 promotes neoplastic transformation by suppressing expression of the INK4a/ARF cell senescence factors." Cancer Res**72**(2): 395-401.

Huang, L., Y. Sowa, T. Sakai and A. B. Pardee (2000). "Activation of the p21WAF1/CIP1 promoter independent of p53 by the histone deacetylase inhibitor suberoylanilide hydroxamic acid (SAHA) through the Sp1 sites." Oncogene**19**(50): 5712-5719.

Isozaki, H., N. Takigawa and K. Kiura (2015). "Mechanisms of Acquired Resistance to ALK Inhibitors and the Rationale for Treating ALK-positive Lung Cancer." Cancers (Basel)**7**(2): 763-783.

Iwahara, T., J. Fujimoto, D. Wen, R. Cupples, N. Bucay, T. Arakawa, S. Mori, B. Ratzkin and T. Yamamoto (1997). "Molecular characterization of ALK, a receptor tyrosine kinase expressed specifically in the nervous system." Oncogene**14**(4): 439-449.

Jackson, R. J., C. U. Hellen and T. V. Pestova (2010). "The mechanism of eukaryotic translation initiation and principles of its regulation." Nat Rev Mol Cell Biol**11**(2): 113-127.

Jiang, P., W. Du, A. Mancuso, K. E. Wellen and X. Yang (2013). "Reciprocal regulation of p53 and malic enzymes modulates metabolism and senescence." Nature**493**(7434): 689-693.

Johannes, G. and P. Sarnow (1998). "Cap-independent polysomal association of natural mRNAs encoding c-myc, BiP, and eIF4G conferred by internal ribosome entry sites." RNA**4**(12): 1500-1513.

Johnstone, T. G., A. A. Bazzini and A. J. Giraldez (2016). "Upstream ORFs are prevalent translational repressors in vertebrates." EMBO J**35**(7): 706-723.

Jopling, C. L. and A. E. Willis (2001). "N-myc translation is initiated via an internal ribosome entry segment that displays enhanced activity in neuronal cells." Oncogene**20**(21): 2664-2670.

Kaeberlein, M., R. W. Powers, K. K. Steffen, E. A. Westman, D. Hu, N. Dang, E. O. Kerr, K. T. Kirkland, S. Fields and B. K. Kennedy (2005). "Regulation of yeast replicative life span by TOR and Sch9 in response to nutrients." Science**310**(5751): 1193-1196.

Kaplon, J., L. Zheng, K. Meissl, B. Chaneton, V. A. Selivanov, G. Mackay, S. H. van der Burg, E. M. Verdegaal, M. Cascante, T. Shlomi, E. Gottlieb and D. S. Peeper (2013). "A key

role for mitochondrial gatekeeper pyruvate dehydrogenase in oncogene-induced senescence." Nature**498**(7452): 109-112.

Klinge, S., F. Voigts-Hoffmann, M. Leibundgut, S. Arpagaus and N. Ban (2011). "Crystal structure of the eukaryotic 60S ribosomal subunit in complex with initiation factor 6." Science**334**(6058): 941-948.

Koivunen, J. P., C. Mermel, K. Zejnullahu, C. Murphy, E. Lifshits, A. J. Holmes, H. G. Choi, J. Kim, D. Chiang, R. Thomas, J. Lee, W. G. Richards, D. J. Sugarbaker, C. Ducko, N. Lindeman, J. P. Marcoux, J. A. Engelman, N. S. Gray, C. Lee, M. Meyerson and P. A. Jänne (2008). "EML4-ALK fusion gene and efficacy of an ALK kinase inhibitor in lung cancer." Clin Cancer Res**14**(13): 4275-4283.

Komar, A. A. and M. Hatzoglou (2011). "Cellular IRES-mediated translation: the war of ITAFs in pathophysiological states." Cell cycle**10**(2): 229-240.

Kondoh, N., M. Shuda, K. Tanaka, T. Wakatsuki, A. Hada and M. Yamamoto (2001). "Enhanced expression of S8, L12, L23a, L27 and L30 ribosomal protein mRNAs in human hepatocellular carcinoma." Anticancer Res**21**(4A): 2429-2433.

Koromilas, A. E. (2015). "Roles of the translation initiation factor eIF2alpha serine 51 phosphorylation in cancer formation and treatment." Biochimica et biophysica acta**1849**(7): 871-880.

Kozak, M. (1987). "An analysis of 5'-noncoding sequences from 699 vertebrate messenger RNAs." Nucleic Acids Res**15**(20): 8125-8148.

Krenacs, L., A. Wellmann, L. Sorbara, A. W. Himmelmann, E. Bagdi, E. S. Jaffe and M. Raffeld (1997). "Cytotoxic cell antigen expression in anaplastic large cell lymphomas of T- and null-cell type and Hodgkin's disease: evidence for distinct cellular origin." Blood**89**(3): 980-989.

Lackner, D. H. and J. Bahler (2008). "Translational control of gene expression from transcripts to transcriptomes." International review of cell and molecular biology**271**: 199-251.

Laimer, D., H. Dolznig, K. Kollmann, P. W. Vesely, M. Schlederer, O. Merkel, A. I. Schiefer, M. R. Hassler, S. Heider, L. Amenitsch, C. Thallinger, P. B. Staber, I. Simonitsch-Klupp, M. Artaker, S. Lagger, S. D. Turner, S. Pileri, P. P. Piccaluga, P. Valent, K. Messana, I. Landra, T. Weichhart, S. Knapp, M. Shehata, M. Todaro, V. Sexl, G. Höfler, R. Piva, E. Medico, B. A. Ruggeri, M. Cheng, R. Eferl, G. Egger, J. M. Penninger, U. Jaeger, R. Moriggl, G. Inghirami and L. Kenner (2012). "PDGFR blockade is a rational and effective therapy for NPM-ALK-driven lymphomas." Nat Med**18**(11): 1699-1704.

Laplante, M. and D. M. Sabatini (2012). "mTOR signaling in growth control and disease." Cell**149**(2): 274-293.

Larsson, O., S. Li, O. A. Issaenko, S. Avdulov, M. Peterson, K. Smith, P. B. Bitterman and V. A. Polunovsky (2007). "Eukaryotic translation initiation factor 4E induced progression of primary human mammary epithelial cells along the cancer pathway is associated with targeted translational deregulation of oncogenic drivers and inhibitors." Cancer Res**67**(14): 6814-6824.

Lee, A. S., P. J. Kranzusch and J. H. Cate (2015). "eIF3 targets cell-proliferation messenger RNAs for translational activation or repression." Nature**522**(7554): 111-114.

Leontieva, O. V., Z. N. Demidenko and M. V. Blagosklonny (2013). "S6K in geroconversion." Cell Cycle**12**(20): 3249-3252.

Leppek, K., R. Das and M. Barna (2018). "Functional 5' UTR mRNA structures in eukaryotic translation regulation and how to find them." Nat Rev Mol Cell Biol**19**(3): 158-174.

Lin, H. K., Z. Chen, G. Wang, C. Nardella, S. W. Lee, C. H. Chan, W. L. Yang, J. Wang, A. Egia, K. I. Nakayama, C. Cordon-Cardo, J. Teruya-Feldstein and P. P. Pandolfi (2010). "Skp2 targeting suppresses tumorigenesis by Arf-p53-independent cellular senescence." Nature**464**(7287): 374-379.

Loreni, F., M. Mancino and S. Biffo (2014). "Translation factors and ribosomal proteins control tumor onset and progression: how?" Oncogene**33**(17): 2145-2156.

Ma, X. M. and J. Blenis (2009). "Molecular mechanisms of mTOR-mediated translational control." Nature reviews. Molecular cell biology**10**(5): 307-318.

Manfrini, N., S. Ricciardi, A. Miluzio, M. Fedeli, A. Scagliola, S. Gallo, D. Brina, T. Adler, D. H. Busch, V. Gailus-Durner, H. Fuchs, M. Hrabě de Angelis and S. Biffo (2017). "High levels of eukaryotic Initiation Factor 6 (eIF6) are required for immune system homeostasis and for steering the glycolytic flux of TCR-stimulated CD4." Dev Comp Immunol**77**: 69-76.

Martin, B., R. Sanz, R. Aragues, B. Oliva and A. Sierra (2008). "Functional clustering of metastasis proteins describes plastic adaptation resources of breast-cancer cells to new microenvironments." Journal of proteome research**7**(8): 3242-3253.

Martineau, Y., R. Azar, D. Müller, C. Lasfargues, S. El Khawand, R. Anesia, J. Pelletier, C. Bousquet and S. Pyronnet (2014). "Pancreatic tumours escape from translational control through 4E-BP1 loss." Oncogene**33**(11): 1367-1374.

Martinelli, P., P. Bonetti, C. Sironi, G. Pruneri, C. Fumagalli, P. R. Raviele, S. Volorio, S. Pileri, R. Chiarle, F. K. McDuff, B. K. Tusi, S. D. Turner, G. Inghirami, P. G. Pelicci and E.

Colombo (2011). "The lymphoma-associated NPM-ALK oncogene elicits a p16INK4a/pRb-dependent tumor-suppressive pathway." Blood**117**(24): 6617-6626.

McHugh, D. and J. Gil (2018). "Senescence and aging: Causes, consequences, and therapeutic avenues." J Cell Biol**217**(1): 65-77.

Medeiros, L. J. and K. S. Elenitoba-Johnson (2007). "Anaplastic Large Cell Lymphoma." Am J Clin Pathol**127**(5): 707-722.

Menne, T. F., B. Goyenechea, N. Sánchez-Puig, C. C. Wong, L. M. Tonkin, P. J. Ancliff, R. L. Brost, M. Costanzo, C. Boone and A. J. Warren (2007). "The Shwachman-Bodian-Diamond syndrome protein mediates translational activation of ribosomes in yeast." Nat Genet**39**(4): 486-495.

Meyer, K. D., D. P. Patil, J. Zhou, A. Zinoviev, M. A. Skabkin, O. Elemento, T. V. Pestova, S. B. Qian and S. R. Jaffrey (2015). "5' UTR m(6)A Promotes Cap-Independent Translation." Cell**163**(4): 999-1010.

Miluzio, A., A. Beugnet, S. Grosso, D. Brina, M. Mancino, S. Campaner, B. Amati, A. de Marco and S. Biffo (2011). "Impairment of cytoplasmic eIF6 activity restricts lymphomagenesis and tumor progression without affecting normal growth." Cancer cell**19**(6): 765-775.

Miluzio, A., A. Beugnet, V. Volta and S. Biffo (2009). "Eukaryotic initiation factor 6 mediates a continuum between 60S ribosome biogenesis and translation." EMBO reports**10**(5): 459-465.

Miluzio, A., S. Oliveto, E. Pesce, L. Mutti, B. Murer, S. Grosso, S. Ricciardi, D. Brina and S. Biffo (2015). "Expression and activity of eIF6 trigger malignant pleural mesothelioma growth in vivo." Oncotarget**6**(35): 37471-37485.

Montagne, J., M. J. Stewart, H. Stocker, E. Hafen, S. C. Kozma and G. Thomas (1999). "Drosophila S6 kinase: a regulator of cell size." Science**285**(5436): 2126-2129.

Montanaro, L., D. Treré and M. Derenzini (2008). "Nucleolus, ribosomes, and cancer." Am J Pathol**173**(2): 301-310.

Mora, J., D. A. Filippa, J. Qin and N. Wollner (2003). "Lymphoblastic lymphoma of childhood and the LSA2-L2 protocol: the 30-year experience at Memorial-Sloan-Kettering Cancer Center." Cancer**98**(6): 1283-1291.

Morris, S. W., M. N. Kirstein, M. B. Valentine, K. G. Dittmer, D. N. Shapiro, D. L. Saltman and A. T. Look (1994). "Fusion of a kinase gene, ALK, to a nucleolar protein gene, NPM, in non-Hodgkin's lymphoma." Science**263**(5151): 1281-1284.

Murakami, M., T. Ichisaka, M. Maeda, N. Oshiro, K. Hara, F. Edenhofer, H. Kiyama, K. Yonezawa and S. Yamanaka (2004). "mTOR is essential for growth and proliferation in early mouse embryos and embryonic stem cells." Mol Cell Biol**24**(15): 6710-6718.

Muñoz-Espín, D., M. Cañamero, A. Maraver, G. Gómez-López, J. Contreras, S. Murillo-Cuesta, A. Rodríguez-Baeza, I. Varela-Nieto, J. Ruberte, M. Collado and M. Serrano (2013). "Programmed cell senescence during mammalian embryonic development." Cell**155**(5): 1104-1118.

Nacarelli, T. and C. Sell (2017). "Targeting metabolism in cellular senescence, a role for intervention." Mol Cell Endocrinol**455**: 83-92.

Nandagopal, N. and P. P. Roux (2015). "Regulation of global and specific mRNA translation by the mTOR signaling pathway." Translation (Austin)**3**(1): e983402.

Nicke, B., J. Bastien, S. J. Khanna, P. H. Warne, V. Cowling, S. J. Cook, G. Peters, O. Delpuech, A. Schulze, K. Berns, J. Mullenders, R. L. Beijersbergen, R. Bernards, T. S. Ganesan, J. Downward and D. C. Hancock (2005). "Involvement of MINK, a Ste20 family kinase, in Ras oncogene-induced growth arrest in human ovarian surface epithelial cells." Mol Cell**20**(5): 673-685.

Nilsson, J., J. Sengupta, J. Frank and P. Nissen (2004). "Regulation of eukaryotic translation by the RACK1 protein: a platform for signalling molecules on the ribosome." EMBO Rep**5**(12): 1137-1141.

Oyadomari, S., H. P. Harding, Y. Zhang, M. Oyadomari and D. Ron (2008). "Dephosphorylation of translation initiation factor 2alpha enhances glucose tolerance and attenuates hepatosteatosis in mice." Cell metabolism**7**(6): 520-532.

Palmer, R. H., E. Vernersson, C. Grabbe and B. Hallberg (2009). "Anaplastic lymphoma kinase: signalling in development and disease." Biochem J**420**(3): 345-361.

Pavitt, G. D. (2018). "Regulation of translation initiation factor eIF2B at the hub of the integrated stress response." Wiley Interdiscip Rev RNA: e1491.

Payne, V. A., W. S. Au, C. E. Lowe, S. M. Rahman, J. E. Friedman, S. O'Rahilly and J. J. Rochford (2009). "C/EBP transcription factors regulate SREBP1c gene expression during adipogenesis." Biochem J**425**(1): 215-223.

Pende, M., S. H. Um, V. Mieulet, M. Sticker, V. L. Goss, J. Mestan, M. Mueller, S. Fumagalli, S. C. Kozma and G. Thomas (2004). "S6K1(-/-)/S6K2(-/-) mice exhibit perinatal lethality and rapamycin-sensitive 5'-terminal oligopyrimidine mRNA translation and reveal a

mitogen-activated protein kinase-dependent S6 kinase pathway." Mol Cell Biol**24**(8): 3112-3124.

Pesce, E., C. Minici, J. Babetaler, E. Hurt, M. Degano, P. Calamita and S. Biffo (2015). "Direct and high throughput (HT) interactions on the ribosomal surface by iRIA." Scientific reports**5**: 15401.

Pestova, T. V., V. G. Kolupaeva, I. B. Lomakin, E. V. Pilipenko, I. N. Shatsky, V. I. Agol and C. U. Hellen (2001). "Molecular mechanisms of translation initiation in eukaryotes." Proc Natl Acad Sci U S A**98**(13): 7029-7036.

Peña-Llopis, S., S. Vega-Rubin-de-Celis, J. C. Schwartz, N. C. Wolff, T. A. Tran, L. Zou, X. J. Xie, D. R. Corey and J. Brugarolas (2011). "Regulation of TFEB and V-ATPases by mTORC1." EMBO J**30**(16): 3242-3258.

Pisarev, A. V., C. U. Hellen and T. V. Pestova (2007). "Recycling of eukaryotic posttermination ribosomal complexes." Cell**131**(2): 286-299.

Pisarev, A. V., M. A. Skabkin, V. P. Pisareva, O. V. Skabkina, A. M. Rakotondrafara, M. W. Hentze, C. U. Hellen and T. V. Pestova (2010). "The role of ABCE1 in eukaryotic posttermination ribosomal recycling." Mol Cell**37**(2): 196-210.

Poon, R. Y., W. Jiang, H. Toyoshima and T. Hunter (1996). "Cyclin-dependent kinases are inactivated by a combination of p21 and Thr-14/Tyr-15 phosphorylation after UV-induced DNA damage." J Biol Chem**271**(22): 13283-13291.

Powers, R. W., M. Kaeberlein, S. D. Caldwell, B. K. Kennedy and S. Fields (2006). "Extension of chronological life span in yeast by decreased TOR pathway signaling." Genes Dev**20**(2): 174-184.

Pradet-Balade, B., F. Boulmé, H. Beug, E. W. Müllner and J. A. Garcia-Sanz (2001). "Translation control: bridging the gap between genomics and proteomics?" Trends Biochem Sci**26**(4): 225-229.

Preiss, T. and M. W. Hentze (1999). "From factors to mechanisms: translation and translational control in eukaryotes." Curr Opin Genet Dev**9**(5): 515-521.

Pulford, K., L. Lamant, S. W. Morris, L. H. Butler, K. M. Wood, D. Stroud, G. Delsol and D. Y. Mason (1997). "Detection of anaplastic lymphoma kinase (ALK) and nucleolar protein nucleophosmin (NPM)-ALK proteins in normal and neoplastic cells with the monoclonal antibody ALK1." Blood**89**(4): 1394-1404.

Raught, B. and A. C. Gingras (1999). "eIF4E activity is regulated at multiple levels." Int J Biochem Cell Biol**31**(1): 43-57.

Raught, B., A. C. Gingras, S. P. Gygi, H. Imataka, S. Morino, A. Gradi, R. Aebersold and N. Sonenberg (2000). "Serum-stimulated, rapamycin-sensitive phosphorylation sites in the eukaryotic translation initiation factor 4GI." EMBO J**19**(3): 434-444.

Raught, B., F. Peiretti, A. C. Gingras, M. Livingstone, D. Shahbazian, G. L. Mayeur, R. D. Polakiewicz, N. Sonenberg and J. W. Hershey (2004). "Phosphorylation of eucaryotic translation initiation factor 4B Ser422 is modulated by S6 kinases." The EMBO journal**23**(8): 1761-1769.

Redaelli, S., M. Ceccon, L. Antolini, R. Rigolio, A. Pirola, M. Peronaci, C. Gambacorti-Passerini and L. Mologni (2016). "Synergistic activity of ALK and mTOR inhibitors for the treatment of NPM-ALK positive lymphoma." Oncotarget**7**(45): 72886-72897.

Rizza, S., S. Cardaci, C. Montagna, G. Di Giacomo, D. De Zio, M. Bordi, E. Maiani, S. Campello, A. Borreca, A. A. Puca, J. S. Stamler, F. Cecconi and G. Filomeni (2018). "-nitrosylation drives cell senescence and aging in mammals by controlling mitochondrial dynamics and mitophagy." Proc Natl Acad Sci U S A**115**(15): E3388-E3397.

Robichaud, N., N. Sonenberg, D. Ruggero and R. J. Schneider (2018). "Translational Control in Cancer." Cold Spring Harb Perspect Biol.

Rosso, P., G. Cortesina, F. Sanvito, A. Donadini, B. Di Benedetto, S. Biffo and P. C. Marchisio (2004). "Overexpression of p27BBP in head and neck carcinomas and their lymph node metastases." Head Neck**26**(5): 408-417.

Roux, P. P. and I. Topisirovic (2012). "Regulation of mRNA translation by signaling pathways." Cold Spring Harb Perspect Biol**4**(11).

Roux, P. P. and I. Topisirovic (2018). "Signaling Pathways Involved in the Regulation of mRNA Translation." Mol Cell Biol**38**(12).

Ruggero, D. (2013). "Translational control in cancer etiology." Cold Spring Harbor perspectives in biology**5**(2).

Ruggero, D. and P. P. Pandolfi (2003). "Does the ribosome translate cancer?" Nat Rev Cancer**3**(3): 179-192.

Russell, D. W. and L. L. Spremulli (1979). "Purification and characterization of a ribosome dissociation factor (eukaryotic initiation factor 6) from wheat germ." The Journal of biological chemistry**254**(18): 8796-8800.

Ruvinsky, I., N. Sharon, T. Lerer, H. Cohen, M. Stolovich-Rain, T. Nir, Y. Dor, P. Zisman and O. Meyuhas (2005). "Ribosomal protein S6 phosphorylation is a determinant of cell size and glucose homeostasis." Genes & development**19**(18): 2199-2211.

Salaverria, I., S. Beà, A. Lopez-Guillermo, V. Lespinet, M. Pinyol, B. Burkhardt, L. Lamant, A. Zettl, D. Horsman, R. Gascoyne, G. Ott, R. Siebert, G. Delsol and E. Campo (2008). "Genomic profiling reveals different genetic aberrations in systemic ALK-positive and ALK-negative anaplastic large cell lymphomas." Br J Haematol**140**(5): 516-526.

Sanvito, F., S. Piatti, A. Villa, M. Bossi, G. Lucchini, P. C. Marchisio and S. Biffo (1999). "The beta4 integrin interactor p27(BBP/eIF6) is an essential nuclear matrix protein involved in 60S ribosomal subunit assembly." The Journal of cell biology**144**(5): 823-837.

Sanvito, F., F. Vivoli, S. Gambini, G. Santambrogio, M. Catena, E. Viale, F. Veglia, A. Donadini, S. Biffo and P. C. Marchisio (2000). "Expression of a highly conserved protein, p27BBP, during the progression of human colorectal cancer." Cancer research**60**(3): 510-516.

Schmitt, C. A., J. S. Fridman, M. Yang, S. Lee, E. Baranov, R. M. Hoffman and S. W. Lowe (2002). "A senescence program controlled by p53 and p16INK4a contributes to the outcome of cancer therapy." Cell**109**(3): 335-346.

Serrano, M., A. W. Lin, M. E. McCurrach, D. Beach and S. W. Lowe (1997). "Oncogenic ras provokes premature cell senescence associated with accumulation of p53 and p16INK4a." Cell**88**(5): 593-602.

Shankland, K. R., J. O. Armitage and B. W. Hancock (2012). "Non-Hodgkin lymphoma." Lancet**380**(9844): 848-857.

Shi, Y., H. Zhai, X. Wang, Z. Han, C. Liu, M. Lan, J. Du, C. Guo, Y. Zhang, K. Wu and D. Fan (2004). "Ribosomal proteins S13 and L23 promote multidrug resistance in gastric cancer cells by suppressing drug-induced apoptosis." Exp Cell Res**296**(2): 337-346.

Shirokikh, N. E. and A. S. Spirin (2008). "Poly(A) leader of eukaryotic mRNA bypasses the dependence of translation on initiation factors." Proc Natl Acad Sci U S A**105**(31): 10738-10743.

Shor, B., D. Cavender and C. Harris (2009). "A kinase-dead knock-in mutation in mTOR leads to early embryonic lethality and is dispensable for the immune system in heterozygous mice." BMC Immunol**10**: 28.

Shuda, M., N. Kondoh, K. Tanaka, A. Ryo, T. Wakatsuki, A. Hada, N. Goseki, T. Igari, K. Hatsuse, T. Aihara, S. Horiuchi, M. Shichita, N. Yamamoto and M. Yamamoto (2000). "Enhanced expression of translation factor mRNAs in hepatocellular carcinoma." Anticancer Res**20**(4): 2489-2494.

Si, K. and U. Maitra (1999). "The Saccharomyces cerevisiae homologue of mammalian translation initiation factor 6 does not function as a translation initiation factor." Molecular and cellular biology**19**(2): 1416-1426.

Silvera, D., S. C. Formenti and R. J. Schneider (2010). "Translational control in cancer." Nat Rev Cancer**10**(4): 254-266.

Sinvani, H., O. Haimov, Y. Svitkin, N. Sonenberg, A. Tamarkin-Ben-Harush, B. Viollet and R. Dikstein (2015). "Translational tolerance of mitochondrial genes to metabolic energy stress involves TISU and eIF1-eIF4GI cooperation in start codon selection." Cell Metab**21**(3): 479-492.

Soda, M., Y. L. Choi, M. Enomoto, S. Takada, Y. Yamashita, S. Ishikawa, S. Fujiwara, H. Watanabe, K. Kurashina, H. Hatanaka, M. Bando, S. Ohno, Y. Ishikawa, H. Aburatani, T. Niki, Y. Sohara, Y. Sugiyama and H. Mano (2007). "Identification of the transforming EML4-ALK fusion gene in non-small-cell lung cancer." Nature**448**(7153): 561-566.

Sonenberg, N. and A. G. Hinnebusch (2009). "Regulation of translation initiation in eukaryotes: mechanisms and biological targets." Cell**136**(4): 731-745.

Storer, M., A. Mas, A. Robert-Moreno, M. Pecoraro, M. C. Ortells, V. Di Giacomo, R. Yosef, N. Pilpel, V. Krizhanovsky, J. Sharpe and W. M. Keyes (2013). "Senescence is a developmental mechanism that contributes to embryonic growth and patterning." Cell**155**(5): 1119-1130.

Tejada, S., M. V. Lobo, M. García-Villanueva, S. Sacristán, M. I. Pérez-Morgado, M. Salinas and M. E. Martín (2009). "Eukaryotic initiation factors (eIF) 2alpha and 4E expression, localization, and phosphorylation in brain tumors." J Histochem Cytochem**57**(5): 503-512.

Truitt, M. L., C. S. Conn, Z. Shi, X. Pang, T. Tokuyasu, A. M. Coady, Y. Seo, M. Barna and D. Ruggero (2015). "Differential Requirements for eIF4E Dose in Normal Development and Cancer." Cell**162**(1): 59-71.

Truitt, M. L. and D. Ruggero (2016). "New frontiers in translational control of the cancer genome." Nat Rev Cancer**16**(5): 288-304.

Turner, S. D., R. Tooze, K. Maclennan and D. R. Alexander (2003). "Vav-promoter regulated oncogenic fusion protein NPM-ALK in transgenic mice causes B-cell lymphomas with hyperactive Jun kinase." Oncogene**22**(49): 7750-7761.

Valenzuela, D. M., A. Chaudhuri and U. Maitra (1982). "Eukaryotic ribosomal subunit anti-association activity of calf liver is contained in a single polypeptide chain protein of Mr =

25,500 (eukaryotic initiation factor 6)." The Journal of biological chemistry**257**(13): 7712-7719.

Volta, V., A. Beugnet, S. Gallo, L. Magri, D. Brina, E. Pesce, P. Calamita, F. Sanvito and S. Biffo (2013). "RACK1 depletion in a mouse model causes lethality, pigmentation deficits and reduction in protein synthesis efficiency." Cellular and molecular life sciences : CMLS**70**(8): 1439-1450.

Wang, C., Z. Huang, Y. Du, Y. Cheng, S. Chen and F. Guo (2010). "ATF4 regulates lipid metabolism and thermogenesis." Cell Res**20**(2): 174-184.

Warner, J. R. (1999). "The economics of ribosome biosynthesis in yeast." Trends Biochem Sci**24**(11): 437-440.

Wek, R. C. (2018). "Role of eIF2α Kinases in Translational Control and Adaptation to Cellular Stress." Cold Spring Harb Perspect Biol**10**(7).

Wendel, H. G., R. L. Silva, A. Malina, J. R. Mills, H. Zhu, T. Ueda, R. Watanabe-Fukunaga, R. Fukunaga, J. Teruya-Feldstein, J. Pelletier and S. W. Lowe (2007). "Dissecting eIF4E action in tumorigenesis." Genes Dev**21**(24): 3232-3237.

Wiley, C. D., M. C. Velarde, P. Lecot, S. Liu, E. A. Sarnoski, A. Freund, K. Shirakawa, H. W. Lim, S. S. Davis, A. Ramanathan, A. A. Gerencser, E. Verdin and J. Campisi (2016). "Mitochondrial Dysfunction Induces Senescence with a Distinct Secretory Phenotype." Cell Metab**23**(2): 303-314.

Wilson, F. H., C. M. Johannessen, F. Piccioni, P. Tamayo, J. W. Kim, E. M. Van Allen, S. M. Corsello, M. Capelletti, A. Calles, M. Butaney, T. Sharifnia, S. B. Gabriel, J. P. Mesirov, W. C. Hahn, J. A. Engelman, M. Meyerson, D. E. Root, P. A. Jänne and L. A. Garraway (2015). "A functional landscape of resistance to ALK inhibition in lung cancer." Cancer Cell**27**(3): 397-408.

Wong, C. C., D. Traynor, N. Basse, R. R. Kay and A. J. Warren (2011). "Defective ribosome assembly in Shwachman-Diamond syndrome." Blood**118**(16): 4305-4312.

Woolford, J. L., Jr. and S. J. Baserga (2013). "Ribosome biogenesis in the yeast Saccharomyces cerevisiae." Genetics**195**(3): 643-681.

Wu, J., J. Savooji and D. Liu (2016). "Second- and third-generation ALK inhibitors for non-small cell lung cancer." J Hematol Oncol**9**: 19.

Xing, X. and A. L. Feldman (2015). "Anaplastic large cell lymphomas: ALK positive, ALK negative, and primary cutaneous." Adv Anat Pathol**22**(1): 29-49.

Yang, H. S., A. P. Jansen, A. A. Komar, X. Zheng, W. C. Merrick, S. Costes, S. J. Lockett, N. Sonenberg and N. H. Colburn (2003). "The transformation suppressor Pdcd4 is a novel eukaryotic translation initiation factor 4A binding protein that inhibits translation." Mol Cell Biol**23**(1): 26-37.

Yang, S., J. Cui, Y. Yang, Z. Liu, H. Yan, C. Tang, H. Wang, H. Qin, X. Li, J. Li, W. Wang, Y. Huang and H. Gao (2016). "Over-expressed RPL34 promotes malignant proliferation of non-small cell lung cancer cells." Gene**576**(1 Pt 3): 421-428.

Zhang, Q., F. Wei, H. Y. Wang, X. Liu, D. Roy, Q. B. Xiong, S. Jiang, A. Medvec, G. Danet-Desnoyers, C. Watt, E. Tomczak, M. Kalos, J. L. Riley and M. A. Wasik (2013). "The potent oncogene NPM-ALK mediates malignant transformation of normal human CD4(+) T lymphocytes." Am J Pathol**183**(6): 1971-1980.

Zheng, L., S. Cardaci, L. Jerby, E. D. MacKenzie, M. Sciacovelli, T. I. Johnson, E. Gaude, A. King, J. D. Leach, R. Edrada-Ebel, A. Hedley, N. A. Morrice, G. Kalna, K. Blyth, E. Ruppin, C. Frezza and E. Gottlieb (2015). "Fumarate induces redox-dependent senescence by modifying glutathione metabolism." Nat Commun**6**: 6001.

Zhou, J., J. Wan, X. Gao, X. Zhang, S. R. Jaffrey and S. B. Qian (2015). "Dynamic m(6)A mRNA methylation directs translational control of heat shock response." Nature**526**(7574): 591-594.

Zoncu, R., A. Efeyan and D. M. Sabatini (2011). "mTOR: from growth signal integration to cancer, diabetes and ageing." Nature reviews. Molecular cell biology**12**(1): 21-35.

7. Appendix

Manuscript in preparation

Alessandra Scagliola is the co-principal investigator of a side-project aimed to investigate the effects of eIF6 depletion in metabolic disorders. She is responsible for experimental design, analysis of data and management of the project.
The manuscript is in preparation. Please find here a brief report with the aim of the project and the main results obtained.

eIF6 depletion directly protects against the metabolic syndrome reducing lipid metabolism and increasing mitochondrial activity through the compensatory activation of the mTOR pathway

eIF6 (Eukaryotic Initiation Factor 6) is a master regulator of metabolism: eIF6 expression grade is rate-limiting in the maintenance of cellular metabolic homeostasis and its levels correlate with insulin resistance and obesity in humans (Brina, Miluzio et al. 2015)[1]. eIF6 translational activity is mTORc1-independent[2] and it positively regulates the translation of uORF-containing mRNAs encoding for lipogenic transcription factors[1]. Given the physiological role of eIF6 in the regulation of fatty acid synthesis, we decided to investigate the effects of eIF6 inhibition in metabolic syndrome. We defined the response of eIF6 heterozygote (eIF6 het) mice to a High Fat Diet (HFD) regimen. In these mice, obesity, insulin resistance, lipidemia, hepatic steatosis and fibrosis are significantly ameliorated compared to wt ones. Thus, eIF6 heterozygosity protects from HFD-induced Non-alcoholic fatty liver disease (NAFLD). Transcriptome analysis of eIF6 het livers reveals that genes involved in fatty acid, cholesterol and triglycerides biosynthesis are decreased; moreover, eIF6 directly drives the translation of lipogenic transcription factors, such as C/EBPβ, also in severe NAFLD. These data confirm the direct role of eIF6 in lipid metabolism, even in metabolic diseases. Intriguingly, genes involved in oxidative phosphorylation, respiratory

chain assembly and mitochondrial translation were significantly overexpressed in eIF6 het mice. Accordingly, cellular imaging and metabolomic assays show that eIF6 het primary hepatocytes derived from obese mice have a strong increase in ATP production and mitochondrial activity. These results corroborate the new emerging link between eIF6 and mitochondrial functions[3]. It was previously demonstrated that mTORC1 regulates mitochondrial function via the transcriptional regulation of Yin-Yang 1 (YY1)[4]. Using computational analysis, we identified the transcription factor YY1 as the common regulator of mitochondrial genes upregulated in eIF6 het livers. Consistently, upon prolonged high fat diet, eIF6 het livers were found to have a compensatory mTORc1 activation. In high fat diet, in eIF6 het mice, YY1 was not differentially expressed at the transcriptional level, but was translationally induced. Thus, we propose a mechanistically link between the eIF6 and mTORc1 independent pathways and their cooperation in the control of lipid metabolism and mitochondrial activity which results in the protective effects of eIF6 chronic depletion in metabolic syndrome.

References:

1. eIF6 coordinates insulin sensitivity and lipid metabolism by coupling translation to transcription. Brina D, Miluzio A, Ricciardi S, Clarke K, Davidsen PK, et al. Nat Commun. 2015 Sep 18;6:8261. doi: 10.1038/ncomms9261.

2. Impairment of cytoplasmic eIF6 activity restricts lymphomagenesis and tumor progression without affecting normal growth. Miluzio A, Beugnet A, Grosso S, Brina D, Mancino M et al. Cancer Cell. 2011 Jun 14;19(6):765-75. doi: 10.1016/j.ccr.2011.04.018.

3. The Role of Eif6 in Skeletal Muscle Homeostasis Revealed by Endurance Training Co-expression Networks. Clarke K, Ricciardi S, Pearson T, Bharudin I, Davidsen PK, et al. 2017 Cell Rep 21, 1507. doi: 10.1016/j.celrep.2017.10.040.

4. mTOR controls mitochondrial oxidative function through a YY1-PGC-1alpha transcriptional complex. Cunningham JT, Rodgers JT, Arlow DH, Vazquez F, Mootha VK et al. Nature 2007 Nov 29;450(7170):736-40. doi:10.1038/nature06322.

eIF6 depletion directly protects against the metabolic syndrome reducing lipid metabolism and increasing mitochondrial activity through the compensatory activation of mTOR pathway

Alessandra Scagliola[1,2], Annarita Miluzio[1], Roberta Alfieri[3], Gabriele Ventura[2], Chiara Cordiglieri[3], Stefania Oliveto[1,2], Nicola Manfrini[3] and Stefano Biffo[1,2].

[1]Molecular Histology and Cell Growth Unit, Istituto Nazionale Genetica Molecolare, "Romeo ed Enrica Invernizzi", Milano, Italy.
[2]Department of Biosciences, University of Milan, Milan, Italy.
[3] Istituto Nazionale Genetica Molecolare, "Romeo ed Enrica Invernizzi", Milano, Italy.

INTRODUCTION

eIF6 is a master regulator of metabolism. eIF6 translational activity is mTORc1-independent[2] and it positively regulates the translation of uORF-containing mRNAs encoding for lipogenic transcription factors[1]. eIF6 levels correlate with insulin resistance and obesity in humans[1].

AIM

We decided to investigate the effects of eIF6 inhibition in the metabolic syndrome, a cluster of conditions directly correlated with high risk of obesity and hyperglycemia. We defined the response of eIF6 het mice to a High Fat Diet (HFD) regimen.

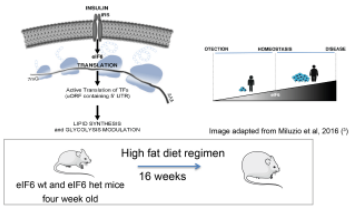

RESULTS

1. eIF6 reduction protects from HFD-induced obesity and insulin resistance

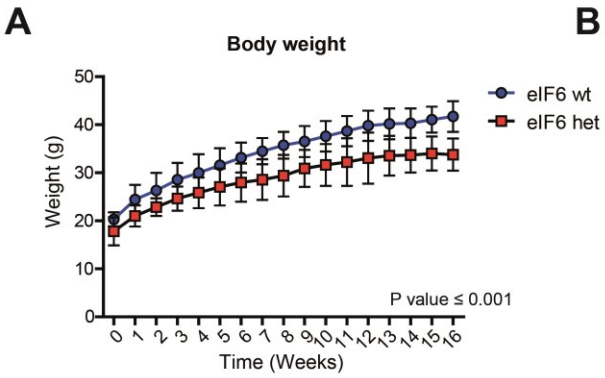

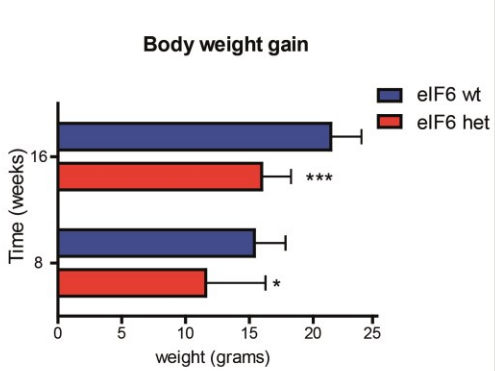

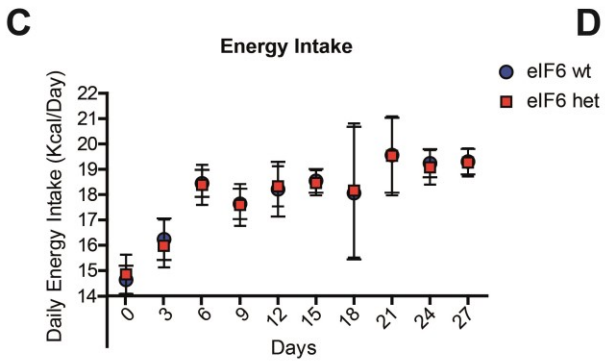

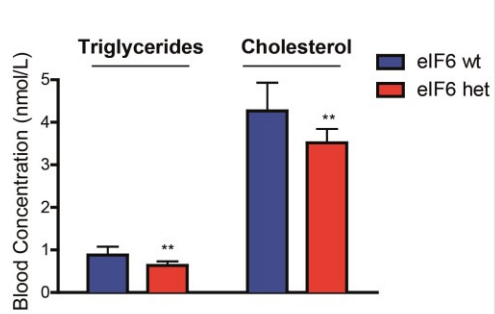

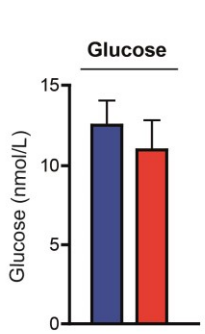

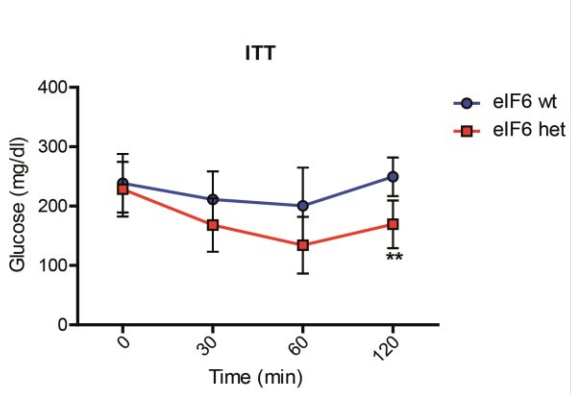

A.eIF6 het mice have a reduced body weight compared to wt ones. Body weight was measured at the indicated time points. N=12 mice for genotype. ***Pvalue<0.001, *Pvalue<0.05.
B.Absolute body weight gain is reduced in eIF6 het mice compared to wt ones. N=12 mice for genotype. **Pvalue<0.01.
C.Cumulative food intake shows no difference between eIF6 het and wt mice. N=12 mice for genotype.
D.Cholesterol and triglycerides levels are reduced in blood of eIF6 het compared to wt ones at the end of HFD regimen. N=7 mice for genotype.**Pvalue<0.001.
E.Glycemia is similar between eIF6 het and wt mice. N=7 mice for genotype.
F. Insulin Tolerance Test (ITT) shows that eIF6 het mice respond better to insulin. N=5 mice for genotype. **Pvalue<0.01.

2. Hepatic steatosis and fibrosis are reduced in eIF6 het mice

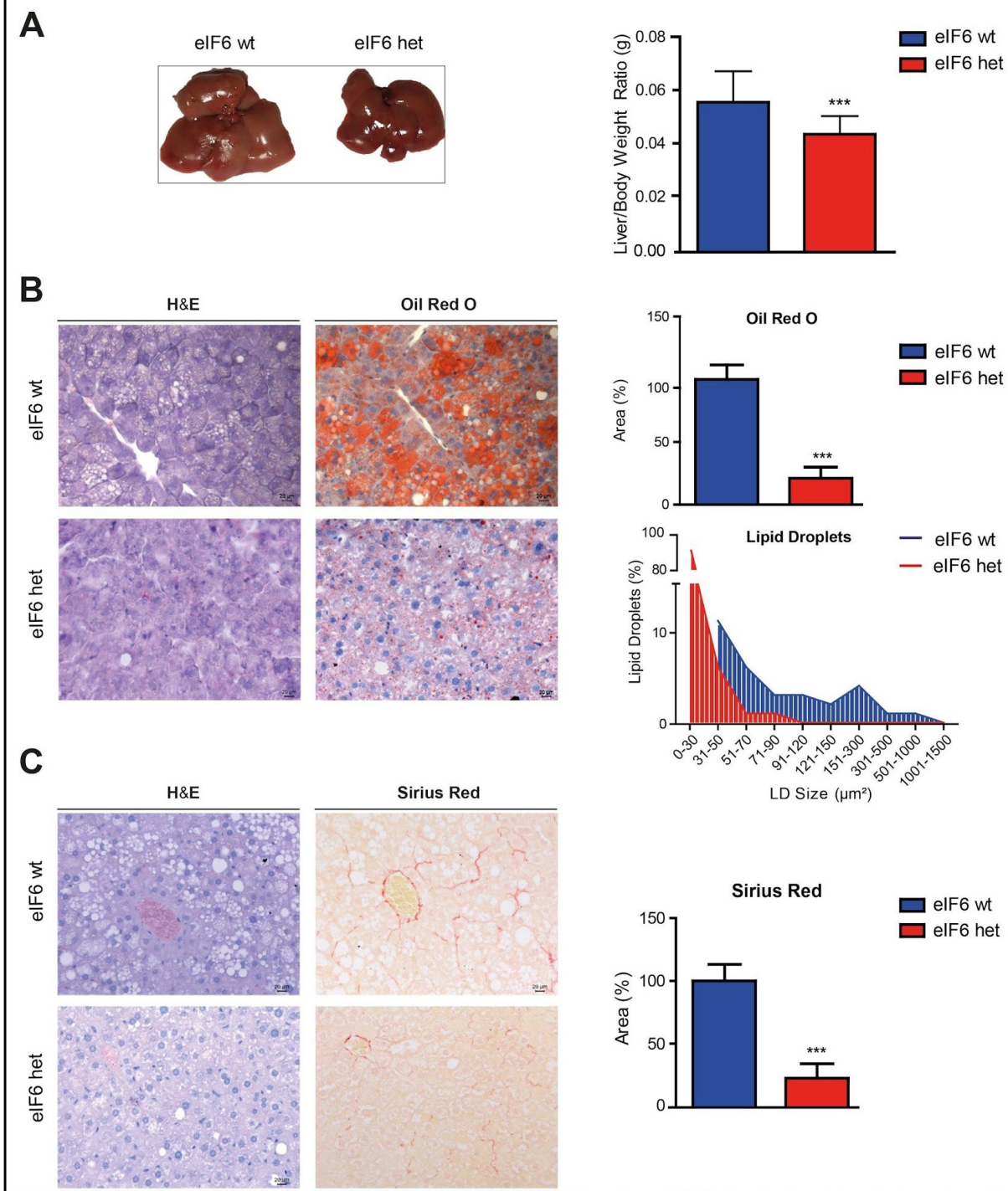

A. LEFT: Representative images of eIF6 wt and het livers after 16 weeks of HFD regimen. RIGHT: Liver/Body weight ratio shows that eIF6 het livers are less enlarged compared to wt ones. N=18 mice for genotype. ***Pvalue<0.001.

B. LEFT: Representative liver sections stained with H&E and Oil Red O show that eIF6 het mice have reduced hepatic lipid accumulation compared to wt ones. Scale bar is indicated. RIGHT, TOP: quantification of Oil Red O positive area in eIF6 het and wt livers. N= 3–4 for genotype.***P<0.001.RIGHT, BOTTOM:Frequency distribution shows that het mice have smaller lipid droplets compared to wt ones.

C. LEFT: Representative liver sections stained with H&E and Sirius Red show that eIF6 het mice have reduced collage deposition compared to wt ones. Scale bar is indicated. RIGHT: quantification of Sirius Red positive Area in eIF6 wt and het mice. N= 3–4 mice for genotype.***P < 0.001.

3. eIF6 depletion affects lipid metabolism

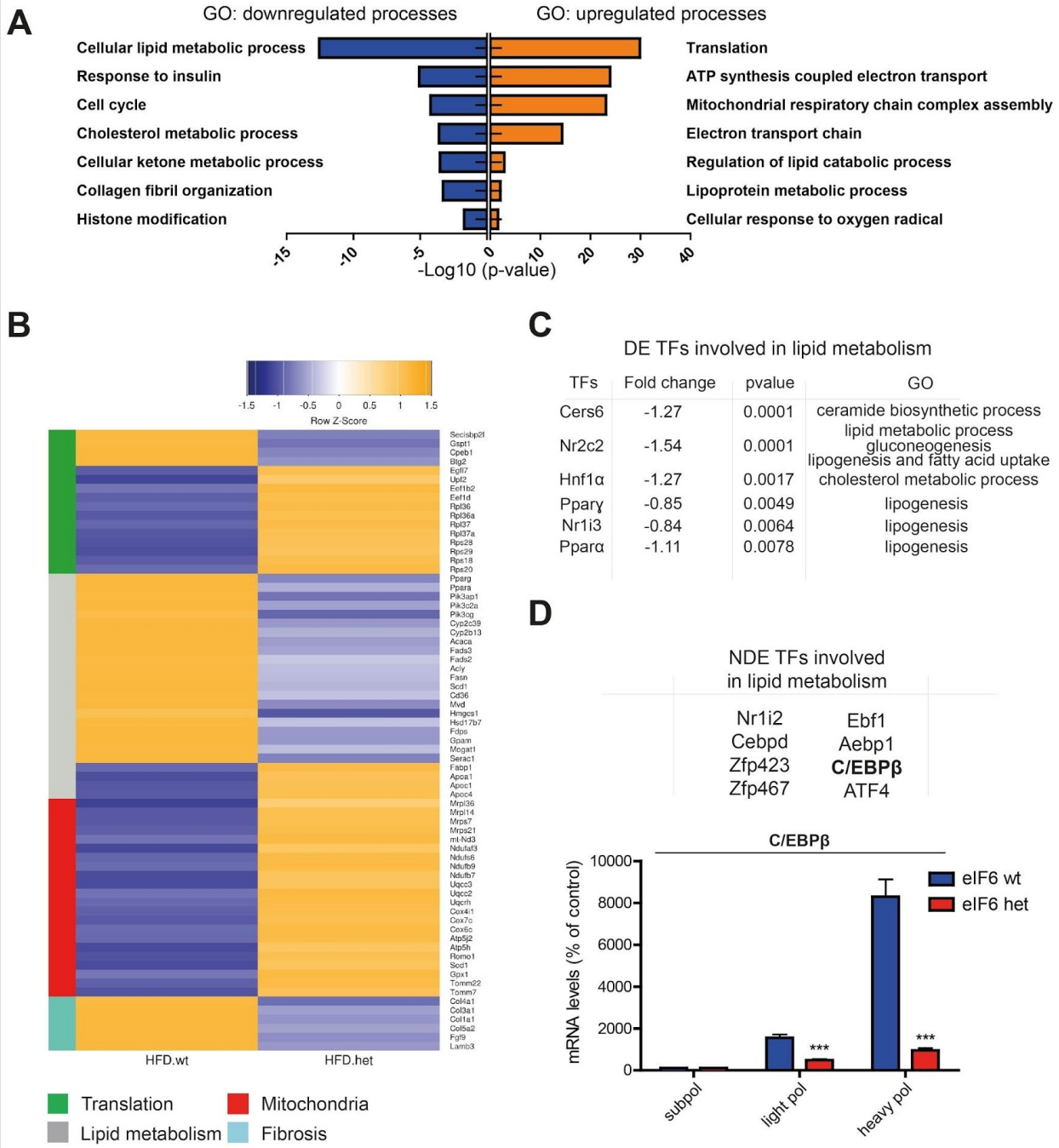

A.RNA-Seq analysis of eIF6 wt and het livers (N=4 for genotype) after 16 weeks of HFD regimen. Gene Ontology analysis identifies a pro found metabolic reprogramming in eIF6 het livers compared to wt ones. eIF6 het livers show a consistent transcritional reduction of lipid and cholesterol metabolic processes.

B.Heat map analysis showing differential gene expression between eIF6 wt and het liver samples.

C.Transcription Factors involved in lipid metabolism are differentially expressed in eIF6 het samples compared to wt ones. Fold change, pvalue and relative GO are indicated.

D.List of lipid metabolism-related transcription factors not differentially expressed in the RNA-Seq analysis but translationally regulated by eIF6 activity[1].Real-time PCR of C/EBPβ mRNA on liver polysome fractions reveals that its association with actively translating ribosomes (heavy polysomes) is reduced in eIF6 het livers compared to wt ones. ***Pvalue<0.001.

4. Mitochondrial function is increased in eIF6 het livers

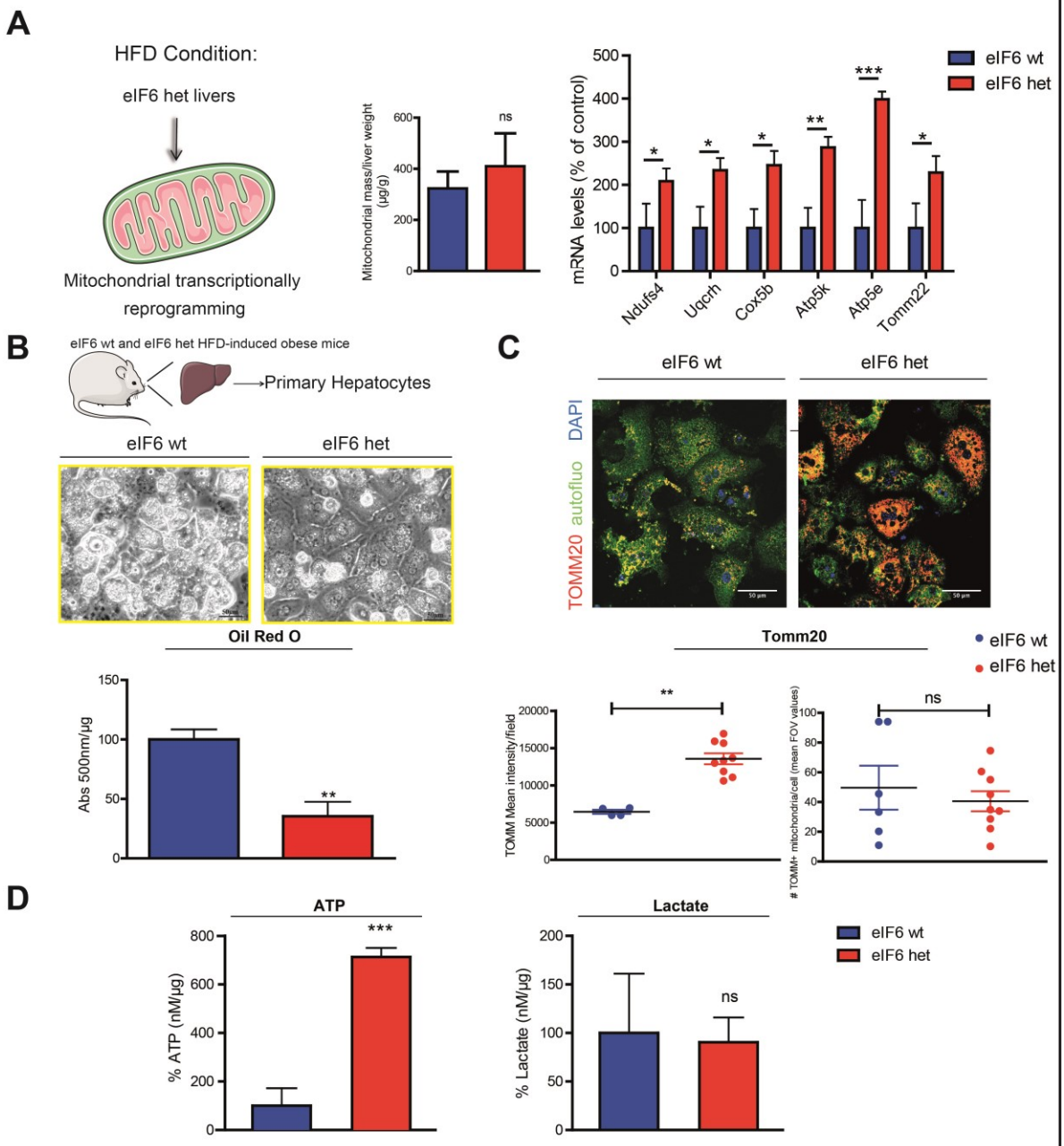

A.LEFT: simplified scheme showing the transcriptionally reprogramming of mithocondrial function identified by GO analysis. RIGHT: eIF6 het and wt mice have similar liver mitochondrial mass. Real-time PCR of the indicated genes confirms the upregulation of mitochondrial transcripts in eIF6 het livers. N=3 for genotype. ***Pvalue<0.001; **Pvalue<0.01, *Pvalue<0.05.

B.TOP: Representative bright-field images of primary hepatocytes isolated from eIF6 het and wt obese mice show that eIF6 wt cells have an increased accumulation of lipid droplets. BOTTOM: Quantification of Red Oil staining performed on primary hepatocytes. N=6 for genotype. **Pvalue<0.01.

C.TOP: Representative images of Immunofluorescence staining with TOMM20 Antibody. BOTTOM, LEFT: TOMM20 mitochondrial protein expression evaluated from fluorescence intensity levels. Mann-whitney paired comparison reveal significant difference between wt and het cells(**P<0.01).RIGHT: Number of mitochondria for each cell as visualized from TOMM20 labelling is similar between wt and het samples. Scale bar is indicated.

D.eIF6 het primary hepatocytes have increased ATP levels; in contrast, lactate secretion, an index of glycolytic flux, is similar between wt and get samples. These results indicate a specific increment of ATP synthesis derived by the Electron Transport Chain in het condition.

5. The transcription factor YY1 regulates the mitochondrial genes overexpressed in eIF6 het livers

A

Functional Gene Network visulalization of mitochondrial genes associated with eIF6 expression:

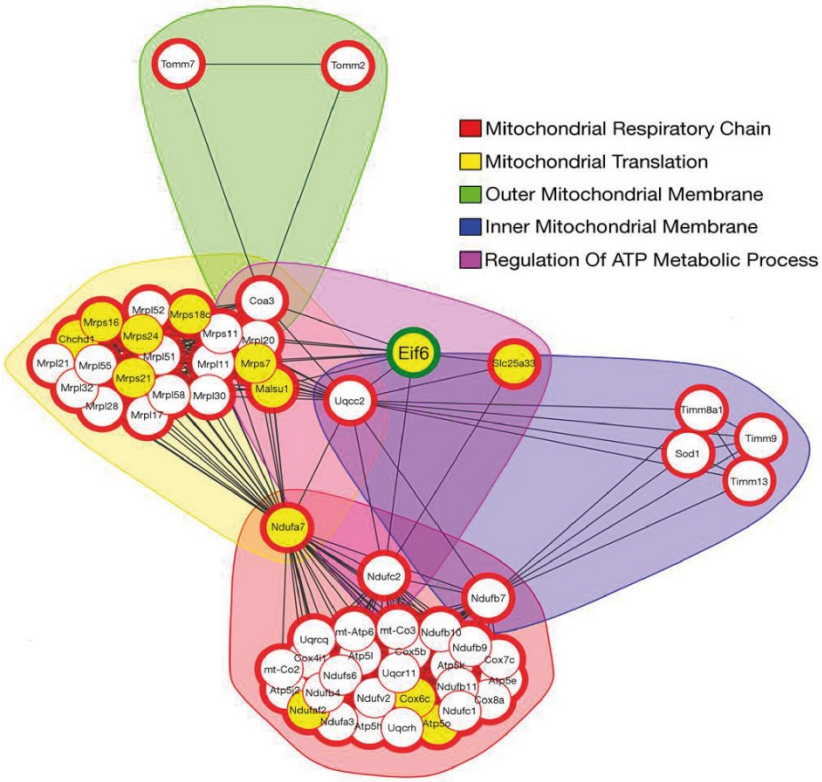

B

Computational analysis reveals that most of mitochondrial genes connected to eIF6 are transcriptionally regulated by YY1

Annotation	Dna binding motif prediction	N^ of associated genes	Associated genes
YY1		143	Ndufa2, Ndufaf, Ndufc1, Uqcrh, Uqcrq, Cox7c, Cox8a, Cox5b, Atp5j2, Atp5e, Atp5k, Atp4a, ...
Ets1		135	Uqcrq, Cox4i1, Tomm7, Atp5e, Slc25a33, Mrpl33...
Elk3		131	Romo1, Uqcrq, Timm10, Ndufa13, Atp5j2, Aurkaip1...

A.Functional Gene Network represents the Mitochondrial genes significantly correlated with eIF6 expression.
B.List of the overrepresented Transcription Factor-Binding Motifs in all mitochondrial genes associated with eIF6 expression. These motifs have been identified using two transcription factor binding site prediction analysis (iRegulon and Juspar softwares). The indicated motifs are recognized by the TFs YY1, Ets1 and ELK3

6. In eIF6 heterozygosity YY1 is translationally induced and mTOR kinase is activated

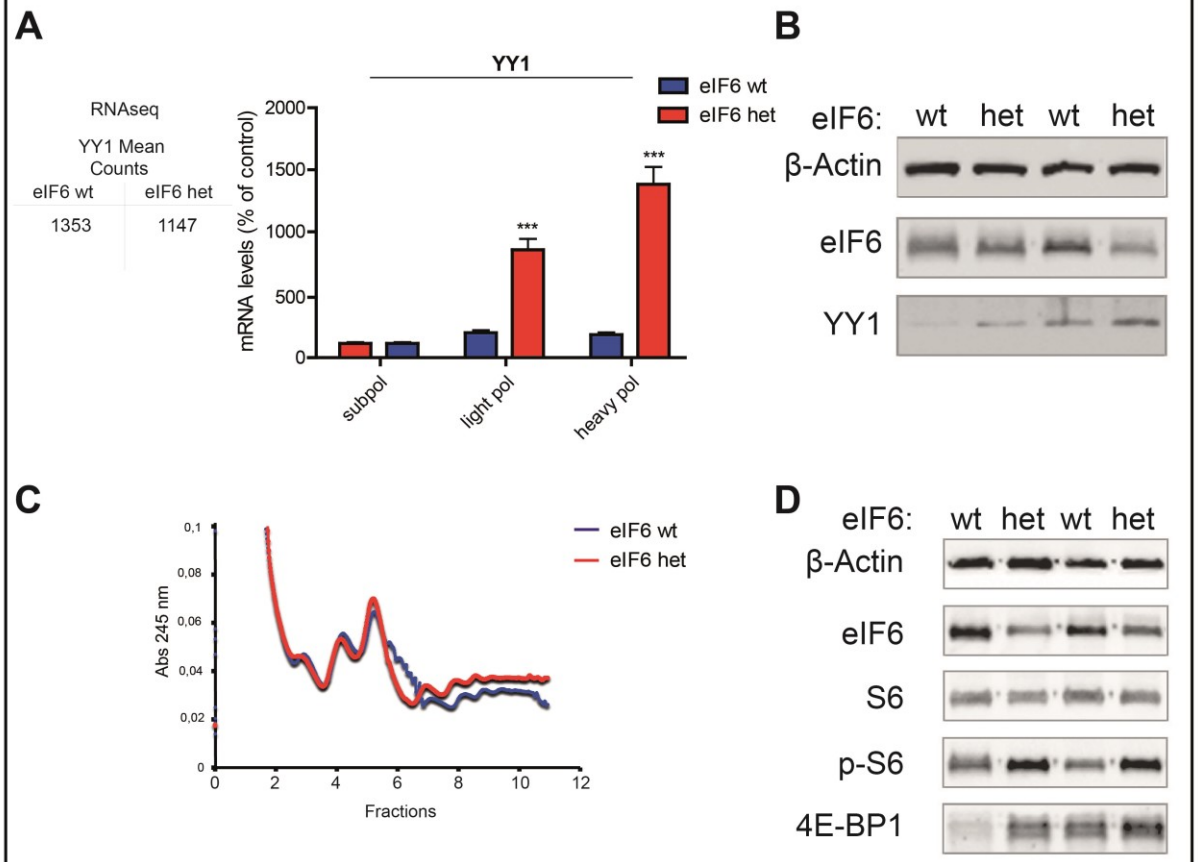

A.LEFT: RNA-Seq Counts show that YY1 is not differentially expressed between eIF6 wt and het livers. RIGHT: Real-time PCR of YY1 mRNA on liver polysome fractions reveals that its association with actively translating ribosomes (heavy polysomes) is increased in eIF6 het livers compared to wt ones. N=3 for genotype.
B: Representative Western Blot analysis indicates that YY1 protein levels are increased in eIF6 het livers.
C: As reported, mTORC1 regulates mitochondrial function via YY1[4]. Representative liver polysomal profiles of wt and eIF6 het livers show increased polysomes in het mice.
D: Representative Western Blot analysis indicates that mTORc1 kinase is activated in eIF6 het livers: phosphorylation of rpS6 and 4E-BP1 are increased in eIF6 het livers compared to wt ones.

CONCLUSIONS

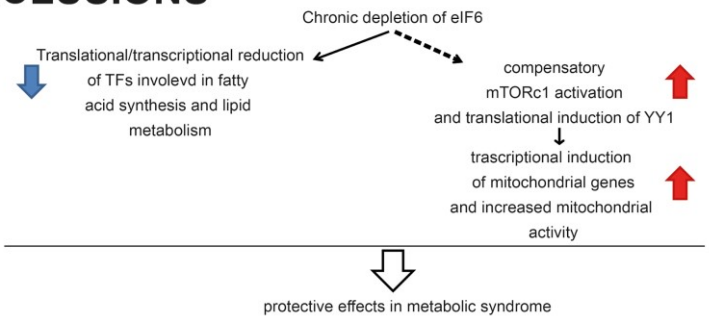

We propose a mechanistically link between the eIF6 and mTORc1 independent pathways and their cooperation in the control of lipid metabolism and mitochondrial activity resulting in the protective effects of eIF6 chronic depletion in metabolic syndrome

List of scientific publications on Journals and Ph.D. student contribution

- Oliveto S, Alfieri R, Miluzio A, Scagliola A, Seclì RS, Gasparini P, Grosso S, Cascione L, Mutti L, Biffo S. "*A polysome-based microRNA screen identifies miR-24-3p as a novel pro-migratory miRNA in mesothelioma*."

This paper identifies miR-24-3p as a novel polysome-associated miRNA up-regulated in Malignant Pleural Mesothelioma (MPM). miR-24-3p positively regulates Rho-GTP activity, and its inhibition reduces the migratory capability of MPM cells. The authors found that miR-24-3p regulates the translation of mRNAs involved in cell migration. Consequently, they confirmed the pro-oncogenic role of miR-24-3p, *in vivo*. miR-24-3p inhibition reduces both tumor growth and metastasis formation in xenografts.
Alessandra Scagliola participated in the execution of experiments involving NOD-SCID mice, evaluating their survival, tumor volumes and metastasis formation. She also performed some experiments aimed to define the proliferation rate of MPM cells.

- Clarke K, RicciardiS, PearsonT, Bharudin I, DavidsenP, BonomoM, BrinaD, Scagliola A, SimpsonD, BeynonR, KhanimF, AnkersJ, SarzynskiM, GhoshS, PiscontiA, BunceC, StewartC, EggintonS, CaddickM, JacksonM, BouchardC, BiffoS and F FalcianiF. "*The Role of eIF6 in Skeletal Muscle Homeostasis Revealed by Endurance Training Co-Expression Networks*." Cell Rep. 2017 Nov 7;21(6):1507-1520. doi: 10.1016/j.celrep.2017.10.040.

This paper describes the application of advanced computational molecular networks to progress our understanding of human skeletal muscle aging. Using this approach, the authors have been able to discover a link between mRNAs translation and age-dependent metabolic reprogramming. In particular, the computational analysis revealed eIF6 as the most connected translation factor linked to energy metabolism. Using eIF6 heterozygous mice, the authors confirmed the capability of eIF6 to regulate the translation of a specific set of energy metabolism-related transcripts, involved in oxidative phosphorylation, acetyl-coenzyme A (CoA) metabolism, TCA cycle, glycolysis, fatty acid metabolism and pyruvate metabolism. They showed that in skeletal muscle fibers of eIF6 het mice mitochondrial respiration efficiency is impaired and ROS production is increased. Accordingly, eIF6 het mice have a reduced performance in a treadmill exercise test.

Alessandra Scagliola managed and performed the treadmill exercise test and she analyzed the data obtained. She was also responsible for the generation, maintenance and handling of eIF6 wt and het mice used for the experiment, as well as responsible for the isolation and processing of organs used for histological analysis.

- Manfrini N, Ricciardi S, Miluzio A, Fedeli M, Scagliola A, Gallo S, Brina D, Adler T, Busch DH, Gailus-Durner V, Fuchs H, Hrabě de Angelis M, Biffo S. (2017) "*High levels of eukaryotic Initiation Factor 6 (eIF6) are required for immune system homeostasis and for steering the glycolytic flux of TCR-stimulated CD4$_+$ T cells in both mice and humans*." Dev Comp Immunol. 2017 Jul 22;77:69-76. doi: 10.1016/j.dci.2017.07.022.

This paper explores a new function of eIF6 for immune regulation in mice and in humans. The authors demonstrated that eIF6 het mice have reduced immune system functionality, revealed by an increased mortality upon spontaneous viral infection and by the reduction of peripheral blood CD4+ Effector Memory T cell. Given the increased eIF6 expression upon TCR-mediated activation of human CD4+T cells, the authors investigated the sensitivity of primary human T cells to eIF6 depletion. eIF6 downregulation affects glycolysis and energy production capacity of activated CD4+ T cells. Consequently, the *in vitro* acquisition of effector functions, as well as inflammatory cytokines secretion, are impaired in human CD4+ T-cell. In summary, this work shows that eIF6 levels are rate limiting for the glycolytic switch occurring upon T cells activation and that high levels of eIF6 are necessary for a complete immunological response *in vivo*.
Alessandra Scagliola participated in the execution of all the experiments involving mice.